Protracted intra- and inter-pluton magmatism during the Acadian orogeny: evidence from new LA-ICP-MS U–Pb zircon ages from northwestern Maine, USA

David Gibson[1], Sandra M. Barr[2], Deanne van Rooyen[3], Chris E. White[4], and Jean-Luc Pilote[5]

1. Department of Natural Sciences - Geology, University of Maine at Farmington, Farmington, Maine 04938 USA
2. Department of Earth and Environmental Science, Acadia University, Wolfville, Nova Scotia B4P 2R6, Canada
3. Department of Mathematics, Physics, and Geology, Cape Breton University, Sydney, Nova Scotia B1P 6L2, Canada
4. Nova Scotia Department of Energy and Mines, Geological Survey Division, Halifax, Nova Scotia B3J 2T9, Canada
5. Geological Survey of Canada, Natural Resources Canada, 490 rue de la Couronne, Québec, G1K 9A9, Canada
*Corresponding author <dgibson@maine.edu>

Date received: 07 November 2020 ¶ Date accepted: 26 February 2021

ABSTRACT

Devonian granitoid plutons comprise a major part of the bedrock of northwestern Maine representing the magmatic expression of the Acadian orogeny in this part of the northern Appalachian orogen. They are petrographically diverse with minerals characteristic of both I- and S-type granites, in some cases within the same intrusion, and some are compositionally zoned. New LA-ICP-MS ages presented here elucidate the timing and duration of this magmatism. The earliest phase of granitoid magmatism began around 410–405 Ma with the emplacement of the Flagstaff Lake Igneous Complex, and the presence of contemporaneous mafic rocks suggests that mantle-derived magmas were also produced at this time. Late Devonian ages, ca. 365 Ma, for many intrusions, such as the Chain of Ponds and Songo plutons, reveal that magmatism continued for 45 million years during which compositionally diverse I- and S-type magmas were produced. In addition, there is evidence that intrusive activity was prolonged within some plutons, for example the Rome-Norridgewock pluton and the Mooselookmeguntic Igneous Complex, with 10–15 myr between intrusive units. The new ages suggest a break in magmatism between 400 Ma and 390 Ma apparently separating Acadian magmatism into early and late pulses. The production of lower crustal I-type magmas appears to have been concentrated later, ca. 380–365 Ma, although several S-type granitoids were also emplaced during this period. These Late Devonian plutons display abundant zircon inheritance with ages around 385 Ma, which suggests that the crust was experiencing enhanced thermal perturbations during this extended timeframe. The new data for granitoid plutons in northwestern Maine are consistent with tectonic models for other parts of Ganderia which propose initial flat slab subduction followed by slab breakoff and delamination.

RÉSUMÉ

Les plutons granitoïdes du Dévonien constituent une tranche importante du substrat rocheux du nord-ouest du Maine représentant l'expression magmatique de l'orogenèse acadienne dans cette partie de l'orogène appalachien septentrional. Ils constituent une succession pétrographiquement diversifiée, composée de minéraux caractéristiques tant des granites de type I que de type S, dans certains cas à l'intérieur de la même intrusion, alors que la composition des autres plutons régionaux est zonée. Les nouvelles datations par ablation laser et spectrométrie de masse à plasma inductif présentées ici élucident le moment où est survenu ce magmatisme et sa durée. L'épisode le plus ancien du magmatisme granitoïde a débuté vers 410–405 Ma avec la mise en place du complexe de roches éruptives du lac Flagstaff, même si la présence de roches mafiques contemporaines laisse supposer que des magmas d'origine mantellique ont également été produits à ce moment. Les datations du Dévonien tardif faisant remonter à environ 365 Ma de nombreuses intrusions, comme les plutons Chain of Ponds et Songo, révèlent que ce magmatisme s'est dans l'ensemble poursuivi durant 45 millions d'années au cours desquelles des magmas de type I et S de compositions diverses ont été produits. Il existe de plus des preuves que l'activité intrusive s'est prolongée à l'intérieur de certains plutons, par exemple le pluton Rome-Norridgewock et le complexe de roches éruptives de Mooselookmeguntic, qui accusent un écart de 10 à 15 Ma entre les unités

ATLANTIC GEOLOGY 57, 147–191 (2021)
0843-5561|21|0147–0191$7.75|0
doi:10.4138/atlgeol.2021.008

intrusives. Les nouvelles datations permettent de supposer une interruption du magmatisme entre 400 et 390 Ma., qui semble séparer le magmatisme acadien en impulsions précoce et tardive. La production de magmas de type I crustaux inférieurs semble s'être concentrée à un moment ultérieur, vers 380 à 365 Ma, bien que plusieurs roches granitoïdes de type S se soient également mises en place durant cette période. Ces plutons du Dévonien tardif présentent un héritage abondant de zircons remontant à peu près à 385 Ma, ce qui laisse entendre que la croûte terrestre a subi des perturbations thermiques de plus en plus prononcées au cours de cet intervalle prolongé. Les nouvelles données sur les plutons granitoïdes du nord-ouest du Maine correspondent aux modèles tectoniques d'autres parties du terrane de Gander, qui supposent une subduction initiale de plaques plates suivie par une rupture des plaques et une délamination.

[*Traduit par la redaction*]

INTRODUCTION

Granitic magmas produced during collisional tectonic events are important repositories of information regarding (i) the duration of orogenesis, (ii) the role of mantle inputs, both physical and thermal, and (iii) the growth/assembly of the continental crust (e.g., Hawkesworth *et al.* 2019). However, any meaningful model that is proposed to explain the interaction between tectonic and magmatic processes during such orogenies relies heavily on accurate age determinations of the plutonic rocks.

Paleozoic granitoid rocks constitute a major component of Ganderia in the northern Appalachian orogen (Fig. 1). They are widely dispersed throughout Maine and adjacent New Brunswick and New Hampshire, but many of these plutons do not have reliable ages.

The focus of this contribution is a dense cluster of plutons that outcrop in western and northwestern Maine. They were emplaced at various crustal levels, as suggested by the presence or absence of thermal aureoles, and appear to lack any patterns of age and tectono-magmatic correlation. This apparent lack may be due at least in part to the range of methodologies used to date them (U–Pb zircon, $^{39}Ar/^{40}Ar$ and Rb–Sr), and/or the extent of intra-pluton petrographic variation, and the fact that some plutons remain undated. We present new LA-ICP-MS ages for a number of these plutons to examine the duration of magmatism in this part of the orogen, enable correlations between the timing of magmatism and possible sources to be investigated, and further elucidate the nature of this prolonged magmatic event(s) – was it continuous or pulsatory? In many ways these plutons are a microcosm of "Acadian" (*sensu latto*) magmatism and may further enhance our understanding of the tectono-magmatic environment in the broader Acadian context.

GRANITOID PLUTONS IN MAINE

Silurian and Devonian plutonic rocks are scattered throughout Maine and New Brunswick but mainly occur in three belts (Fig. 1). The Coastal Maine Magmatic Province (CMMP) of Hogan and Sinha (1989) outcrops south of the Norumbega Fault Zone and extends into southern New Brunswick to include the Saint George Batholith (Mohammadi *et al.* 2017). Plutons in east-central Maine appear to be the southwestern extension of the Miramichi Magmatic Belt in New Brunswick, although it is not clear whether or not those plutons extend south of the Norumbega fault to merge with the CMMP (Fig. 1). The third belt of plutons form a scattered trend across north-central Maine into northern New Brunswick, defining the Piscataquis Magmatic Belt (Pilote *et al.* 2011; Gibson *et al.* 2006), located south of the inferred boundary between peri-Laurentian and peri-Gondwanan terranes known as the Red Indian Line (Fig. 1).

Based on a compilation of available geochronological data (Bradley *et al.* 2000; Pilote *et al.* 2011), one-third of the approximately 170 reliable U–Pb zircon ages from Silurian and Devonian plutons in Maine, eastern New Hampshire, and New Brunswick (area shown in Figure 1) have Silurian to earliest Devonian ages between 444 and 416 Ma (Fig. 2). These plutons vary from metaluminous to peraluminous and peralkaline compositions and intruded mainly south of the Norumbega Fault Zone in Maine extending into southwestern New Brunswick and the Miramichi Magmatic Belt of central and northern New Brunswick. They are generally attributed to the Salinic orogeny. A second group, about 40% of dated plutons, have early to middle Devonian ages of ca. 415–395 Ma (Fig. 2). These rocks also vary considerably in composition and intruded mainly throughout the Piscataquis Magmatic Belt in northern and western Maine and into eastern New Hampshire. The remaining one-third of the ages are middle to late Devonian age (ca. 390–360 Ma) and are from plutons scattered throughout New Brunswick, Maine, and eastern New Hampshire. These Devonian plutons have often been termed "Acadian" and "Late Acadian" in the literature (Fig. 2). Their distribution shows no clear pattern in space and time, and the wide geographic separation of some contemporaneous plutons suggests that they are not all related to a specific or the same orogenic event.

Pluton ages in the Coastal Maine and Miramichi belts are reasonably well constrained, but this is not the case for plutons in western Maine, where the broad distribution of varied plutons is especially enigmatic. Some of these plutons are the focus of the present study (Fig. 3).

FIELD RELATIONS AND PETROGRAPHY

The plutons dated in this study are in northwestern Maine bordering with Quebec in the north and New Hampshire in

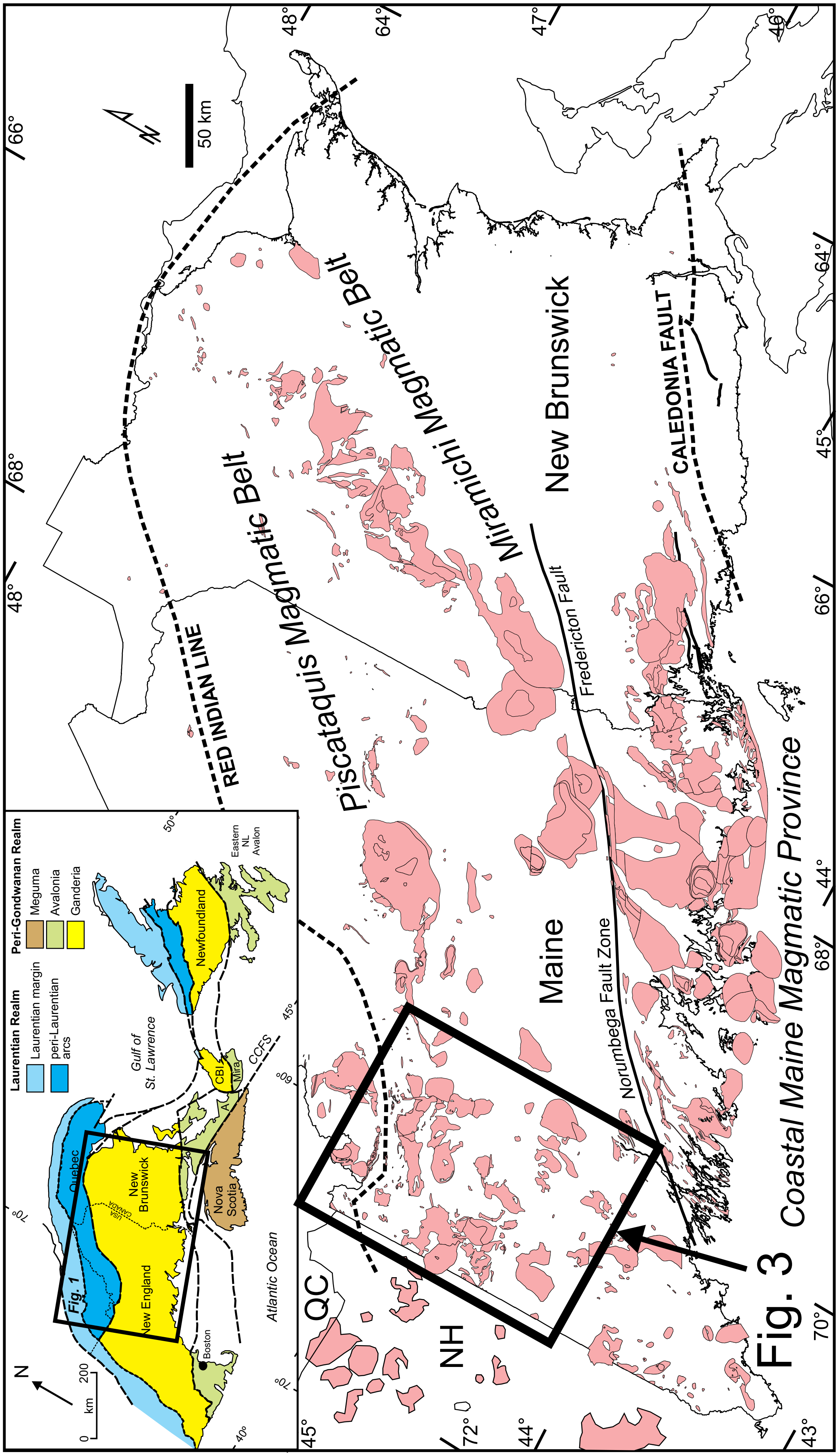

Figure 1. Geologic map of part of the northern Appalachian orogen showing the distribution of Silurian and Devonian plutons. Area outlined in black is shown in more detail in Figure 3. Inset map shows the location of the map in Figure 1 on the tectonic divisions of the northern Appalachian orogen after Hibbard *et al.* (2006).

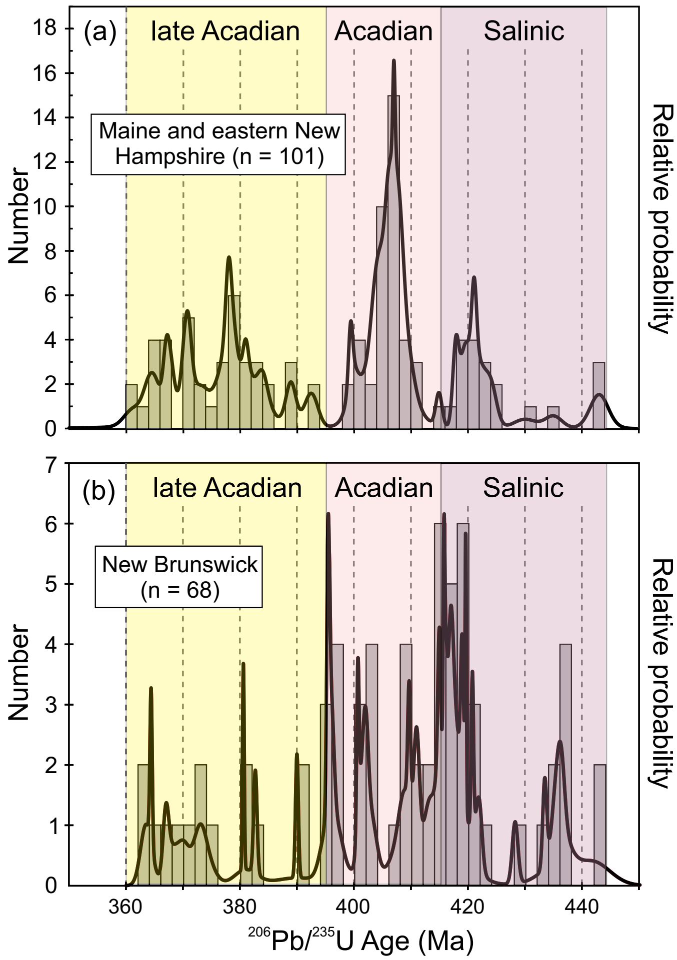

Figure 2. Probability plots of U–Pb zircon igneous crystallization ages for Silurian and Devonian plutons from (a) Maine and eastern New Hampshire and (b) New Brunswick. Data are from the compilations of Bradley *et al.* (2000) and Pilote *et al.* (2011).

the west (Fig. 3). They intruded a variety of country rocks with ages from Precambrian to Devonian and vary in mineralogy and emplacement form. Both I- and S-type compositions are evident, in some cases forming different units of the same intrusion, such as in the Mooselookmeguntic Igneous Complex and the Lexington composite pluton (Tomascak *et al.* 2005). Field relationships suggest that some of the plutons may be high-level ring-dike intrusions whereas others are deeper level sill-like or tabular intrusions. Both zoned and composite intrusions are present, although the lack of exposure in many areas precludes evidence from internal contacts to definitively determine which. Most, if not all, of these plutons truncate either major stratigraphic and/or structural boundaries, suggesting that they were emplaced after crustal assembly in this part of the northern Appalachian orogen.

The Mooselookmeguntic Igneous Complex (MIC), the Redington and Phillips plutons and the Lexington composite pluton in northwestern Maine have been dated previously by the U–Pb zircon method (Tomascak *et al.* 2005; Solar *et al.* 1998). As summarized in Table 1, these plutons display petrographic and compositional characteristics similar to those of the plutons described below which were dated in this study.

Chain of Ponds pluton

The Chain of Ponds (COP) pluton outcrops over approximately 220 km^2 in northern Maine and extends northward into Quebec (Fig. 3). It intruded Precambrian basement rocks of the Chain Lakes massif, and is mapped as two granitoid bodies, the most northerly of which is zoned with a core of biotite-hornblende granite and a marginal zone of biotite granite. Several "screens" of country rock outcrop within both units in a semi-circular concentric outcrop pattern parallel to the outer contact of the intrusion (Harwood 1973). Westerman (1980) mapped a large number of brittle fractures, which together with the outcrop relationships suggest that the intrusion has a high-level ring dike form. A few kilometres to the north in Quebec, the Spider Lake pluton is similarly zoned but due to lack of exposure its relative age relationship to the COP pluton is unclear. The COP pluton was dated by Heitzler *et al.* (1988) using the $^{40}Ar/^{39}Ar$ hornblende step-heating technique which yielded an age of 373 ± 2 Ma based on the average of 6 plateau ages. The Spider Lake pluton gave a U–Pb zircon age of 383 ± 3 Ma (Simonetti and Doig 1990).

Dated sample COP-1 was collected from the northerly zoned part of the COP pluton close to the Quebec border. It consists of equigranular, medium-grained biotite granite with a colour index (CI) ~20. Biotite is the predominant mafic mineral and occurs as euhedral flakes 2–3 mm in size. It has pale brown to dark brown pleochroism with numerous zircon inclusions. Minor hornblende is also present. Plagioclase forms larger euhedral grains, up to 4 mm in length, commonly displaying compositional zoning, and is more abundant than K-feldspar. Some grains show minor sericitic alteration. K-feldspar occurs as mostly interstitial, anhedral grains. Quartz occurs as anhedral grains, commonly in clusters (glomerocrysts), with some grains displaying undulatory extinction. Zircon is the most abundant accessory mineral and is hosted predominantly in biotite. Some larger grains, up to 0.25 mm, are present. In addition, opaque minerals and titanite are present. Some epidote

Figure 3. (next page) Generalized geologic map of northwestern Maine (after Osberg *et al.* 1985 and Moench and Pankiwskji 1988) showing the plutons dated in this study along with other Devonian plutons including those which have previously published U–Pb ages. Only major tectonic or lithological boundaries are shown; BMF = Blueberry Mountain fault (Moench and Hildreth 1976), WBF = Winter Brook fault (Moench and Pankiwskji 1988).

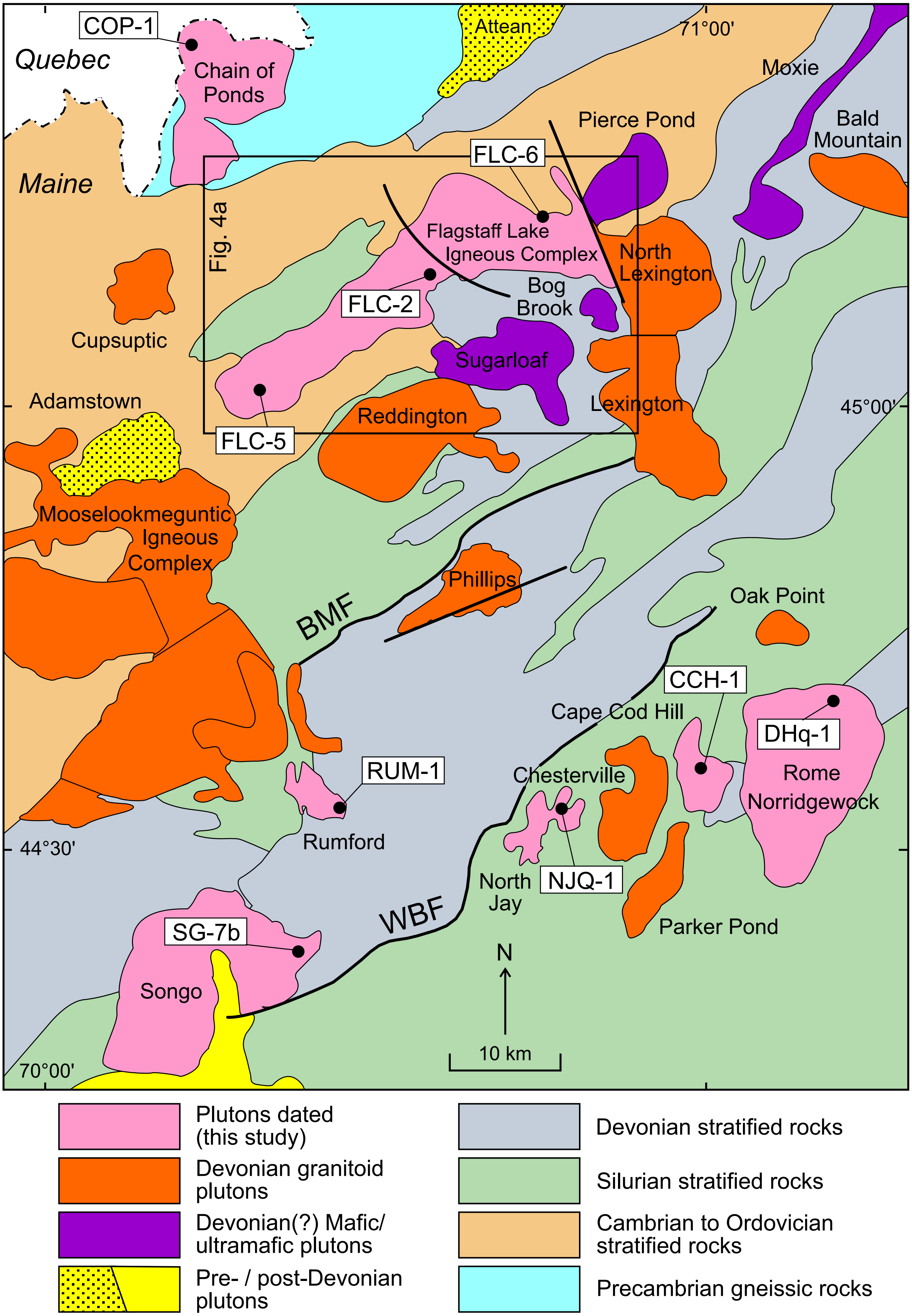

COP-1
Quebec
Chain of Ponds
Maine
Attean
71°00'
Moxie
Pierce Pond
Bald Mountain
FLC-6
Fig. 4a
Flagstaff Lake Igneous Complex
North Lexington
Bog Brook
FLC-2
Cupsuptic
Sugarloaf
Adamstown
Lexington
45°00'
Reddington
FLC-5
Mooselookmeguntic Igneous Complex
Phillips
BMF
Oak Point
CCH-1
Cape Cod Hill
DHq-1
Rome Norridgewock
RUM-1
Chesterville
Rumford
44°30'
North Jay
NJQ-1
Parker Pond
WBF
SG-7b
N
Songo
10 km
70°00'
Plutons dated (this study)
Devonian granitoid plutons
Devonian(?) Mafic/ ultramafic plutons
Pre- / post-Devonian plutons
Devonian stratified rocks
Silurian stratified rocks
Cambrian to Ordovician stratified rocks
Precambrian gneissic rocks

Table 1. Summary of field relationships, petrography, and published ages for plutons of northwestern Maine.

Pluton/Complex	Field relationships and petrography	Dates and methods
Mooselookmeguntic Igneous Complex (MIC)	Outcrops over an area of ~ 925 km². It intruded a metamorphosed sequence of Cambrian to Silurian rocks and the Ordovician (?) Adamstown pluton. Contact relations suggest it is a subhorizontal, sheet-like intrusion. It is a composite pluton with a biotite ± hornblende granodiorite and tonalite, that contains titanite and epidote (Guidotti, pers comm), and a two-mica granite. A separate intrusion, the Umbagog pluton, outcrops adjacent to the main body. Solar *et al.* (1998) and Tomascak *et al.* (2005) proposed amalgamating all the above rocks into the MIC subdividing it into a monzodiorite suite (the tonalite and Umbagog pluton) and a more felsic biotite and two-mica granite, the granite suite. Inclusions of the former are observed in the more felsic rocks.	Monzodiorite suite: ca. 377 Ma [U–Pb zircon; Tomascak *et al.* (2005)]; 378 ± 2 Ma [Moench and Aleinikoff (2003)]. Granite suite: 370 ± 1 Ma [U–Pb monazite; Solar *et al.* (1998)]. Granodiorite inclusion: 388.9 ± 1.6 Ma [(U–Pb zircon, Solar *et al.* (1998)].
Phillips pluton	Intruded Devonian metasedimentary rocks and is a medium-grained, equigranular two-mica leucogranite with muscovite > biotite and garnet. Minor granodiorite is also present as large blocks and enclaves (Pressley and Brown 1999). It also contains numerous but discontinuous biotite schlieren probably produced by magmatic flow during emplacement.	403.6 ± 2.2 Ma [U–Pb zircon and monazite; Solar *et al.* (1998)].
Reddington pluton	Intruded a Silurian metamorphic package of rocks covering an area of 185 km². It is a medium- to coarse-grained, equigranular to porphyritic granite with large ~ 3 cm K-feldspar phenocrysts. Biotite typically displays distinct red-brown pleochroism.	407.6 ± 4.7 Ma [U–Pb zircon; Solar *et al.* (1998)].
Lexington Composite Pluton	Outcrops over an area of 325 km². It intruded predominantly Devonian metamorphic rocks and was previously mapped as having a northern, central, and southern lobe. The northern unit appears to intrude the rest of the pluton (corroborated by the ages) and we propose referring to this unit as the North Lexington pluton. It is a medium-grained, equigranular granodiorite to granite with biotite + hornblende + titanite. The central and southern units form the Lexington pluton with the former comprised of a coarse-grained, porphyritic quartz monzonite, which contains large, zoned K-feldspar megacrysts up to 20 cm in length which are aligned suggesting a flow origin. Abundant coeval mafic enclaves are present. The southern unit is a finer-grained granite with smaller and less abundant K-feldspar phenocrysts.	North Lexington biotite + hornblende + titanite granodiorite: ca. 365 Ma [U–Pb zircon; Tomascak *et al.* (2005)]. Lexington pluton - central and southern quartz monzonite and granite: 404 ± 2 Ma [U–Pb zircon; Solar *et al.* (1998)].
Rome-Norridgewock pluton	Large, 300 km² pluton which intruded Silurian strata. It is composed of medium- to coarse-grained, equigranular two-mica leucocratic granite with muscovite > biotite. Some microscopic evidence for deformation.	378 ± 1 Ma [U–Pb zircon; Tucker *et al.* (2001)].

grains are also observed and their euhedral and zoned, suggesting a possible magmatic origin.

Flagstaff Lake Igneous Complex

The Flagstaff Lake Igneous Complex (FLIC) is one of the largest intrusions (420 km²) of the central/northern Maine belt outcropping from Rangeley to the Long Falls Dam, about 60 km in an orogen-parallel SW–NE direction (Fig. 4a). It intruded Cambrian–Ordovician rocks along its northern border and an Ordovician–Silurian metasedimentary sequence along its southern margin and has not been previously dated. Moench and Pankiwskyj (1988) mapped the complex as a composite intrusion composed of three units, from southwest to northeast: gabbro with garnet "granofels", a central area of porphyritic granite, and gabbro in the northeast. Neilsen *et al.* (1989) described more complex field relations including garnet tonalite (as opposed to granofels) and evidence for the comingling/mixing of mafic and felsic magmas especially in the gabbroic area in the northeast of the complex. However, the reconnaissance fieldwork for this study has revealed further variations. The southwestern unit, although predominantly gabbro, also contains diorite and granite in close field association. Similarly, the central unit is petrographically variable with coarse-grained, porphyritic granite in contact with fine-grained quartz diorite (Fig. 4b). The contact is sharp, defined by a thin (<1 cm) biotite-rich zone, but it does not appear to be a chilled, intrusive contact. The northeastern unit is predominantly a commingled zone of mafic and felsic rocks. Medium-grained

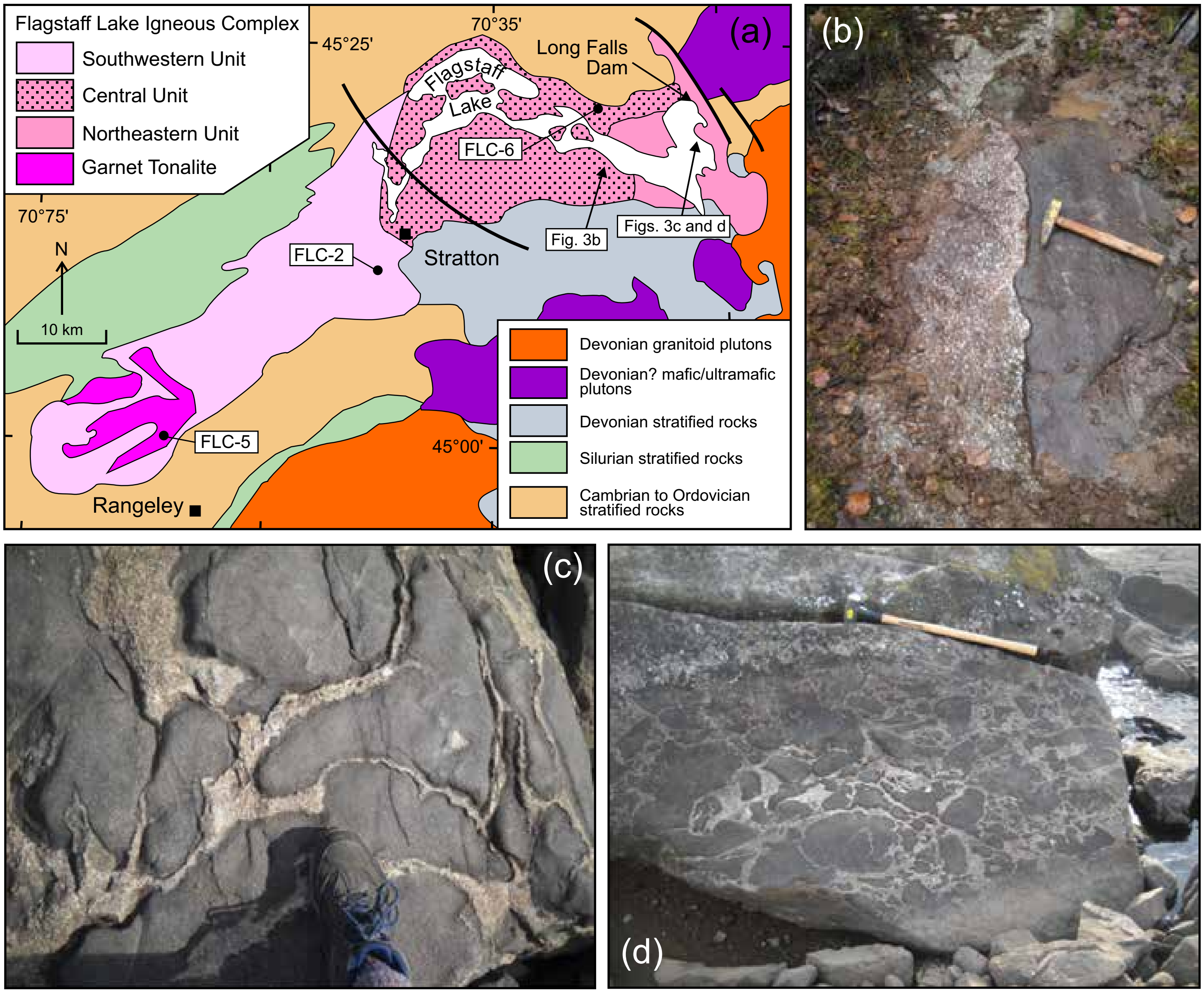

Figure 4. (a) Geological map of the Flagstaff Lake Igneous Complex (after Moench and Pankiwskji 1988 and Neilsen *et al.* 1989) showing the main field relations and sample locations. (b) Contact between porphyritic granite and quartz diorite south shore of Flagstaff Lake (hammer handle is 30 cm in length and oriented to the north). (c) and (d) lobate contacts between co-mingled felsic and mafic rocks (boot in (c) is 12 cm across; in (d) hammer handle is 1 m).

gabbro and diabase are surrounded by, and in lobate contact with, intermediate "hybrid" rocks and granitic material (Figs. 4c, d). Some quartz and feldspar grains are observed in the mafic rocks whereas some mafic minerals (hornblende?) exchanged to the felsic portion. Acicular apatite, formed by quenching during magma mixing, was observed microscopically in intermediate rocks, although evidence of more intensive mixing, such as rapakivi-textured feldspars or quartz ocelli, is absent. It is clear however, that these mafic and felsic magmas were contemporaneous.

A particularly enigmatic rock type observed in the FLIC is garnet tonalite, which outcrops both in the southwestern part of the complex and near its northeastern contact. Nielsen *et al.* (1989) suggested two possible origins for these rocks — either by the differentiation of mantle-derived magma or by country rock anatexis. They pointed to the close association of the garnet tonalite with sulfidic, Fe-rich metapelite as an important petrogenetic observation. However, either process would have required significant heat input and therefore determining the age of these rocks might be significant in elucidating the timing of mantle-derived magmatic activity. Three samples were dated from the FLIC: *Sample FLC-2* is equigranular, coarse-grained, biotite granite with CI ~15 and was collected from the central unit of the FLIC just west of the town of Stratton. The dominant mafic mineral is biotite which displays distinctive pale to deep red-brown pleochroism. It forms euhedral grains up to 2.5 mm with minor chloritic alteration along cleavage planes. Muscovite is also present and appears to be primary as it occurs both as discrete grains (Figs. 5a, b) and as inclusions in both K-feldspar and plagioclase. K-feldspar occurs as large (up to 5 mm) euhedral to subhedral twinned grains showing perthitic texture. Quartz is more abundant than plagioclase with some grains being up to 4 mm in length and locally displaying undulatory extinction. Plagioclase forms subhedral to anhedral grains which are interstitial or larger, up to 4 mm, some of which display concentric zoning. Zircon is again the dominant accessory phase occurring as small equant grains <0.2 mm in size, although some acicular forms are also present. Minor amounts of apatite are also observed.

Sample FLC-5 was collected from workings at an abandoned garnet quarry at the southwestern end of the FLIC. The rock is equigranular, medium-grained and dominated by garnet which comprises over 60% of the sample. The garnet occurs as mostly euhedral to subhedral grains which range in size from 2–3 mm (Fig. 5c) and contain numerous opaque inclusions. Most are fractured in a consistent orientation. Biotite is the dominant mafic mineral and is commonly around the margins of the garnet grains. It displays pale red to deeper red-brown pleochroism. Plagioclase forms subhedral grains between the garnet grains and typically displays concentric zoning, supporting an igneous origin for this rock (Fig. 5d). Quartz occurs interstitially as small (<1 mm) grains that show normal (non-undulatory) extinction. The main accessory phases are zircon, hosted by the biotite, and opaque minerals, which are generally observed within the garnet grains.

Sample FLC-6 was collected from the northeastern part of the FLIC just inland from the northern shoreline of Flagstaff Lake. It is a medium-grained, mainly equigranular biotite granite with a CI ~25. Biotite occurs as small, euhedral flakes up to 2 mm wide with some minor chloritic alteration. It displays pale to deeper red-brown pleochroism and hosts abundant zircon grains. Muscovite is also present and is interpreted to be mostly of primary origin, although it also occurs as an alteration product. Plagioclase is more abundant than K-feldspar and some larger grains, up to 4 mm, are present. Most plagioclase forms smaller euhedral to subhedral grains with sericitization of core areas suggesting higher Ca contents. K-feldspar is typically subhedral and around 4 mm across with quartz about the same size, the latter displaying normal extinction. Zircon is the dominant accessory phase with minor amounts of opaque minerals.

Rumford pluton

The Rumford pluton, mapped by Moench and Hildreth (1976), is a small, composite intrusion which outcrops over an area of 25 km^2 but is poorly exposed in a bowl-shaped topographic depression. It intruded mostly Devonian metasedimentary rocks but also some Silurian strata to the northwest and therefore cross cuts an important structural boundary, the Blueberry Mountain fault (Fig. 3). Moench and Hildreth 1976) mapped a number of rock types in the Rumford pluton. An area of gabbro-diorite with hornblende, biotite, and calcic plagioclase occurs in the western part of the intrusion. The main part of the pluton is more felsic with equal areas of pegmatitic granite and two-mica granite. The pegmatitic granite texture ranges from true pegmatite to aplite with minor garnet and tourmaline. The two-mica granite contains abundant inclusions of granodiorite and tonalite which contain biotite and hornblende with some titanite and zircon, and are similar to rocks in the Mooselookmeguntic Igneous Complex (Table 1).

Sample RUM-1 was collected from the eastern margin of this petrographically diverse pluton. It is a medium-grained, medium-grey equigranular granite. It has a CI of ~20 with biotite as the main mafic mineral and sparse hornblende. The biotite occurs as euhedral flakes 2–3 mm in length. Glomerocrystic quartz is abundant, and plagioclase predominates over K-feldspar. Opaque minerals and rare zircon and apatite are present as accessories but no titanite was observed.

Songo pluton

Outcropping over an area of 325 km^2 the Songo pluton (Fig. 3) intruded a high-grade Devonian metasedimentary sequence, which was metamorphosed to K-feldpsar + sillimanite grade (Guidotti *et al.* 1986 and references therein). The estimated depth of emplacement is ~18 km based on new Al-in-hornblende data (Brock and Gibson, unpublished data) using the calibration method of Mutch *et al.* (2016). The Songo pluton previously yielded a U–Pb zircon age of 382 ± 3 Ma (Lux and Aleinikoff 1985); however, a younger age of 360.7 ± 2.2 Ma was reported by Eusden *et al.* (2020). It is intruded by numerous two-mica leucocratic granite and pegmatite bodies, which range in age from Carboniferous to Permian (Solar and Tomascak 2016). These bodies have played an important role in the development of petrographic variants within the Songo pluton (Gibson *et al.* 1989). Typically, the Songo pluton consists of equigranular, coarse-grained biotite + hornblende + titanite granodiorite to granite with some quartz diorite and is undeformed. However, more proximal to the granite/pegmatite intrusions the granite displays a well-defined fabric, which can be intensely developed to gneissic at its extreme. In addition, hornblende is absent and the biotite has the red-brown pleochroism indicative of high Ti content common in metamorphic varieties (Deer *et al.* 1966). This variation could be related to the forceful emplacement of the younger Carboniferous–Permian leucogranite and pegmatite or perhaps the deformed rocks are vestiges of an older pluton. Recent remapping of the Bethel (Eusden *et al.* 2020) and Waterford quadrangles (C. Koteas, personal communication 2020) have further highlighted the variable petrography evident in the Songo pluton.

Dated sample SG-7b was collected from the northeastern lobe of non-foliated Songo pluton granodiorite. It is an equigranular, medium-grained biotite + hornblende + titanite granodiorite with a CI of ~25 (Figs. 5e, f). Biotite

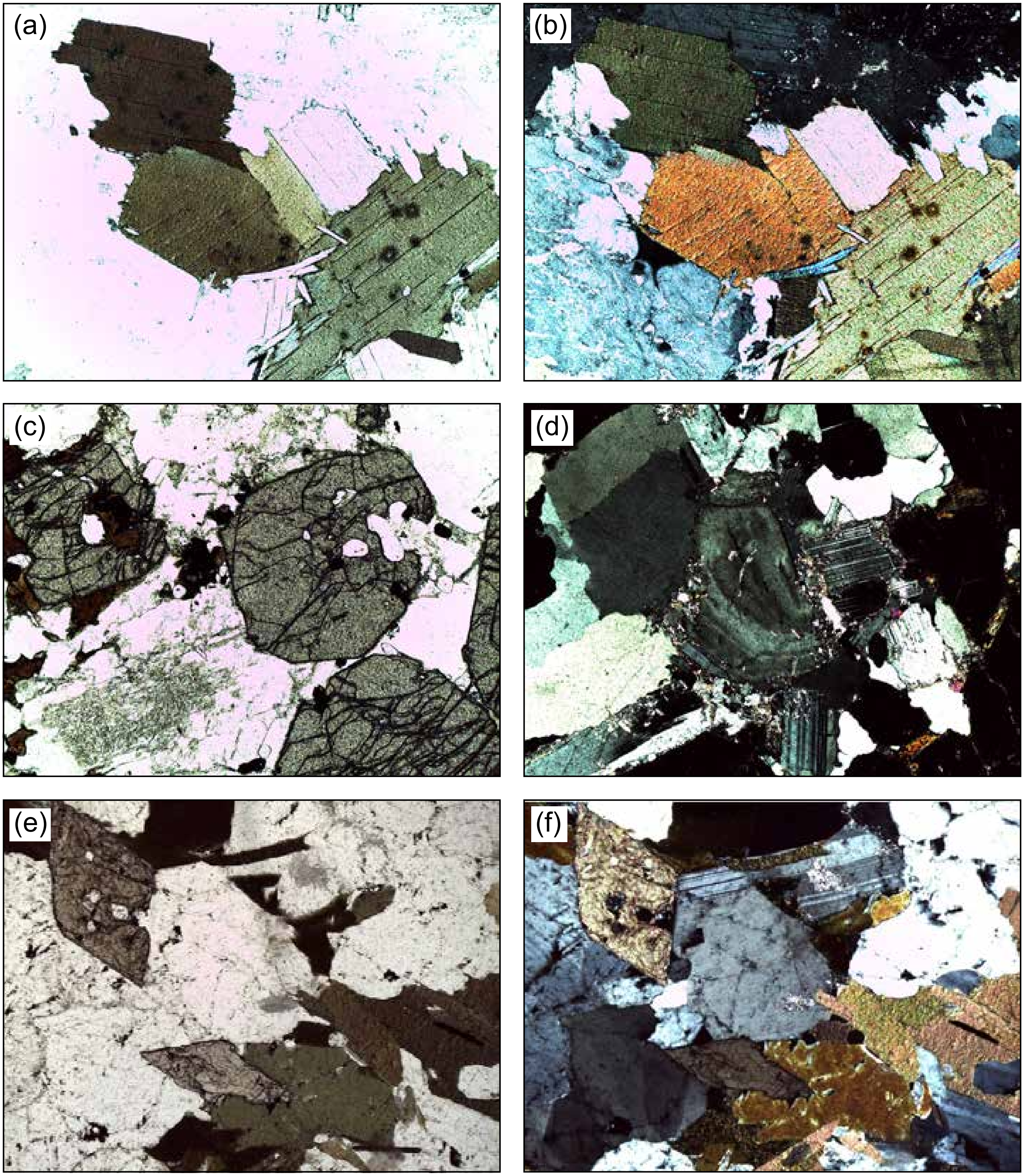

Figure 5. Photomicrographs from the FLIC and Songo pluton. (a) Biotite granite FLC-2, with biotite containing numerous zircon inclusions; primary muscovite grains are also present. (b) Same view with crossed polars. (c) Garnet tonalite (FLC-5) with euhedral garnet grains and alteration of higher Ca core of plagioclase in plane polarized light. (d) Same sample displaying zoned plagioclase grain with garnet grains (crossed polars). (e) Euhedral titanite along with biotite and hornblende in granodiorite from the Songo pluton (sample SG 7b). (f) Same view with crossed polars. Field of view for all photomicrographs is 3.5 mm.

occurs as euhedral grains up to 2.5 mm in diameter and is more abundant than hornblende. It displays pale brown to greenish-brown pleochroism and has minor chloritic alteration along cleavage planes. Minor hornblende occurs as subhedral grains with light to dark green pleochroism. Plagioclase is more abundant than K-feldspar and occurs as ~4 mm subhedral grains, some of which display compositional zoning. K-feldspar forms interstitial subhedral grains up to 4 mm across. Quartz is typically in clusters, with individual grains not exceeding 2 mm across and displays normal extinction. Accessory phases include euhedral titantite grains up to 2.5 mm in length and a lesser amount of zircon forming inclusions in biotite.

West-central Maine plutons

A group of four peraluminous two-mica plutons outcrop in west-central Maine, from west to east the North Jay, Chesterville, Cape Cod Hill, and Rome-Norridgewock plutons (Fig. 3), following the nomenclature proposed in Gibson *et al.* (2006). They intruded an older Silurian metasedimentary succession in a different crustal block than the plutons described above and previously dated plutons (Table 1). They are separated from these plutons by a major structural boundary, the Winter Brook fault, which was interpreted by Moench and Pankiwskyj (1988) "as a west-verging older-over-younger thrust". The Rome-Norridgewock pluton has an overall ovoid outcrop pattern and is exposed over an area of 260 km^2, whereas the North Jay (40 km^2), Chesterville (85 km^2), and Cape Cod Hill (50 km^2) plutons have more irregular outlines but still truncate the regional NE-SW orogen trend. The Chesterville pluton is poorly exposed and intensely weathered and was therefore not sampled for the present study. However, it appears to be petrographically similar to both the North Jay and Cape Cod Hill granites.

North Jay pluton

The North Jay pluton consists of light grey, medium-grained, equigranular muscovite - biotite granite with minor amounts of garnet. It is intruded by several metre-sized pegmatite dikes along with aplitic segregations, which also contain garnet and minor beryl. Abundant metasedimentary xenoliths, that range from large blocks (10–20 cm) to small, thin slivers or surmicaeous enclaves, are also observed. They are obviously of metamorphic origin with garnet and biotite in schistose fabric. Small (1–2 cm) clots of biotite and garnet may represent further disaggregation of the xenoliths. These garnets are euhedral (Fig. 6a) and electron microprobe data reveal that they are chemically zoned in Ca, Mg, Mn, and Y contents (Gibson *et al.* 2006). However, another population of subhedral to anhedral garnet (Fig. 6b), which lacks chemical zoning, is also present. Although the majority of garnet in the North Jay granite is most likely xenocrystic due to the abundance of metamorphic xenoliths, some is magmatic in origin (Gibson *et al.* 2006).

Dated sample NJq-1 was collected from the North Jay granite quarry and is fine- to medium-grained, equigranular two-mica leucocratic granite with a CI ~12. Biotite is slightly more abundant that muscovite. It has pale brown to deeper red-brown pleochoism with numerous zircon inclusions. Muscovite is of primary origin with some large euhedral grains present. Quartz occurs as anhedral grains in clusters and displays evidence of deformation with undulatory extinction and serrated margins. Plagioclase forms subhedral grains up to 2.5 mm in length and some have concentric zoning. K-feldspar (microcline) is common, both as discrete and interstitial grains. Zircon is the dominant accessory mineral but acicular opaque minerals and some garnet grains are also present.

Cape Cod Hill pluton

The Cape Cod Hill (CCH) pluton forms the elevated topography to the south of Farmington and is mapped as a roughly oval body that cuts across the regional NE–SW trend (Fig. 3). It is composed of a medium-grained, white, equigranular granite with minor garnet. It has a similar range of xenoliths as the North Jay pluton and petrographically the two are similar. However, viewed in thin section the CCH granite displays more pronounced deformation features.

Dated sample CCH-1 was collected from the Cape Cod Hill quarry and is an equigranular, medium-grained two-mica leucocratic granite with a CI of 5. Biotite is sparse and occurs as sub- to anhedral grains < 1 mm in size with pale brown to deeper red-brown pleochroism. Zircon inclusions are common and many grains display warped cleavage planes indicating some post-crystallization deformation. Muscovite is more abundant than biotite with larger euhedral grains up to 2.5 mm. Like the biotite grains, muscovite grains show warped and disjointed cleavage planes (Figs. 6c, d). Quartz occurs as 2 to 2.5 mm grains that show undulatory and sectorial extinction and many with irregular serrated margins. Plagioclase commonly contains numerous muscovite inclusions and generally lacks zoning. Plagioclase grains vary in size but some are ~3 mm in length and twin planes are warped and broken. Microcline is also present most commonly in anhedral, interstitial grains. Zircon is the most common accessory mineral.

Rome-Norridgewock pluton

The Rome-Norridgewock (R-N) pluton is the largest pluton of the west-central Maine group covering an area of 260 km^2 and is mapped as a homogeneous granitic intrusion on the bedrock map of Maine (Osberg *et al.* 1985). However, sampling for an $^{40}Ar/^{39}Ar$ cooling history study (Gibson *et al.* 2006) revealed a petrographically different unit in the northeastern part of the pluton south of the town of Norridgewock. The main unit of the pluton is light grey, medium- to coarse-grained equigranular granite with both biotite and muscovite. This rock type forms most of the pluton

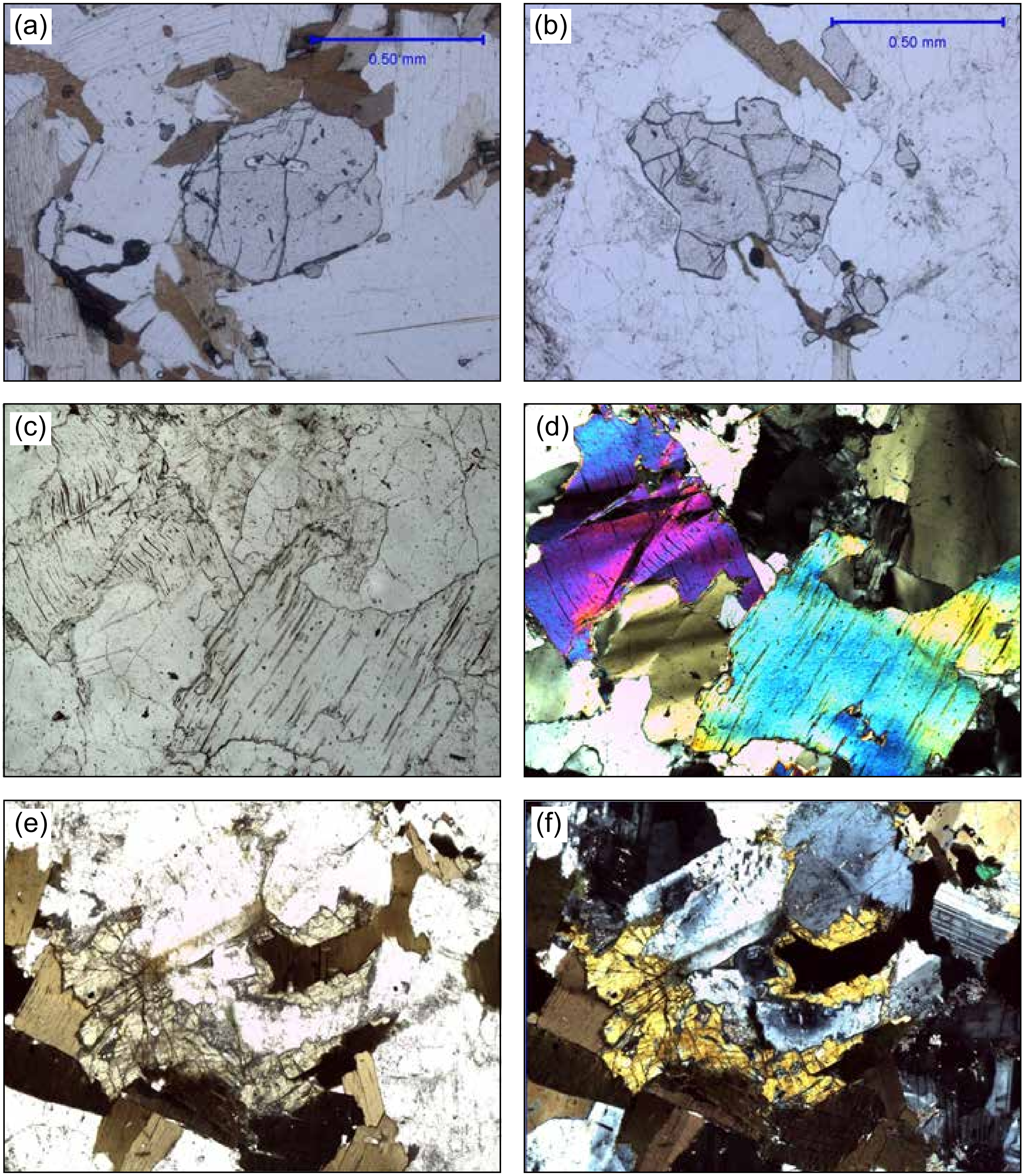

Figure 6. Photomicrographs of the North Jay and CCH granites, and the Norridgewock unit of the R-N pluton. (a) Euhedral garnet grain in a small xenocystic knot of garnet and biotite, North Jay granite. (b) Anhedral garnet in North Jay granite. Scale is shown on the photomicrographs and both are in plane polarized light. (c) and (d) Deformed cleavage planes in muscovite in the CCH granite along with undulatory and sectorial extinction in quartz grains. (e) and (f) Biotite and hornblende in the granodiorite of the Norridgewock unit of the R-N pluton. Possible epidote is also present. Field of view is 3.5 mm.

and closely resembles the CCH and North Jay granites; hence we refer to it as the Rome unit of the R-N pluton in this paper. The only previous age determination on any of the plutons in west-central Maine was from this unit and yielded a U–Pb zircon age of 378 ± 1 Ma (Tucker *et al.* 2001).

The petrographic variant exposed in more northerly outcrops of the R-N pluton is medium-grained, equigranular, biotite ± hornblende + titanite granite/granodiorite, and hence of I-type mineralogic affinity (Chappell and White 2001) in contrast to the two-mica Rome unit described above. This unit is referred to as the Norridgewock unit. No contact relationships were observed, so it is unclear if the Norridgewock unit is a comagmatic part of the R-N pluton or if it should be considered a separate intrusion.

Dated sample DHq-1 was collected from the Dodling Hill quarry which is located in the Norridgewock unit of the R-N pluton. It is equigranular, medium-grained biotite + horn-blende + titanite granite/granodiorite with a CI of ~15 (Figs. 6e, f). Biotite is the dominant mafic mineral and occurs as larger euhedral flakes with pale brown to greenish brown pleochroism. Hornblende forms small subhedral to anhedral grains, typically in mafic knots with biotite. Plagioclase occurs as larger grains, up to 4 mm, that are euhedral to subhedral. Some grains display concentric compositional zoning. K-feldspar forms smaller subhedral crystals. Quartz occurs in glomerocrysts approximately 3 mm in size, some of which display undulatory and sectorial extinction. Zircon and titanite are the dominant accessory phases with minor opaque minerals and allanite also present.

ANALYTICAL METHODS

The samples for this study were sent to Overburden Drilling Management (ODM) in Ottawa, Ontario, for electro-pulse disaggregation and initial zircon separation. Zircon grains for dating were then picked from the zircon concentrates at Cape Breton University in Sydney, Nova Scotia. Selected grains were mounted in an epoxy-covered thin section at the University of New Brunswick, Fredericton, polished to expose the centres of the zircon grains and imaged using cold cathodoluminescence to iden-tify internal zoning and inclusions (Appendix A: Figs. A1 and A2). These images were used to select ablation points (30 μm diameter), avoiding visible inclusions, cracks, or other imperfections.

U and Pb isotopic compositions were measured using the Resonetics S-155-LR 193 nm Excimer laser ablation system connected to an Agilent 7700x quadrupole inductively coupled plasma – mass spectrometer in the Department of Earth Sciences at the University of New Brunswick, following the procedure outlined by McFarlane and Luo (2012) and Archibald *et al.* (2013). Data reduction was done in-house using Iolite software (Paton *et al.* 2011) to process the laser output into data files, and further reduced for U–Pb geochronology using VizualAge (Petrus and Kamber 2012). VizualAge outputs included uncorrected U–Pb ratios that were used to calculate ^{204}Pb-based corrections (Andersen 2002) and ^{208}Pb-based corrections. Data were filtered using ^{204}Pb as a monitor. For grains with <80 counts/s ^{204}Pb, data are uncorrected; for grains where the percentage error on the ^{204}Pb counts per second was <20%, we used a ^{204}Pb-based correction (Andersen 2002), and for grains where the percentage of radiogenic Pb (Pb* in file) is less than 98.5% we used a ^{208}Pb-based correction (Petrus and Kamber 2012). After these corrections were applied, data were sorted by concordance (^{206}Pb/^{238}U versus ^{207}Pb/^{235}U), and by the percentage of radiogenic Pb in the grains as calculated using VizualAge. All analytical data are presented in Appendix B, Table B1, with analyses used in concordia calculations highlighted. All data from reference material FC-1 and Plešovice are presented in Appendix B, Table B2.

Concordia ages were calculated for clusters of three or more near-concordant points using Isoplot versions 3.75 and 4.15 (Ludwig 2003, 2012). All ages are reported at 95% confidence, with decay-constant errors included in the calculations. Data points included in the concordia calculations and reported here are grains that are 98% to 101% concordant and do not require a correction for common Pb (^{204}Pb < 80 counts per second). By using only uncorrected near-concordant grains that overlap within error we can reduce the possibility of misrepresenting the crystallization age as too young which can happen if grains experienced Pb loss (Dickinson and Gehrels 2010). The approach in this study was to calculate concordia ages using as many grains as possible, and hence the MSWD (mean square of weighted deviates) which measures the amount of scatter in the points used to calculate concordia and the reported probability of concordance could in some cases be improved by using fewer grains. In all cases the calculated concordia ages overlap with the weighted mean ages for the samples using all near-concordant data. ^{206}Pb/^{238}U ages are used in all the probability distribution calculations. Concordia ages obtained for standards during this work were presented in Barr *et al.* (2018).

RESULTS

Sample COP-1 (Chain of Ponds pluton)

Abundant zircon grains separated from sample COP-1 range in size from 20 to 150 μm. Most of the grains are clear and euhedral, with bipyramidal terminations preserved. Grains vary in shape from elongate acicular crystals to rectangular. Most grains display weak fluorescence under cathodoluminescence but oscillatory zoning is present in fluorescent grains. Figure A1 (a–d) shows representative grains (backscatter electron and cathodoluminescence for each) with indistinct zoning in their cores, and clear oscillatory zoning around the edges of the grains.

The ages obtained from this sample for grains that are between 98 and 102% concordant (84 out of 129 grains analysed) are mostly in the range between 360 Ma and 400 Ma with no obvious clusters (Fig. 7a). The age distribution is strongly skewed with an older "tail", indicating that inheritance may be a significant factor in the sample. This interpretation is supported by the presence of a few grains as old as Neoproterozoic (Table B1). The cumulative probability plot (Fig. 7b) displays two peaks, a major one ca. 365 Ma, and a secondary one ca. 385 Ma. There is no clear separation between the peaks but they remain distinct with age bins of 2.5 Ma, 5 Ma, and 10 Ma. It is possible to calculate a weighted mean age of ca. 373 Ma for all the grains that are 98–102% concordant (73 grains) but this result has a high MSWD (14) and clearly does not represent a single mean age for the sample. Similarly, it is not possible to calculate a concordia age for the grains around this age without obtaining unacceptably high MSWD values.

Based on the probability distribution we interpret this sample as having two main age components which can produce concordia ages, an older group (Fig. 7c), and a younger group (Fig. 7d). The younger group has a concordia age of 363.4 ± 1.5 Ma with an MSWD of 1.16, and a probability of concordance of 0.28. The older group has a concordia age of 385.3 ± 1.5 Ma with an MSWD of 0.054 and a probability of concordance of 0.94. Hence, we interpret this sample as having a minimum crystallization age of 363 Ma, with inherited older grains. The wide spread of the near-concordant ages and the presence of older grains in this sample shows that these plutons and the terranes into which they intrude are complex and may represent several episodes of igneous activity. This complexity is also present in other samples and will be discussed in subsequent sections.

Samples FLC-2, 5, and 6 (Flagstaff Lake Igneous Complex, FLIC)

The zircon grains from all three FLIC samples are mostly euhedral and clear with few inclusions and the majority of the grains are very small (20 to 150 μm) with only a few grains in the larger range. The smaller grains tend to be acicular in shape, and the larger grains are rectangular, with most showing some oscillatory zoning in cathodoluminescence. Samples FLC-2 and FLC-5 contained abundant zircon, whereas sample FLC-6 had less zircon. However, there are no systematic differences in zircon morphology among the samples and all the grains in all the samples vary in the extent to which zoning is visible, especially in the abundant small grains. Figure A1 (e–h) shows representative grains from FLC-2 (backscatter electron and cathodoluminescence for each) illustrating indistinct zoning (e and f) and non-oscillatory zoning in a smaller grain (g and h). Figure A1 (i–l) shows representative grains from FLC-5 (backscatter electron and cathodoluminescence for each) illustrating variable oscillatory zoning (i and j) and non-oscillatory zoning in a smaller grain (k and l). Figure A1 (m–p) shows representative grains from FLC-6 (backscatter electron and cathodoluminescence for each) illustrating non-oscillatory zoning (m and n) and variable oscillatory zoning in a larger grain (o and p). The images of the smaller grains also illustrate the difficulty in analysing these grains where it is impossible to limit the laser spot to only one zone even if imaging indicates zoning is present because the grains are so small. The ages obtained from the samples differ and hence the samples are discussed separately below.

Sample FLC-2 is the least complicated of the three FLC samples. It has a clear peak in the cumulative probability diagram using all the 98–102% concordant grains (38 out of 57 grains analysed) (Fig. 7e) and has a strong right-tailed distribution with a small secondary peak around 430 Ma, interpreted as a result of inheritance. The concordia age with 25 grains is 409.3 ± 1.6 Ma with an MSWD of 0.57, and a probability of concordance of 0.45 (Fig. 7f).

Sample FLC-5 has two peaks in the cumulative probability diagram (Fig. 8a), both of which can be seen in a weighted mean plot of the 98–102% concordant grains (25 out of 53 grains analysed). The older group (6 grains) has a concordia age of 401 ± 1 Ma with an MSWD of 1.8, and a probability of concordance of 0.18 (Fig. 8c) and the younger group (10 grains) has a concordia age of 383.8 ± 2.2 Ma with MSWD of 2.3 and a probability of concordance of 0.13 (Fig. 8d). While the statistics on these two ages are not very good, they overlap with the weighted mean ages of the two groups of grains, which are 383.2 ± 2 Ma (MSWD = 0.84, probability = 0.58) and 400.3 ± 3.4 Ma (MSWD = 0.33, probability = 0.90), respectively (Fig. 8b).

Sample FLC-6 has a single major peak in the cumulative probability diagram (Fig. 8e) of the 98–102% concordant grains (22 out of 58 grains analysed). Using the largest possible group of grains (15) for a concordia age produces an age of 399.9 ± 3.6 Ma with a high MSWD of 4.0, and low probability of concordance of 0.045. The weighted mean age of the same group of 15 grains is slightly younger at 397.5±5.3 Ma with an MSWD of 1.8 and a probability of 0.039. When only the grains in the main peak of the probability diagram are used, they produce a concordia age of 403.2 ±4.6 Ma with an MSWD of 0.72, and a probability of concordance of 0.40 (Fig. 8f). This age includes only 6 grains but given the age distribution in this sample we interpret it as the main age of crystallization. As with the other FLC samples older inherited grains are present as well, in this case ca. 410 Ma and 450 Ma. Given that sample FLC-5 also has a major group of younger grains with an age of ca. 383 Ma, it is possible that the younger grains with an apparent peak ca. 390 Ma seen in the cumulative probability diagram for FLC-6 could be part of a younger episode of crystallization. Alternatively, they could be the result of minor Pb loss.

Figure 9 shows the U/Th ratios of all the grains included in concordia or weighted mean calculations for the FLIC samples. Of the three samples from this complex FLC-2 has the oldest calculated age, and also the widest spread in U/Th ratios. FLC-5 has two main group of grains that were used to calculate the two possible ages for this sample (inheritance vs. crystallization). There is no difference between the U/Th ratios of the older and younger groups and each cluster is a tight grouping (Fig. 9). This result suggests that Pb loss is likely not a factor in generating the younger ages,

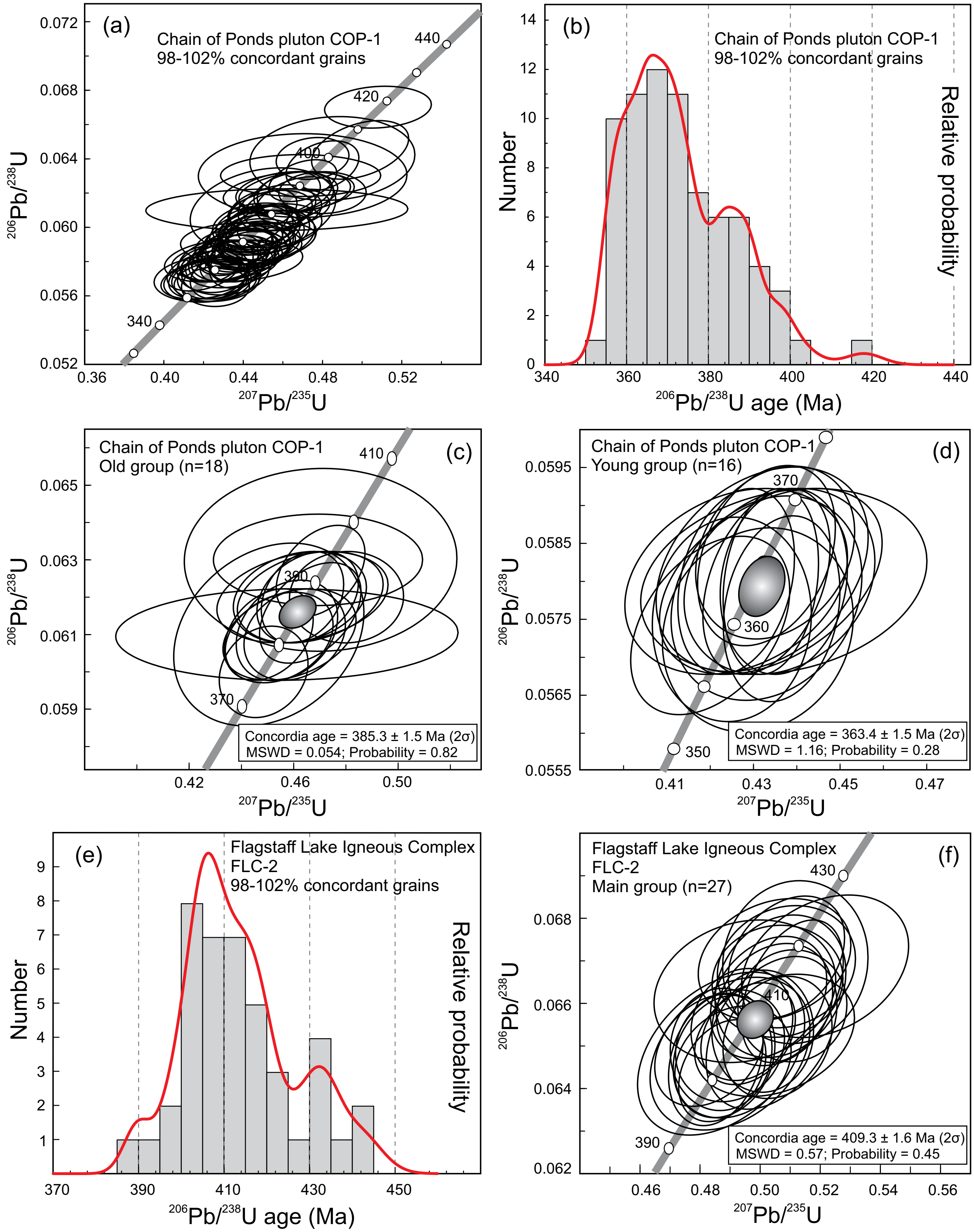

Figure 7. Concordia diagrams and relative probability plot for data for sample COP-1 from the Chain of Ponds pluton showing all the grains that are between 98 and 102% concordant (a), the same grains in a relative probability plot (b), with two concordia diagrams for the older and younger clusters of grains (c and d, respectively). (e) and (f) Concordia diagram and relative probability plot for sample FLC-2 from the Flagstaff Lake Igneous Complex.

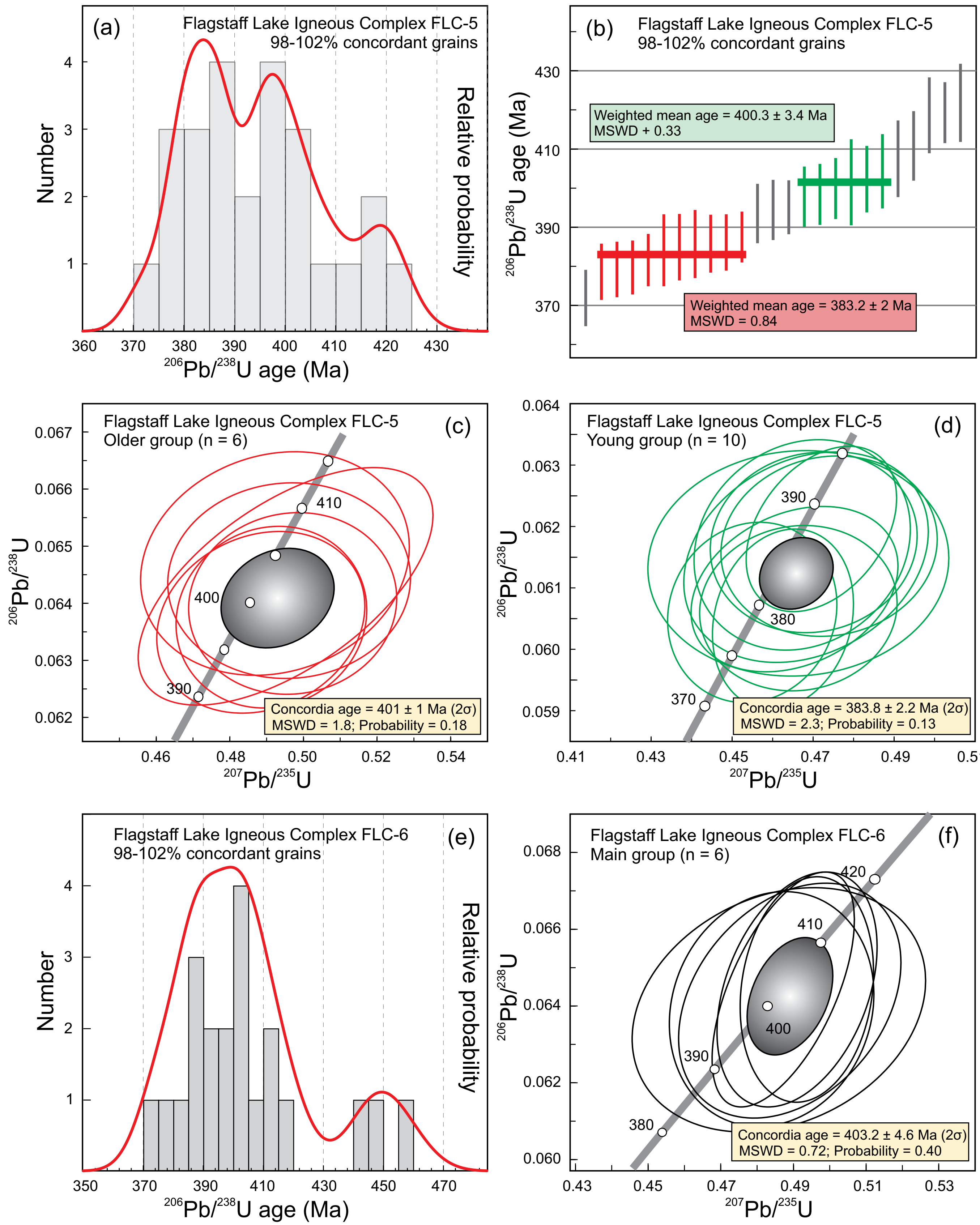

Figure 8. Data for sample FLC-5 showing a relative probability plot for all the grains between 98 and 102% concordant (a), weighted mean plot of the same grains showing two distinct clusters of grains (b), and concordia diagrams for those two groups (c and d); the relative probability plot for grains between 98 and 102% concordant (e), and concordia diagram for the main cluster of grains for sample FLC-6 (f).

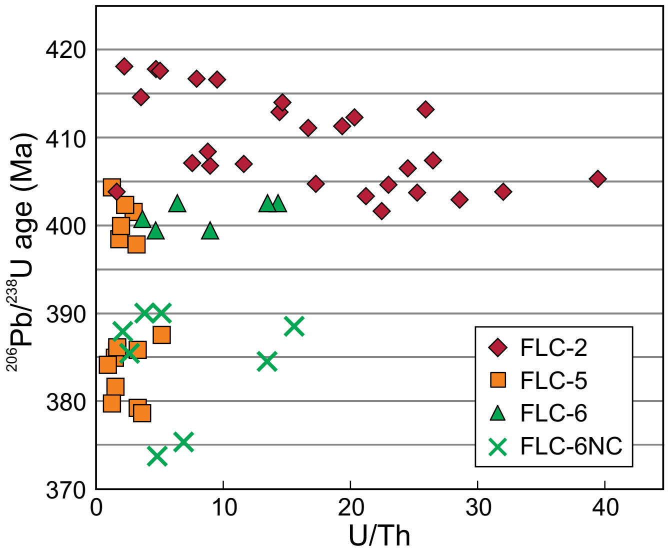

Figure 9. U/Th ratios of zircon grains used in concordia and weighted mean calculations in the FLIC samples.

supporting the interpretation that the older age represents inheritance and the younger one is the crystallization age. The older cluster also overlaps with the ratios from sample FLC-2, providing additional support for the interpretation of inheritance of zircons from the older phase of activity. For FLC-6 the main concordia age for the sample is ca. 400 Ma and those grains have U/Th ratios that again overlap with both sample FLC-2 and with the older group in FLC-5. Figure 9 also includes the U/Th ratios for the younger grains in FLC-6 that were not included in the calculated concordia age and make up the younger tail of the distribution as shown in Figure 8e. These ratios again overlap with those from all the other samples, but their U/Pb ratios obtained from analysis are not concordant enough to define a clear cluster of ages that would support the interpretation of a distinct younger phase of crystallization. This supports the interpretation that the younger grains in FLC-6 are simply part of the normal distribution of data around the most likely crystallization age.

Taken together, the three samples from the Flagstaff Lake Igneous Complex indicate that the complex is a composite pluton containing a large range of inherited ages, and variations in youngest crystallization phases of different segments of the pluton. A major older episode of crystallization at ca. 409 Ma is recorded in sample FLC-2, the major phase for FLC-6 is likely ca. 403 Ma, and sample FLC-5 has a big group of inherited ages ca. 401 Ma, likely derived from the older intrusive units, and a younger episode of crystallization at ca. 383 Ma.

Sample RUM-1 (Rumford pluton)

Zircon grains from sample RUM-1 are very small (most under 40 μm) and many were too small to analyse so the total number of data points for this sample is lower than most others. The grains are acicular and most are subhedral to anhedral with reddish-brown surface staining. Under cathodoluminescence most grains showed only weak fluorescence and only some grains showed oscillatory zoning. Figure A2 (a–d) shows representative grains from RUM-1 (backscatter electron and cathodoluminescence for each) illustrating clear oscillatory zoning (a and b) and indistinct oscillatory zoning in a more elongate grain (c and d).

Only 7 of 12 grains analysed are between 98 and 102% concordant, but they display a clear peak in the cumulative probability distribution (Fig. 10a). The four grains with ages that overlap within error produce a concordia age of 373.2 ± 2.3 Ma with a MSWD of 0.34 and a probability of concordance of 0.56 (Fig. 10b) interpreted as the main age of crystallization in this sample. Additional concordant grains at ca. 490 Ma are interpreted as inherited.

Sample SG-7b (Songo pluton)

Zircon grains in sample SG-7b are mostly euhedral with bipyramidal terminations intact. They are clear and colourless with few visible inclusions and no surface staining. The grains show clear oscillatory zoning under cathodoluminescence. Figure A2 (e–j) shows representative grains from SG-7B (backscatter electron and cathodoluminescence for each) illustrating clear oscillatory zoning seen in grains from this sample.

The data for this sample display a major peak in the cumulative probability diagram for the 98–102 % concordant grains (36 out of 51 grains analysed) (Fig. 10c), and a strong right-tailed distribution, with two minor peaks ca. 375 Ma and 385 Ma that can be interpreted as inherited grains. The concordia age of the major peak using 17 grains is 364.0 ± 1.3 Ma with MSWD of 0.83, with a probability of concordance of 0.36 (Fig. 10d).

Sample NJq-1 (North Jay pluton)

Zircon grains in sample NJq-1 are very small (most less than 40 μm) and generally acicular and euhedral. Most are clear with few visible inclusions but have brown surface staining. Most of the grains show weak oscillatory zoning under cathodoluminescence. Although the sample contained abundant zircon, most grains are too small to analyse so the total number of data points for this sample is lower than most others. Figure A2 (k–p) shows representative grains from NJq-1 (backscatter electron and cathodoluminescence for each) illustrating that some grains have distinct cores (k–l), some grains have indistinct zoning in cores (m and n), and some have partial oscillatory zoning (o and p), illustrating the variability of zoning observed in this sample. Only 10 out of 25 grains analysed are between 98 and 102% concordant and give a clear peak in the cumulative probability distribution (Fig. 10e). Four grains with ages that overlap within error produce a concordia age of 369.6 ± 3.0 Ma with MSWD of 0.93 and a probability of concordance of 0.34 (Fig. 10f), interpreted as the main age of crystallization

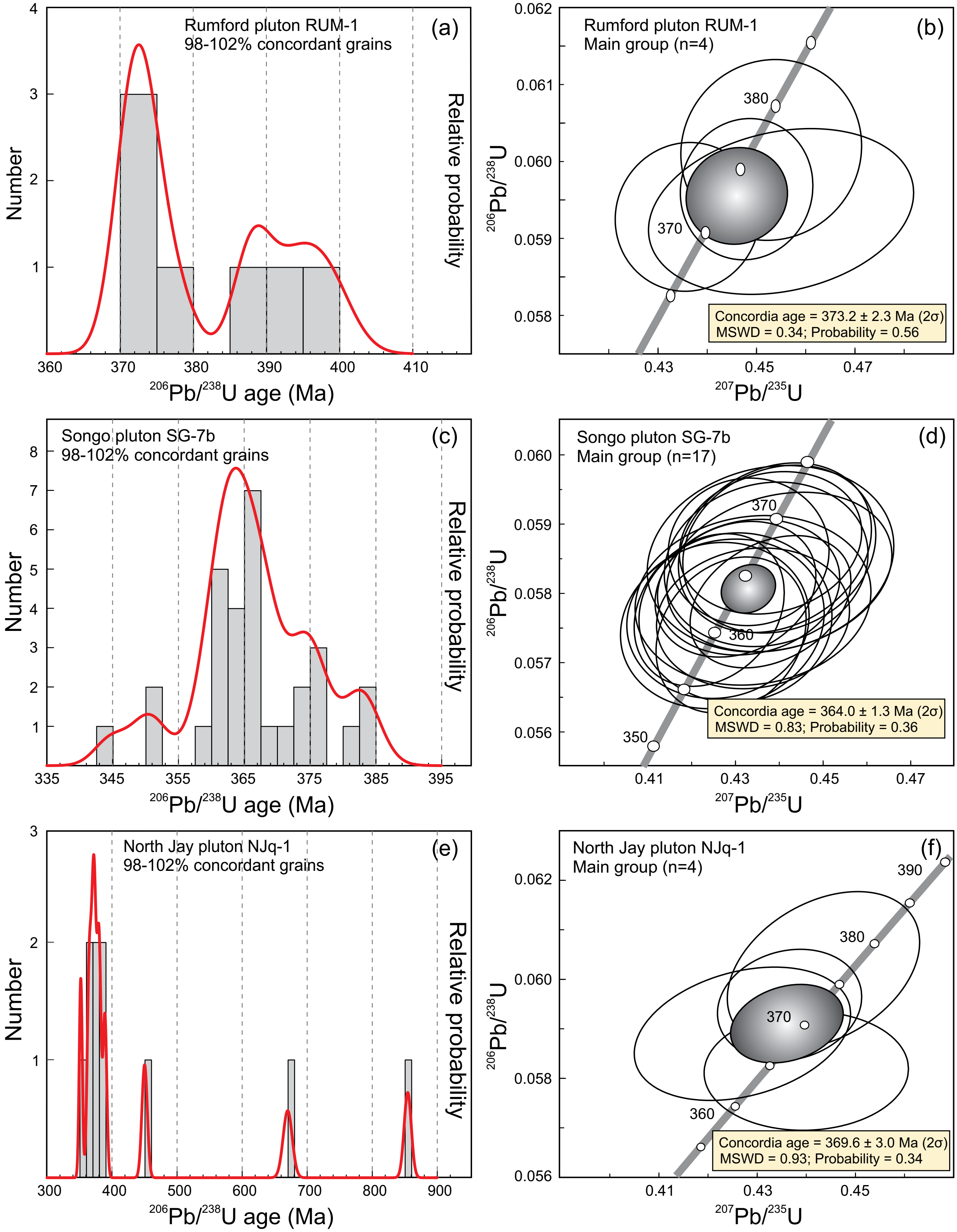

Figure 10. Relative probability plots for all grains between 98 and 102% concordant and concordia diagrams for the main clusters of grains for samples from the Rumford pluton RUM-1 (a and b), the Songo pluton SG-7b (c and d) and the North Jay pluton NJq-1 (e and f).

in this sample. Additional concordant grains at ca. 450 Ma, 670 Ma, and 850 Ma are interpreted as inherited.

Sample CCH-1 (Cape Cod Hill pluton)

Zircon grains in sample CCH-1 are generally acicular and subhedral, with a few euhedral grains. Sizes are varied and range from 20 to 150 µm. Some grains are clear but most have visible inclusions and reddish-brown surface staining. They show very low fluorescence under cathodoluminescence and some of the larger grains show indistinct oscillatory zoning.

The cumulative probability distribution of the 98–102% concordant grains for this sample (39 out of 50 grains analysed) shows three distinct peaks (Fig. 11a). Although no clear separations between them is apparent in the probability distribution, it is possible to resolve three separate concordia ages for different groups of grains (Fig. 11b). These groups of grains do not overlap, and neither the concordia ages nor the weighted mean ages overlap within error (Fig. 11c). The youngest group has a weighted mean age of 370.1 ±1.3 Ma with an MSWD of 1.15, the middle group has a weighted mean age of 383.0 ± 2.3 Ma and an MSWD of 2.1, and the oldest group has a weighted mean age of 396.8 ± 2.5 Ma with an MSWD of 0.118.

Sample DHq-1 (Rome-Norridgewock pluton)

Zircon grains in sample DHq-1 vary from acicular and subhedral, with a few euhedral grains, to subhedral rectangular shapes. Sizes are varied and range from 20 to 150 µm. Some grains are clear but most have visible inclusions and reddish-brown surface staining. The grains in this sample show very low fluorescence under cathodoluminescence and only some of the larger grains show indistinct oscillatory zoning.

The cumulative probability distribution of the 98–102% concordant grains for this sample (42 out of 62 grains analysed) shows three distinct peaks (Fig. 11d). Although no clear separations are apparent between them in the probability distribution, it is possible to resolve three separate concordia ages for different groups of grains (Fig. 11e). These groups of grains do not overlap, and neither the concordia ages nor the weighted mean ages overlap within error. The youngest group (18 grains) has a concordia age of 366.2 ± 1.2 Ma with an MSWD of 4.6 and a probability of concordance of 0.031. Since the statistics on this age are not good we prefer to use the weighted mean age for the same group of grains at 365.9±1.5 with an MSWD of 1.4 (Fig. 11f). The middle group has a concordia age of 377.3 ± 1.3 Ma with an MSWD of 1.3 and a probability of concordance of 0.25 (weighted mean age of 376.9 ± 1.4 Ma with an MSWD of 0.96). The oldest group has a concordia age of 388.0 ± 2.1 Ma with an MSWD of 0.54 and a probability of concordance of 0.46 (weighted mean age of 387.8 ± 2.2 Ma with an MSWD of 0.86).

DISCUSSION

Magmas produced during collisional tectonic events can be generally assigned to what could be considered as three distinct "end-member" compositions each with a mineralogical/chemical fingerprint of its source: (i) magmas produced by melting of meta- and/or sedimentary upper crustal rocks, which yield peraluminous magmas that crystallize to S-type mineralogies; (ii) deeper level melting of lower crust of igneous/intermediate composition produc-ing I-type mineralogies in the crystallized granitic rocks, and (iii) mafic magmas derived from partial melting of the mantle beneath such subduction/collisional regimes (Pearce 1996; Harris *et al.* 1986). The latter may serve a dual role in that they may be emplaced as mafic bodies but can also provide the thermal input responsible for the formation of the other two magma types. However, it would be unlikely that pure end-member compositions of these three magma types would be totally preserved during their subsequent crystallization, ascent, and emplacement during the dynamic kinematics of a collisional plate tectonic event. For example, transitional variations are likely with contamination of both S-and I-type magmas. Indeed, more evolved fractionation of the latter could result in some primary muscovite in these rocks, thus resembling less evolved S-type granites. Mantle-derived melts could evolve to more basaltic andesite or andesitic (dioritic) compositions.

The concentration of Devonian, broadly Acadian, plutons from northwestern Maine, as described in this paper, is characterized by a petrographically diverse suite of granitoid rocks. They can be assigned to three groups: (i) those that display a typical I-type mineral assemblage of biotite + hornblende + titanite, such as the COP and Songo plutons (Figs. 5e and f) , the Norridgewock unit of the R-N pluton, and the North Lexington pluton; (ii) those plutons that have peraluminous S-type mineralogy with biotite + muscovite together with microcline and apatite, exemplified by the North Jay pluton (Figs. 6a and b), Cape Cod Hill pluton (Figs. 6c and d), and the Rome unit of the R-N pluton; and (iii) a group of biotite granite plutons which contain primary

Figure 11. (next page) Data for sample CCH-1 from the Cape Cod Hill pluton showing the relative probability plot for all the grains between 98 and 102% concordant (a), the concordia diagram for the same grains showing three main clusters of grains (b), and a plot showing the weighted means of the same three clusters (c). Figures d, e, and f show data for sample DHq-1 from Norridgewock unit of the Rome-Norridgewock pluton with the probability plot for all the grains between 98 and 102% concordant (d), the concordia diagram for the same grains showing three main clusters of grains (e) and a plot showing the weighted means of the same three clusters (f).

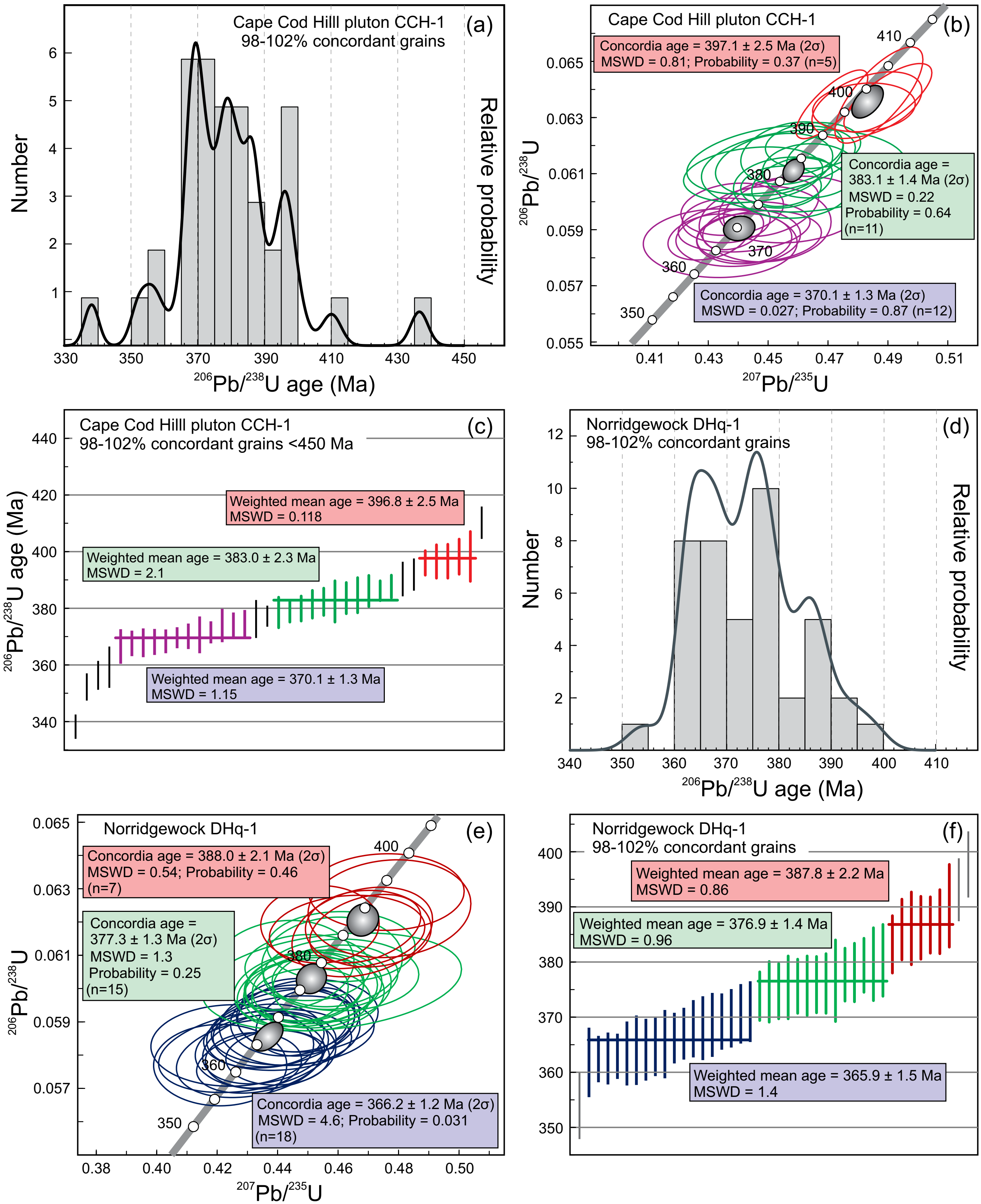
Cape Cod Hilll pluton CCH-1
98-102% concordant grains
(a)
Number
Relative probability
206Pb/238U age (Ma)
Cape Cod Hill pluton CCH-1
(b)
Concordia age = 397.1 ± 2.5 Ma (2σ)
MSWD = 0.81; Probability = 0.37 (n=5)
Concordia age =
383.1 ± 1.4 Ma (2σ)
MSWD = 0.22
Probability = 0.64
(n=11)
Concordia age = 370.1 ± 1.3 Ma (2σ)
MSWD = 0.027; Probability = 0.87 (n=12)
206Pb/238U
207Pb/235U
Cape Cod Hilll pluton CCH-1
98-102% concordant grains <450 Ma
(c)
Weighted mean age = 396.8 ± 2.5 Ma
MSWD = 0.118
Weighted mean age = 383.0 ± 2.3 Ma
MSWD = 2.1
Weighted mean age = 370.1 ± 1.3 Ma
MSWD = 1.15
206Pb/238U age (Ma)
Norridgewock DHq-1
98-102% concordant grains
(d)
Number
Relative probability
206Pb/238U age (Ma)
Norridgewock DHq-1
(e)
Concordia age = 388.0 ± 2.1 Ma (2σ)
MSWD = 0.54; Probability = 0.46
(n=7)
Concordia age =
377.3 ± 1.3 Ma (2σ)
MSWD = 1.3
Probability = 0.25
(n=15)
Concordia age = 366.2 ± 1.2 Ma (2σ)
MSWD = 4.6; Probability = 0.031
(n=18)
206Pb/238U
207Pb/235U
Norridgewock DHq-1
98-102% concordant grains
(f)
Weighted mean age = 387.8 ± 2.2 Ma
MSWD = 0.86
Weighted mean age = 376.9 ± 1.4 Ma
MSWD = 0.96
Weighted mean age = 365.9 ± 1.5 Ma
MSWD = 1.4

muscovite and high Ti biotite, examples being the Reddington pluton, granitic rocks of the FLIC (Figs. 5a and b), leucogranite of the MIC and most likely the felsic rocks of the Rumford pluton. These plutons are distinct from the S-type granitoids as (i) muscovite is much less abundant,(ii) commonly they are associated with mafic material (ei-ther as contemporaneous magmas such as the northeastern unit of the FLIC or as mafic enclaves), and (iii) metased-imentary xenoliths are rare. They could be considered as "modified" or more evolved I-types comparable to biotite granite of the Main Range of the Malaysia peninsula which has transitional I-S characteristics (Ghani *et al.* 2013).

No pattern in spatial distribution of plutons of each group is apparent in the study area. Although there is a concentration of S-type plutons in west-central Maine south of Farmington (Fig. 3), other two-mica granites, such as the Lexington pluton and units in the MIC further to the north and west, intruded Devonian strata. The west-central Maine plutons intruded Silurian strata and display the most distinct deformational textures at the microscopic scale. The I-type plutons outcrop across the entire area from the COP pluton to the north to the Songo pluton some 150 km to the south and were emplaced at various crustal levels as described above and detailed in Guidotti *et al.* (1986).

Our new ages (Table 2) in conjunction with published ages for other plutons of the area, show that magmatism began in northwestern Maine at ca. 410 Ma and continued to ca. 365 Ma, and hence was a protracted magmatic event(s) of approximately 45 Ma duration, during which compositionally variable magmas were produced. The overall distribution of pluton ages suggests that magmatism was not continuous over this time period but instead that there were breaks or lulls in magma production, for example between 400 Ma and 390 Ma and perhaps as late as 385 Ma (Fig. 12). Whether these breaks are actual or the result of incomplete sampling of plutons in those age intervals is uncertain. However, Miles *et al.* (2016) reported a similar magmatic hiatus for the Caledonian granites of Britain and Ireland during subduction of the Iapetus Ocean. Possible explanations they discussed include shallow angle subduction or the extensive erosion and removal of the arc.

In addition, ages for components in individual intrusions are also variable and point to protracted magmatism at the intra-pluton scale, which is consistent with research on pluton assembly (e.g., Glazner *et al.* 2004). Ages for the MIC, the Lexington and North Lexington plutons and the Rome-Norridgewock pluton suggest that they were emplaced in temporally distinct magma batches, some of which were separated by 10 to 15 myr. Even the Songo and COP plutons, which yield younger ca. 365 Ma crystallization

Table 2. Summary of new LA-ICP-MS age data for the Chain of Ponds pluton, Flagstaff Lake Igneous Complex, Rumford, Songo, North Jay, and Cape Cod Hill plutons and the Norridgewock unit (DHq-1) of the Rome-Norridgewock pluton. Ages are given as concordia and weighted mean ages (italics). Ages in bold are considered the crystallization ages.

Sample	Location	Overall distribution	Concordia / weighted mean ages(s) (younger)	(middle)	(older)	Comments
COP-1	45° 22′52.90″ N 70° 48′05.89″ W	Strongly skewed with older "tail".	**363.4 ± 1.5 Ma**		385.3 ± 1.5 Ma	Crystallization age of 363.4 ± 1.5 Ma with older inherited grains at 384 Ma.
FLC-2	45° 08′06.63″ N 70° 27′09.07″ W	Clear single peak with right tailed distribution.		**409.3 ± 1.6 Ma**		Crystallization age of 409.3 ± 1.6 Ma.
FLC-5	45° 00′01.33″ N 70° 39′35.85″ W	Two peaked distribution.	**383.8 ± 2.2 Ma** *383.2 ± 2 Ma*		401 ± 1 Ma *400.3 ± 3.4 Ma*	Crystallization age of 383.8 ± 2.2 Ma with older inherited grains at 401 Ma.
FLC-6	45° 12′34.08″ N 70° 14′06.46″ W	Single major peak.		**403.2 ± 4.6 Ma**		Main age of crystallization is 403.2 ± 4.6 Ma with older inherited grains.
RUM-1	44° 32′43.55″ N 70° 32′34.07″ W	Clear single peak.		**373.2 ± 2.3 Ma**		Crystallization age of 373.2 ± 3.0 Ma.
SG-7b	44° 23′06.71″ N 70° 38′25.69″ W	Clear major peak with right tailed distribution.		**364.0 ± 1.3 Ma**		Crystallization age of 364.0 ± 1.3 Ma with older inherited grains at 375 and 385 Ma.
NJq-1	44° 32′40.20″ N 70° 13′39.37″ W	Clear single peak.		**369.6 ± 3.0 Ma.**		Crystallization age of 369.6 ± 3.0 Ma, with older inherited grains of 450 Ma, 670 Ma and 850 Ma.
CCH-1	44° 37′02.82″ N 70° 00′47.04″ W	Distribution shows three distinct peaks.	**370.1 ± 1.3 Ma** *370.1 ± 1.3 Ma*	383.1 ± 1.4 Ma *383.0 ± 2.3 Ma*	397.1 ± 2.5 Ma *396.8 ± 2.5 Ma*	Crystallization age of 370.1 ± 1.3 Ma with older inherited grains at 383 and 397 Ma.
DHq-1	44° 40′37.59″ N 69° 47′39.97″ W	Distribution shows three distinct peaks.	366.2 ± 1.2 Ma ***365.9 ± 1.5 Ma***	377.3 ± 1.3 Ma *370.9 ± 1.4 Ma*	388.0 ± 2.1 Ma *387.8 ± 2.2 Ma*	Crystallization age of 365.9 ± 1.5 Ma with older inherited grains at 377 and 388 Ma.

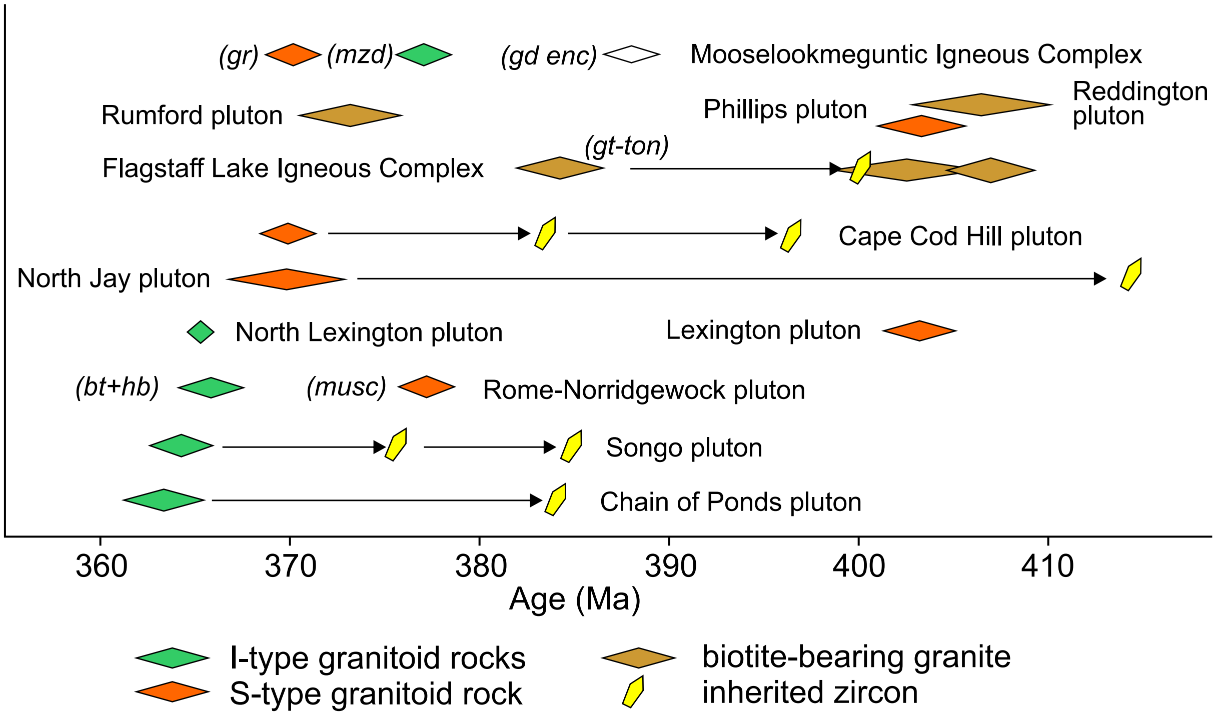

Figure 12. Diagram summarizing age and compositional characteristics of plutons from northwestern Maine. Ages are from this study and previous work (Table 1). Length of each symbol reflects error on the age. Ages of inherited zircons from several plutons are also depicted. Abbreviations for the Mooselookmeguntic Igneous Complex: granodiorite enclave (*gd enc*), monzodiorite unit (*mzd*), granite unit (*gr*); Flagstaff Lake Igneous Complex: garnet-bearing tonalite (*gt-ton*); biotite (*bt*), hornblende (*hb*), and muscovite (*musc*)

ages, have evidence through inherited grains of older precursors (Fig. 12) which cluster around 385 Ma.

It has been proposed by Bradley *et al.* (2000) and Bradley and Tucker (2002) that the migrating front of deformation associated with Acadian shortening was located in northern Maine during the Early Emsian (408–406 Ma) but only the FLIC was geographically and temporally close to this front with its ca. 405 Ma age. The FLIC is also the only intrusion in northwestern Maine to contain significant amounts of mafic rocks (Fig. 4c and d). The majority of Devonian plutons in this area were emplaced later, stitching together the already assembled continental crust.

The new LA-ICP-MS ages presented here, in combination with previously published data, enable an evaluation of sys-tematic variations in the timing of magmatic activity and the nature of magmas generated across northwestern Maine (Fig. 12). The I-type granites in the COP and Songo plutons yield some of the youngest ages in the area at ca. 365 Ma (Fig. 12). However, the presence of ca. 385 Ma inherited grains in these plutons suggest that they were assembled over a lon-ger timeframe, or sampled ca. 385 Ma rocks in their source area(s) or during magma ascent. Indeed, Lux and Aleinikoff (1985) originally suggested an age of ca. 385 Ma for the Son-go pluton. The I-type granodiorite of the North Lexington pluton also yields an age of ca. 365 Ma, as does the I-type granodiorite of the Norridgewock unit of the R-N pluton (Fig. 12). These ages, (along with the 377 Ma age for the monzodiorite suite of the MIC (Tomascak *et al.* 2005), bracket the production of a significant volume of I-type magmas in the lower crust between 380–365 Ma in this area. However, I-type magmas were also produced some 25 myr earlier in this protracted event, as discussed below.

The S-type two-mica granites such as the North Jay and CCH plutons have ages at ca. 370 Ma which is coincident with the ages for the leucogranite suite of the MIC (Tomas-cak *et al.* 2005), the Rome unit of the R-N pluton (Tucker *et al.* 2001) and the Rumford pluton (this study). However, ages for the Lexington and Phillips plutons (ca. 404 and 403 Ma, respectively) point to an older episode of upper crustal melting.

The biotite granite of the FLIC is older than 400 Ma (Table 2, Fig. 12), and among the oldest plutons in the region. This result constrains the age of the coeval mafic rocks in the northeastern part of FLIC (Fig. 4) to ca. 405 Ma and indicates an earlier phase of lower crustal I-type melts and mantle involvement. These results are consistent with the ca. 408 and 404 Ma ages for the Reddington and Phillips plutons, respectively (Table 1), which are petrographically similar to the FLIC granites. The garnet tonalite phase of the FLIC is apparently younger than the main phase at 383.8 ± 2.2 Ma and is another example where an assumed coeval complex was probably constructed over a longer timeframe.

The age obtained for the garnet tonalite is similar to the ages obtained for inherited zircon from the COP and Songo plu-tons (Fig. 12) and suggests a cryptic pulse of magmatism at this time. The increased thermal perturbation necessary to produce the garnet tonalite as discussed previously in this paper is consistent with the occurrence of a coeval magmatic event.

Generally, many of the transitional or modified biotite granites are older than the I-type plutons *(sensu stricto)* and the generation of the latter apparently began at around 385 Ma. This range of ages implies that not only were there periods of higher heat flow at various levels of the crust but that indeed the crust remained at higher temperatures over a significant period of time. The initial production of deeper sourced I-type magmas appears to have been coincident with the formation of the garnet tonalite of the FLIC. This timing implies that mantle-generated mafic magmas were present at ca. 405 Ma as evidenced at the FLIC and that the nearby mafic/ultramafic intrusions of the area such as Sugarloaf, Bog Brook, and Pierce Pond plutons might be of similar age. Mafic magmas likely played a major role in the surge of activity around 380 and 370 Ma with extensive melting of both lower and middle- to upper crust.

Tectonic models for Ganderia during the Acadian orogeny have focused on collision and subsequent flat-slab subduction of Avalonia under Ganderia (e.g., van Staal *et al.* 2009; van Staal and Barr 2012). Continued thermal activity and pluton emplacement in Ganderia through middle and late Devonian have been linked to subsequent slab breakoff and delamination. This model is consistent with the changes documented in northwestern Maine, where a change in the thermal regime of the orogen is indicated by an increase in the role of mafic magmas, both directly, in the co-mingled rocks of the FLIC, and indirectly, melting at different crustal levels. Slab breakoff and/or delamination of the basal lower crust would have resulted in greater heat flow to shallower parts of the crust, creating the conditions for the production of I-type magmas and, not long afterward, the further melting of upper crustal levels as observed in the west-central Maine peraluminous plutons at ca. 370 Ma.

CONCLUSIONS

Northwestern Maine is host to a large number of granitoid plutons diverse in both petrography and age. The earliest magmatic phase began around 410–405 Ma with the production and crystallization of both peraluminous and metaluminous magmas, forming the Lexington and Phillips plutons, the biotite granites of the Reddington pluton and the FLIC. The coeval mafic rocks intimately associated with the latter suggest that mantle-derived magmas were not only a heat source for the production of upper crustal melts but contributed to the assembly of the crust.

A hiatus in magmatic activity occurred between 400 and 385 Ma, the cause of which is at present enigmatic. Magmatism resumed around 385 Ma with the emplacement of the garnet tonalite of the FLIC, as well as a cryptic magmatic phase evidenced by an abundance of inherited zircon ages ca. 385 Ma. This magmatism continued until the Late Devonian (ca. 360 Ma), but with a major burst at ca. 370 Ma with the emplacement of both S-type magmas (the west-central Maine plutons) and I-type magmas (the COP, Songo, and North Lexington plutons).

The initial magmatic "burst" at ca. 410–400 Ma and its resumption at around 385 Ma require greater mantle involvement both materially, as observed in the FLIC, and as a major heat source around 385 Ma with the production of the garnet tonalite and both I- and S-type magmas. Therefore, although overall this is a protracted magmatic event it seems that it also had two distinct pulses. The middle to late Devonian magmatism can be explained by underplating of the mantle by a slab breakoff mechanism resulting in pronounced heat flow into the lower and upper levels of the crust. However, it is interesting to speculate that the earlier Devonian magmatism resulted from flat-slab subduction and delamination whereas the younger episode was produced by full-fledged slab breakoff or even slab disintegration. Alternatively, both magmatic episodes could be related to separate slab breakoff events. Further testing of these models is required by comparisons of the timing of magmatism to the west in New Hampshire and northeast across central Maine and New Brunswick, in conjunction with combined geochemical and isotopic data.

ACKNOWLEDGEMENTS

We thank Brandon Boucher and Chris McFarlane for assisting D. van Rooyen with the U–Pb dating at the University of New Brunswick and for providing invaluable advice in processing and interpreting the age data. We also thank journal reviewers Michael Dorais and Chris Koteas and editor David West for their insightful comments and suggestions which greatly improved the manuscript. We thank Cameron Morrell for his assistance with draughting some of the diagrams, and Polycor Inc. and Dodlin Hill Stone for access to their quarries. This work was funded in part by a Natural Sciences and Engineering Research Council of Canada Discovery Grant to Sandra Barr.

REFERENCES

Anderson, T. 2002. Correction of common lead in U–Pb analyses that do not report ^{204}Pb. Chemical Geology, 192, pp. 59–79. https://doi.org/10.1016/S0009-2541(02)00195-X

Archibald, D.B., Barr, S.M., Murphy, J.B., White, C.E., MacHattie, T.G., Escarraga, E.A., Hamilton, M.A., and McFarlane, C.R.M. 2013. Field relationships, petrology, age, and tectonic setting of the Ordovician West Barneys River Plutonic Suite, southern Antigonish Highlands, Nova Scotia, Canada. Canadian Journal of Earth Sciences, 50, pp. 727–745. https://doi.org/10.1139/cjes-2012-0158

Barr, S. M., van Rooyen, D., and White, C.E. 2018. Granitoid plutons in peri-Gondwanan terranes of Cape Breton Island, Nova Scotia, Canada: new U–Pb (zircon) age constraints. Atlantic Geology, 54, pp. 21–44. https://doi.org/10.4138/atlgeol.2018.002

Bradley, D.C. and Tucker, R. 2002. Emsian synorogenic paleogeography of the Maine Appalachians. Journal of Geology, 110, pp. 483–492. https://doi.org/10.1086/340634

Bradley, D.C., Tucker, R.D., Lux, D.R., Harris, A.G., and McGregor, D.C. 2000. Migration of the Acadian orogen and foreland basin across the northern Appalachians of Maine and adjacent areas. U.S. Geological Survey Professional Paper 1624, 49 p. https://doi.org/10.3133/pp1624

Chappell, B.W. and White, A.J.R. 2001. Two contrasting granite types: 25 years later. Australian Journal of Earth Sciences, 48, pp. 489–499. https://doi.org/10.1046/j.1440-0952.2001.00882.x

Deer, W.A., Howie, B.A., and Zussman, J. 1966. An introduction to the rock forming minerals. Publ. Wiley, 528 p.

Dickinson, W.R. and Gehrels, G.E. 2010. Insights into North American Paleogeography and Paleotectonics from U–Pb ages of detrital zircons in Mesozoic strata of the Colorado Plateau, USA. International Journal of Earth Sciences, 99(6), pp. 1247–1265. https://doi.org/10.1007/s00531-009-0462-0

Eusden, J. D., Brady, J. J., Eusden, R. M., Felch, M. M., Merrill, T. K., and Niiler, K. A. 2020. Bedrock geology of the Bethel quadrangle, Maine. Maine Geological Survey, Open-File Map 20-11, scale 1:24 000. https://digitalmaine.com/mgs_maps/2126.

Ghani, A.A., Searle, M., Robb, L., and Chung, S-L. 2013. Transitional I-S type characteristics in the Main Range granite, Peninsula Malaysia. Journal of Asian Earth Sciences, 76, pp. 225–240. https://doi.org/10.1016/j.jseaes.2013.05.013

Gibson, D. and Lux, D.R. 1989. Petrographic and geochemical variations within the Songo pluton. Western Maine. Maine Geological Survey Studies in Maine Geology, 4, pp. 87–100.

Gibson, D., Lux., D.R., Seaman, S., Williamson, K., and Day, K. 2006. Field relations, petrology and cooling history of Devonian plutons, western interior Maine. *In* Guidebook for field trips in Western Maine. *Edited by* D. Gibson, J. Daly, and D. Reusch. New England Intercollegiate Geological Conference, 98th annual meeting, Trip A-3, pp. 25–42.

Glazner, A.F., Bartley, J.M., Coleman, D.S., Gray, W., and Taylor, R.Z. 2004. Are plutons assembled over millions of years by amalgamation from smaller magma chambers? GSA Today, 14, pp. 4–11. https://doi.org/10.1130/1052-5173(2004)014<0004:APAOMO>2.0.CO;2

Guidotti, C.V., Gibson, D., Lux, D.R., DeYoreo, J.J., and Cheney, J.T. 1986. Carboniferous metamorphism on the north (upper) side of the Sebago batholith. *In* New England Intercollegiate Geological Conference. *Edited by* D.W. Newburg., D.W., Trip C-4, pp. 306–341.

Harris, N.B.W., Pearce, J.A., and Tindle, A.G. 1986. Geochemical characteristics of collision-zone magmatism. Geological Society of London, Special Publications, 19, pp. 67–81. https://doi.org/10.1144/GSL.SP.1986.019.01.04

Harwood, D. S. 1973. Bedrock geology of the Cupsuptic and Arnold Pond quadrangles, west-central Maine. United States Geological Survey Bulletin 1346, 90 p.

Hawkesworth, C., Cawood, P.A., and Dhuime, B. 2019. Rates of generation and growth of the continental crust. Geoscience Frontiers, 10, pp. 165–173. https://doi.org/10.1016/j.gsf.2018.02.004

Heitzler, M.T., Lux, D.R., and Decker, E.R. 1988. The age and cooling history of the Chain of Ponds and Big Island plutons and the Spider Lake granite, west-central Maine and Quebec. American Journal of Science, 288, pp. 925–952. https://doi.org/10.2475/ajs.288.9.925

Hibbard, J.P., van Staal, C.R., Rankin, D., and Williams, H. 2006 Lithotectonic map of the Appalachian orogen (north), Canada-United States of America: Geological Survey of Canada Map 02041A, scale 1:1 500 000. https://doi.org/10.4095/221932

Hogan, J.P. and Sinha, K. 1989. Compositional variation of plutonism in the coastal Maine magmatic province: mode of origin and tectonic setting. *In* Studies in Maine geology; igneous and metamorphic geology; Volume 4. *Edited by* R.D. Tucker and R.G. Marvinney. Maine Geological Survey, pp. 1–33.

Ludwig, K.R. 2003. Isoplot 3.75: A Geochronological Toolkit for Microsoft Excel; Berkeley Geochronological Center.

Ludwig, K.R. 2012. Isoplot 4.15: A Geochronological Toolkit for Microsoft Excel. Berkeley Geochronological Center.

Lux, D.R and Aleinikoff, J.N. 1985. $^{40}Ar/^{39}Ar$ geochronology of the Songo pluton, western Maine. Geological Society of America abstratcs with programs, 17, p. 32.

McFarlane, C.R.M. and Luo, Y. 2012. Modern analytical facilities: U–Pb geochronology using 193nm Excimer LA-ICP-MS optimized for in situ accessory mineral dating in thin sections. Geoscience Canada, 39, pp. 158–172.

Miles, A.J., Woodcock, N.H., and Hawkesworth, C.J. 2016. Tectonic controls on post-subduction granite genesis and emplacement: the late Caledonian suite of Britain and Ireland. Gondwana Research, 39, pp. 250–260. https://doi.org/10.1016/j.gr.2016.02.006

Moench, R.H. and Aleinikoff, J.N. 2003. Stratigraphy, geochronology, and accretionary terrane settings of two Bronson Hill arc sequences, northern New England. Physics and chemistry of the Earth, 28, pp. 113–160. https://doi.org/10.1016/S1474-7065(03)00012-3

Moench, R.H. and Hildreth, C. T. 1976. Geologic map of the Rumford quadrangle, Oxford and Franklin counties, Maine. United States Geological Survey, Geologic Quadrangle Map GQ-1272, scale 1:62 500.

Moench, R.H. and Pankiwskyj, K.A. 1988. Geological map of western interior Maine. United States Geological Survey, Miscellaneous Investigations Series Map I-1692, scale 1:250 000.

Mohammadi, N., Fyffe, L., McFarlane, C.R.M., Thorne, K.G., Lentz, D. R., Charnley, B., Branscombe, L., and Butler, S. 2017. Geological relationships and laser ablation ICP-MS U–Pb geochronology of the Saint George Batholith, southwestern New Brunswick, Canada: implications for its tectonomagmatic evolution. Atlantic Geology, 53, pp. 207–240. https://doi.org/10.4138/atlgeol.2017.008

Mutch, E.J.F., Blundy, J.D., Tattich, B.C., Cooper, F.J., and Brooker, R.A. 2016. An experimental study of amphibole stability in low-pressure granitic magmas and a revised Al-in-hornblende geobarometer. Contributions to Mineralogy and Petrology, 171, pp. 1–27. https://doi.org/10.1007/s00410-016-1298-9

Neilsen, R.L., Landis, E.S., Ceci, V.M., and Poston, C.J. 1989. The commingling of diverse magma types in the Flagstaff Lake Igneous complex. *In* Studies in Maine Geology. *Edited by* R.D. Tucker and R.G. Marvinney. Maine Geological Survey, 3, pp. 67–78.

Osberg, P.H., Hussey III, A.M., and Boone, G.M. 1985. Bedrock geologic map of Maine: Maine Geological Survey, scale 1:500 000.

Paton, C., Hellstrom, J.C., Paul, B., Woodhead, J.D., and Hergt, J.M. 2011. Iolite: Freeware for the visualisation and processing of mass spectrometric data. Journal of Analytical Atomic Spectrometry, 26, pp. 2508–2518. https://doi.org/10.1039/c1ja10172b

Pearce J. 1996. Sources and setting of granitic rocks. Episodes, 19, pp. 120–125. https://doi.org/10.18814/epiiugs/1996/v19i4/005

Petrus, J.A. and Kamber, B.S. 2012. VizualAge: A novel approach to laser ablation ICP-MS U–Pb geochronology data reduction. Geostandards and Geoanalytical Research, 36, pp. 247–270. https://doi.org/10.1111/j.1751-908X.2012.00158.x

Pilote, J-L, Barr, S.M., and Gibson, D. 2011. A cross-border geochronological compilation for Late Silurian–Devonian granitoid rocks in Maine (USA) and New Brunswick (Canada): Pulses or a continuum? Geological Society of America, abstracts with programs, 43, no. 1, p. 159.

Pressley, R.A. and Brown, M. 1999. The Phillips pluton, Maine, USA: evidence of heterogeneous crustal sources and implications for granite ascent and emplacement mechanisms in convergent orogens. Lithos, 43, pp. 335–366. https://doi.org/10.1016/S0024-4937(98)00073-5

Simonetti, A. and Doig, R. 1990. U–Pb and Rb–Sr geochronology of Acadian plutonism in the Dunnahe zone of the southeastern Quebec Appalachians. Canadian Journal of Earth Sciences, 27, pp. 881–892. https://doi.org/10.1139/e90-091

Solar, G.S. and Tomascak, P.B. 2016. The migmatite-granite complex of Southern Maine: its structure, petrology, geochemistry, geochronology, and relation to the Sebago pluton. *In* Guidebook for field trips along the Maine coast from Maquoit Bay to Muscongus Bay. *Edited by* H.N. Berry, IV and D.P. West. New England Intercollegiate Geological Conference, pp. 19–42. https://doi.org/10.1130/abs/2016NE-272917

Solar, G.S., Pressley, R.A., Brown, M., and Tucker, R.D. 1998. Granite ascent in convergent orogenic belts: Testing a model. Geology, 26, pp. 711–714. https://doi.org/10.1130/0091-7613(1998)026<0711:GAICOB>2.3.CO;2

Tomascak, P.B., Brown, M., Solar, G.S., Becker, H.J., Centorbi, T.Y., and Tian, J. 2005. Source contributions to Devonian granite magmatism near the Laurentian border, New Hampshire and Western Maine, USA. Lithos, 80, pp. 75–99. https://doi.org/10.1016/j.lithos.2004.04.059

Tucker, R.D., Osberg, P.H., and Berry IV, H.N 2001. The geology of a part of Acadia and the nature of the Acadian orogeny across central and eastern Maine. American Journal of Science, 301, pp. 205–260. https://doi.org/10.2475/ajs.301.3.205

van Staal, C.R. and Barr, S.M. 2012. Lithospheric architecture and tectonic evolution of the Canadian Appalachians. *In* Tectonic Styles in Canada Revisited: the LITHOPROBE perspective. *Edited by* J.A. Percival, F.A. Cook, and R.M. Clowes, R.M. Geological Association of Canada Special Paper, 49, pp. 41–95.

van Staal, C.R., Whalen, J.B., Valverde-Vaquero, P., Zagorevski, A., and Rogers, N. 2009. Pre-Carboniferous, episode accretion-related, orogenesis along the Laurentian margin of the northern Appalachians. Geological Society, London, Special Publications, 327, pp. 271–316. https://doi.org/10.1144/SP327.13

Westerman, D. 1980. Geologic structures of the Chain of Pond pluton and vicinity, Northwestern Maine. Geological Survey of Maine, Open-File report no. 80-36, 34 p.

Editorial responsibility: David P. West, Jr.

APPENDIX A

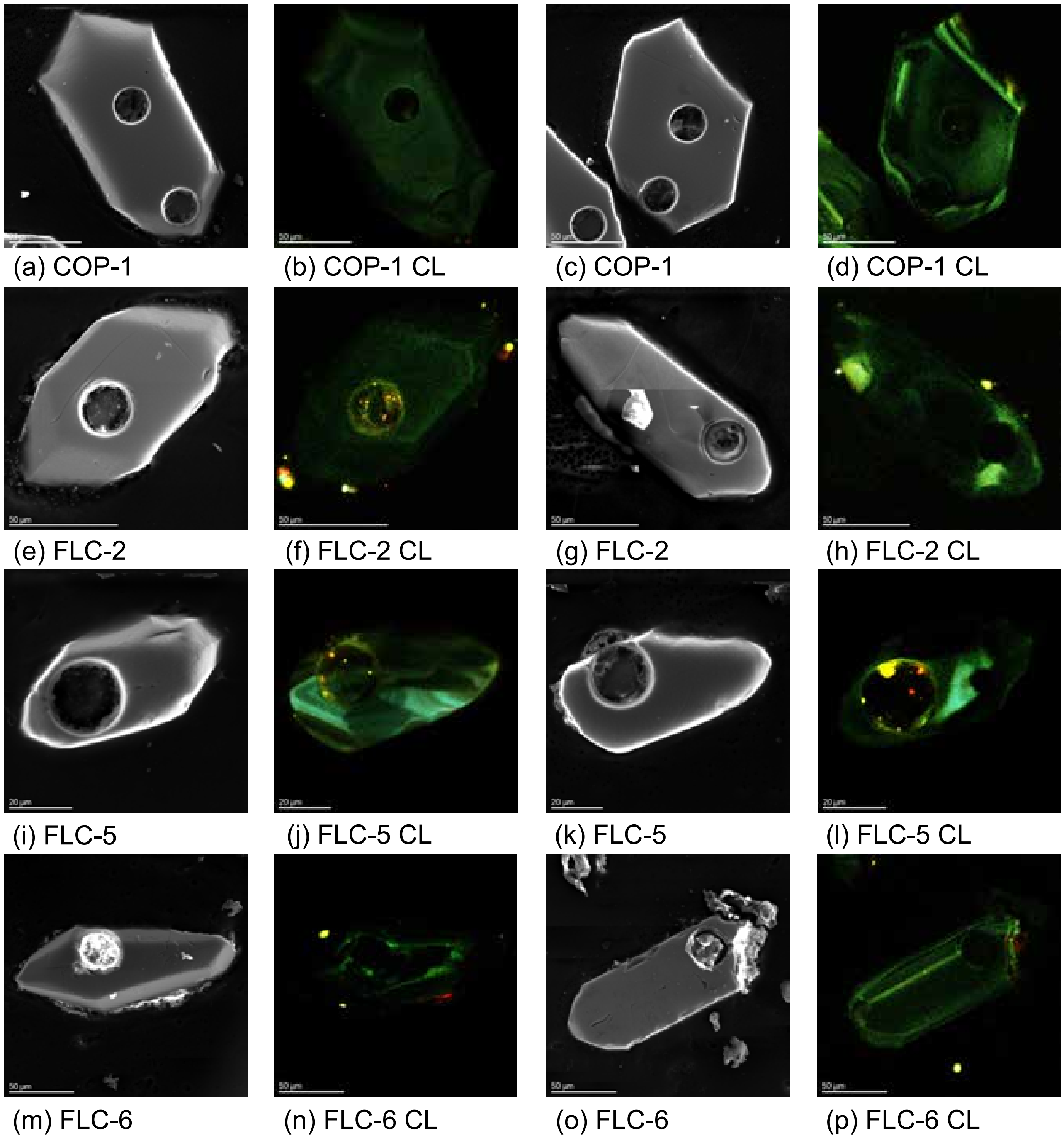

Figure A1. Scanning electron micrographs in backscatter electron mode and catholuminescence mode of representative zircon morphologies from the Chain of Ponds pluton (a–d for sample COP-1) and the Flagstaff Lake Igneous Complex (e–h for sample FLC-2, i–l for sample FLC-5, and m–p for sample FLC-6). The scale bar on each image is 50 μm.

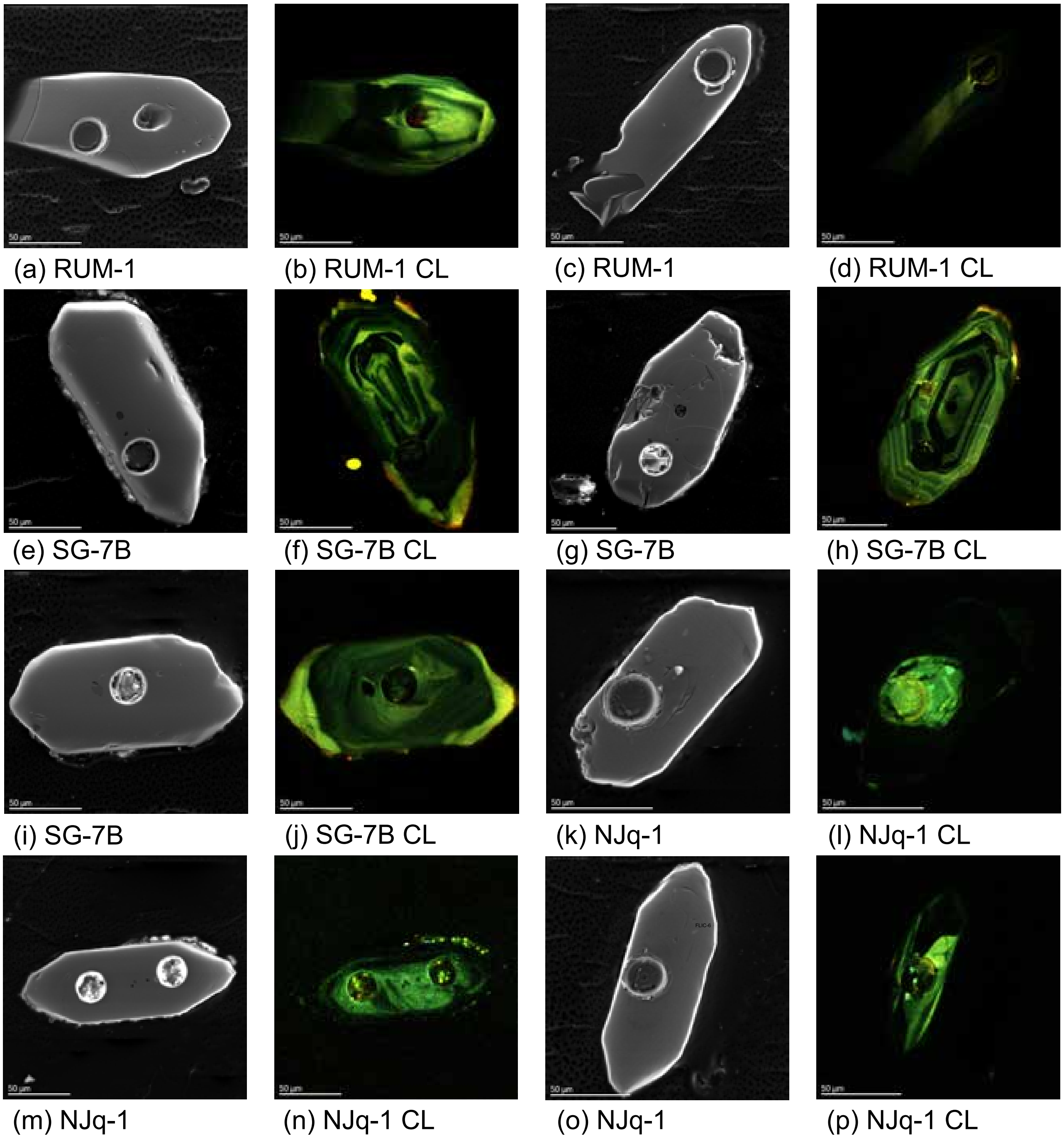

Figure A2. Scanning electron micrographs in backscatter electron mode and catholuminescence mode of representative zircon morphologies from the Rumford pluton (a–d for sample RUM-1), the Songo pluton (e–j for sample SG-7b) and the North Jay pluton (k–p for sample NJq-1). The scale bar on each image is 50 µm. (The extreme bright spots are from the diamond polishing paste.).

APPENDIX B

Table B1. LA-ICP-MS U-Pb isotopic analyses of zircons (University of New Brunswick).

Grains included in concordia calculations are shaded in grey
In samples with two or more age groups, light grey for young groups, darked grey for older groups

Corrections = C* — cps = counts per second — [1] = (after Hg correction)
1 threshold 204cps for no correction — 80 cps
2 threshold % for 204-based correction — 21 % error
3 threshold % for 208-based correction — 98.5 %Pb*

Sample	Zr90 cps	U (ppm)	Th (ppm)	Th/U	^{204}Pb cps[1]	2σ error on 204 cps	% error on 204 cps	cps ^{206}Pb/^{204}Pb	%Pb*	C*	Isotopic ratios ^{207}Pb/^{235}U	2σ ±	^{206}Pb/^{238}U	2σ ±	err. corr.	^{207}Pb/^{206}Pb	2σ ±	Calculated ages ^{207}Pb/^{206}Pb	2σ ±	^{207}Pb/^{235}U	2σ ±	^{206}Pb/^{238}U	2σ ±	% conc
Chain of Ponds pluton COP-1																								
COP-1 - 1	1.09E+08	437	218	2	3	13	433	6373	99.73	1	0.441	0.011	0.059	0.001	0.186	0.0546	0.0014	377	58	370	8	367	5	99.2
COP-1 - 2	1.15E+08	435	247	1.76	27	11	41	730	99.77	1	0.447	0.015	0.059	0.001	0.3	0.0547	0.0017	391	70	374	10	371	6	99.1
COP-1 - 3	1.07E+08	312	139.8	2.23	6	15	250	2192	99.6	1	0.445	0.019	0.058	0.001	0.149	0.0561	0.0024	413	89	372	13	362	6	97.2
COP-1 - 3b - 1	1.09E+08	227	156.4	1.45	-3	12	*-400*	*-3350*	*99.94*	1	*0.442*	*0.019*	0.06	0.001	0.146	0.0535	0.0023	330	90	372	14	376	6	101.1
COP-1 - 4	9.75E+07	174	100.2	1.74	2	15	750	9800	99.68	1	1.55	0.061	0.159	0.004	0.584	0.07	0.0021	927	66	947	24	951	24	96.1
COP-1 - 5	1.10E+08	666	238	2.8	2	13	650	13950	99.78	1	0.433	0.012	0.058	0.001	0.375	0.0544	0.0015	377	61	365	9	363	5	99.4
COP-1 - 6	1.04E+08	447.7	155	2.89	12	12	100	1768	99.43	1	0.505	0.019	0.063	0.001	0.507	0.0579	0.0019	500	71	414	13	394	8	95.1
COP-1 - 6b - 1	1.27E+08	461	203	2.27	-6	20	-333	-3603	99.75	1	0.469	0.033	0.063	0.001	0.003	0.055	0.0041	380	160	389	23	391	8	100.6
COP-1 - 7	1.11E+08	377	184	2.05	7	12	171	2349	99.62	1	0.445	0.013	0.058	0.001	0.019	0.0556	0.0018	408	68	373	9	365	5	97.9
COP-1 - 7b - 1	1.10E+08	505.7	145.9	3.47	4	13	325	15968	99.84	1	1.668	0.022	0.169	0.002	0.209	0.0718	0.001	980	28	997	9	1005	10	97.4
COP-1 - 8	1.17E+08	531	172	3.09	-6	14	-233	-4000	99.85	1	0.438	0.014	0.059	0.001	0.131	0.0538	0.0017	342	70	368	10	371	5	100.8
COP-1 - 9	9.23E+07	158.9	9.54	16.66	6	20	333	2535	99.4	1	1.352	0.057	0.138	0.004	0.412	0.0709	0.0026	939	74	866	24	834	21	88.9
COP-1 - 9b - 1	1.29E+08	179	59.8	2.99	0	20			99.9	1	0.456	0.038	0.062	0.002	0.187	0.0542	0.0044	340	170	379	26	385	10	101.5
COP-1 - 9b - 1a	9.48E+07	115.7	9.5	12.18	-6	17	-283	-2358	99.57	1	1.758	0.094	0.174	0.004	0.642	0.0727	0.003	975	82	1023	33	1031	24	91
COP-1 - 10	1.22E+08	506	368	1.38	9	19	211	2544	99.86	1	0.426	0.021	0.058	0.001	0.262	0.0536	0.0025	330	100	359	15	362	7	100.9
COP-1 - 10a	9.61E+07	521	81	6.43	2	20	1000	25700	99.66	1	1.327	0.054	0.142	0.005	0.657	0.0678	0.0022	855	67	856	23	855	29	99.6
COP-1 - 11	1.08E+08	348	203	1.71	6	12	200	2512	100	1	0.432	0.015	0.06	0.001	0.282	0.0527	0.0018	297	73	363	11	373	6	102.7
COP-1 - 12	1.20E+08	381	128	2.98	21	26	124	781	99.92	1	0.457	0.054	0.061	0.001	0.043	0.0547	0.0065	360	250	380	37	384	7	101
COP-1 - 13	1.24E+08	298	140	2.13	-3	17	-567	-4900	99.9	1	0.462	0.021	0.062	0.001	0.218	0.054	0.0024	348	94	385	14	388	7	100.7
COP-1 - 14	1.25E+08	369	175	2.11	-1	17	-1700	-17840	99.83	1	0.447	0.02	0.061	0.001	0.045	0.0538	0.0026	330	100	374	14	379	6	101.3
COP-1 - 15	1.33E+08	351	160	2.19	-3	26	-867	-5433	99.66	1	0.423	0.02	0.057	0.001	0.354	0.0543	0.0025	365	99	358	14	357	9	99.7
COP-1 - 16	1.09E+08	252.1	190.3	1.32	18	14	78	647	99.82	1	0.46	0.016	0.061	0.001	0.219	0.0544	0.0019	362	73	383	11	384	6	100.3
COP-1 - 17	1.11E+08	289	176	1.64	9	14	156	1524	100.1	1	0.445	0.014	0.062	0.001	0.151	0.0524	0.0018	278	72	373	10	389	7	104.4
COP-1 - 18	1.12E+08	549	277	1.98	-5	11	-220	-4856	99.81	1	0.426	0.011	0.058	0.001	0.262	0.0536	0.0013	336	54	359	8	361	5	100.5
COP-1 - 19	1.09E+08	163	68.3	2.39	-6	12	-200	-1237	99.92	1	0.458	0.021	0.061	0.001	0.321	0.0539	0.0023	346	92	381	15	383	6	100.5
COP-1 - 20	1.13E+08	51.9	53.8	0.96	12	16	133	951	99.14	1	4	0.15	0.287	0.007	0.334	0.1013	0.0037	1626	69	1629	31	1627	34	99
COP-1 - 21	9.39E+07	277	74.1	3.74	1	14	1400	34000	99.03	1	2.006	0.087	0.179	0.006	0.769	0.0814	0.0022	1220	52	1113	28	1058	33	86.3
COP-1 - 22	1.06E+08	900	259	3.47	-3	13	-433	-12507	99.73	1	0.434	0.009	0.058	0.001	0.197	0.0545	0.0012	375	50	366	7	364	5	99.6
COP-1 - 22b - 1	1.14E+08	611	183	3.34	8	15	188	3663	99.75	1	0.463	0.013	0.062	0.001	0.282	0.0544	0.0014	389	52	386	9	389	6	100.8
COP-1 - 23	9.76E+07	457	206	2.22	-	22	*-314*	*-2771*	*99.71*	1	*0.448*	*0.017*	0.06	0.001	0.401	0.0546	0.002	380	79	375	12	375	8	100.1
COP-1 - 24	1.27E+08	145	90	1.61	- 7	21	-300	-966	99.81	1	0.47	0.043	0.063	0.002	0.018	0.055	0.005	360	190	388	29	392	9	100.9
COP-1 - 24a	8.31E+07	263	128.2	2.05	7	26	1300	11000	99.12	1	1.373	0.058	0.137	0.003	0.275	0.0723	0.0031	976	90	875	25	826	18	85
COP-1 - 25	1.32E+08	362	163	2.22	-212	22	-105	*-829*	*99.81*	1	*0.45*	0.03	0.061	0.002	0.243	0.0544	0.0035	370	140	376	21	379	9	100.7

Table B1. Continued.

Sample	Zr90 cps	U (ppm)	Th (ppm)	Th/U	^{204}Pb cps[1]	2σ error on 204 cps	% error on 204 cps	cps ^{206}Pb/^{204}Pb	%Pb*	C*	Isotopic ratios ^{207}Pb/^{235}U	2σ ±	^{206}Pb/^{238}U	2σ ±	err. corr.	^{207}Pb/^{206}Pb	2σ ±	Calculated ages ^{207}Pb/^{206}Pb	2σ ±	^{207}Pb/^{235}U	2σ ±	^{206}Pb/^{238}U	2σ ±	% conc
COP-1 - 25a	*9.15E+07*	*146.9*	*94.2*	*1.56*	-2	15	-750	-8895	99.46	1	1.851	0.064	0.177	0.003	0.118	0.0757	0.0027	1085	67	1061	23	1049	14	96.8
COP-1 - 26	1.03E+08	328	124.6	2.63	9	13	144	1499	99.67	1	0.44	0.016	0.057	0.001	0.189	0.0557	0.002	412	79	371	11	360	6	97
COP-1 - 27	1.19E+08	576	230.2	2.5	3	15	500	9167	99.98	1	0.45	0.014	0.061	0.001	0.326	0.0535	0.0015	339	62	378	10	382	6	101
COP-1 - 28	1.15E+08	177	92.7	1.91	13	11	85	620	99.53	1	0.446	0.023	0.057	0.001	0.015	0.0567	0.0029	420	110	371	16	359	5	96.6
COP-1 - 29	1.00E+08	494	173	2.86	18	15	83	1113	99.72	1	0.425	0.014	0.056	0.001	0.185	0.055	0.0019	390	77	359	10	349	6	97.1
COP-1 - 29b - 1	1.16E+08	451	224	2.01	6	13	217	3150	99.69	1	0.422	0.016	0.057	0.001	0.255	0.0542	0.0021	353	81	357	11	358	5	100.2
COP-1 - 30	1.23E+08	275	157	1.75	8	28	350	1688	99.66	1	0.485	0.034	0.064	0.002	0.089	0.0557	0.004	410	150	400	23	398	9	99.4
COP-1 - 30a	8.81E+07	95.6	47.3	2.02	0	23			99.52	1	1.85	0.12	0.182	0.006	0.248	0.0738	0.0048	1000	130	1055	41	1077	33	89.7
COP-1 - 31	1.11E+08	510	294	1.73	-3	12	-400	-7523	99.71	1	0.437	0.012	0.058	0.001	0.141	0.0546	0.0015	375	59	368	8	365	4	99.2
COP-1 - 32	1.13E+08	275	108.2	2.54	-1	15	-1500	-11830	99.66	1	0.438	0.02	0.057	0.001	0.116	0.0557	0.0025	410	100	367	14	359	7	97.7
COP-1 - 32b - 1	1.05E+08	132.9	84.6	1.57	18	11	61	324	100.1	1	0.443	0.02	0.062	0.001	0.03	0.0525	0.0026	272	98	374	14	386	7	103.2
COP-1 - 33	1.19E+08	154.2	83.6	1.84	14	14	100	529	99.87	1	0.463	0.027	0.062	0.001	0.272	0.0548	0.0032	370	120	388	20	389	7	100.3
COP-1 - 34	1.08E+08	389	222	1.75	-5	12	-240	-3414	99.82	1	0.448	0.014	0.06	0.001	0.186	0.0541	0.0018	354	71	376	11	378	5	100.6
COP-1 - 35	1.08E+08	151.9	79.7	1.91	-1	14	-1400	-6590	100	1	0.432	0.018	0.059	0.001	0.016	0.053	0.0023	299	91	363	13	372	6	102.5
COP-1 - 36	1.09E+08	258	133.3	1.94	3	13	433	3960	99.78	1	0.465	0.016	0.062	0.001	0.312	0.055	0.0019	386	72	386	11	387	6	100.2
COP-1 - 37	1.07E+08	275.3	149.2	1.85	-18	12	-67	-707	99.68	1	0.48	0.018	0.062	0.001	0.024	0.0559	0.0023	414	86	396	13	390	5	98.5
COP-1 - 38	9.36E+07	180.5	200.6	0.9	25	15	60	288	99.75	1	0.437	0.027	0.058	0.001	0.217	0.0548	0.0034	370	130	366	20	362	7	99
COP-1 - 39	1.24E+08	207	129	1.6	5	15	300	1888	99.95	1	0.423	0.024	0.058	0.001	0.185	0.0534	0.0031	320	120	357	17	362	8	101.5
COP-1 - 40	1.32E+08	420	258	1.63	9	20	222	2314	99.72	1	0.466	0.023	0.062	0.001	0.282	0.0552	0.0026	400	100	387	15	386	7	99.7
COP-1 - 41	6.73E+07	593.2	84.9	6.99	1	11	1100	50300	99.82	1	1.899	0.031	0.183	0.003	0.668	0.0754	0.0009	1080	24	1079	11	1083	16	99.9
COP-1 - 42	1.04E+08	377	180	2.09	3	11	367	5133	99.82	1	0.448	0.015	0.059	0.001	0.256	0.0546	0.0016	395	68	374	10	369	6	98.6
COP-1 - 43	1.07E+08	129.3	90.3	1.43	5	11	220	1130	99.53	1	0.46	0.024	0.06	0.001	0.157	0.0569	0.0033	420	110	387	18	377	8	97.3
COP-1 - 44	1.11E+08	337	304.7	1.11	-4	13	-325	-3658	99.74	1	0.428	0.012	0.057	0.001	0.198	0.0547	0.0015	380	61	361	9	357	5	98.8
COP-1 - 45	1.15E+08	435.5	268	1.63	2	15	750	10050	99.66	1	0.453	0.013	0.06	0.001	0.173	0.0554	0.0017	407	67	379	9	375	5	99
COP-1 - 46	1.16E+08	458.4	326	1.41	4	16	400	5123	99.74	1	0.424	0.014	0.057	0.001	0.105	0.0542	0.0019	357	76	358	10	356	5	99.5
COP-1 - 47	8.96E+07	184.1	61.7	2.98	8	26	325	3023	99.09	1	2.236	0.099	0.194	0.004	0.165	0.0836	0.0037	1269	88	1190	31	1143	21	89.8
COP-1 - 48	1.02E+08	371.2	161.3	2.3	-1	15	-1500	-17210	99.92	1	0.475	0.015	0.064	0.001	0.151	0.0544	0.0019	366	75	395	11	398	6	100.9
COP-1 - 49	1.00E+08	442	145.6	3.04	12	17	142	1532	99.67	1	0.434	0.021	0.058	0.001	0.413	0.0545	0.0023	364	91	364	14	362	8	99.4
COP-1 - 50	1.01E+08	210	87.8	2.39	20	13	65	501	99.7	1	0.508	0.022	0.067	0.001	0.131	0.056	0.0027	410	100	418	16	418	9	99.9
COP-1 - 51	1.18E+08	290	146.8	1.98	9	14	156	1438	99.7	1	0.436	0.018	0.058	0.001	0.218	0.055	0.0022	385	85	366	12	361	5	98.6
COP-1 - 52	1.08E+08	214.4	118.2	1.81	0	11			99.86	1	0.439	0.019	0.059	0.001	0.157	0.0539	0.0023	331	90	367	13	371	6	101.1
COP-1 - 53	1.18E+08	241.1	115.3	2.09	26	19	73	412	99.78	1	0.447	0.024	0.059	0.001	0.418	0.0554	0.0034	390	130	374	17	371	7	99.1
COP-1 - 53a	7.32E+07	362	111.7	3.24	-13	19	-146	-2423	99.47	1	1.534	0.092	0.155	0.006	0.433	0.0721	0.0039	970	120	942	36	927	33	95.9
COP-1 - 54	1.21E+08	280	86	3.26	-5	13	-260	-2596	99.99	1	0.435	0.019	0.06	0.001	0.285	0.053	0.0026	300	100	366	13	376	6	102.8
COP-1 - 55	9.60E+07	855	715	1.2	-2	17	-850	-17800	99.76	1	0.447	0.013	0.06	0.001	0.584	0.0545	0.0013	384	53	375	9	373	8	99.5
COP-1B - 1	1.48E+08	7.93	3.37	2.35	6	10	170	2661	99.60	1	0.431	0.017	0.056	0.001	0.020	0.0555	0.0020	402	78	365	12	354	6	97.0
COP-1B - 2	1.61E+08	7.13	4.95	1.44	7	10	134	2018	99.68	1	0.426	0.018	0.057	0.001	0.085	0.0549	0.0021	380	84	359	13	357	6	99.3
COP-1B - 3	1.49E+08	3.199	1.125	2.84	-1	9	-669	6456	99.91	1	0.433	0.024	0.059	0.001	0.035	0.0537	0.0029	310	110	362	17	367	7	101.4
COP-1B - 4	1.48E+08	5.8	2.354	2.46	2	9	567	7727	99.82	1	0.439	0.019	0.059	0.001	0.069	0.0543	0.0021	356	81	368	13	368	6	99.9
COP-1B - 5	1.47E+08	14.47	6.25	2.32	10	9	95	3253	99.12	1	0.539	0.018	0.064	0.001	0.502	0.0610	0.0014	624	50	437	12	400	7	91.6

Table B1. Continued.

Sample	Zr90 cps	U (ppm)	Th (ppm)	Th/U	^{204}Pb cps[1]	2σ error on 204 cps	% error on 204 cps	cps ^{206}Pb/^{204}Pb	%Pb*	C*	Isotopic ratios ^{207}Pb/^{235}U	2σ ±	^{206}Pb/^{238}U	2σ ±	err. corr.	^{207}Pb/^{206}Pb	2σ ±	Calculated ages ^{207}Pb/^{206}Pb	2σ ±	^{207}Pb/^{235}U	2σ ±	^{206}Pb/^{238}U	2σ ±	% conc
COP-1B - 6	1.46E+08	9.2	3.208	2.87	-4	10	-250	18000	99.74	1	0.444	0.016	0.059	0.001	0.179	0.0549	0.0016	384	64	373	11	369	6	98.9
COP-1B - 7	1.74E+08	9.42	1.665	5.66	-22	15	-68	21500	100.12	1	0.442	0.032	0.062	0.002	0.511	0.0529	0.0033	310	140	371	23	390	13	105.1
COP-1B - 8	1.47E+08	6.55	2.72	2.41	1	10	1650	21150	99.78	1	0.426	0.017	0.057	0.001	0.187	0.0541	0.0019	357	78	359	12	356	6	99.2
COP-1B - 9	1.45E+08	9.06	5.6	1.62	-1	10	-1000	17890	99.47	1	0.457	0.015	0.058	0.001	0.072	0.0567	0.0016	458	62	383	10	366	6	95.6
COP-1B - 10	1.49E+08	5.282	2.244	2.35	5	10	200	2138	99.65	1	0.441	0.020	0.058	0.001	0.054	0.0555	0.0024	399	94	372	14	361	6	96.9
COP-1B - 11	1.45E+08	11.29	6.48	1.74	8	10	125	3000	99.77	1	0.470	0.014	0.063	0.001	0.392	0.0544	0.0012	383	50	391	10	392	6	100.3
COP-1B - 12	1.57E+08	13.56	7.52	1.80	8	10	125	3508	99.79	1	0.433	0.013	0.058	0.001	0.312	0.0545	0.0012	384	51	365	10	366	6	100.2
COP-1B - 13	1.53E+08	10.29	3.83	2.69	10	10	100	2139	99.04	1	0.494	0.016	0.059	0.001	0.316	0.0610	0.0016	617	59	407	11	368	7	90.5
COP-1B - 14	1.46E+08	9.01	5.05	1.78	0	10	#DIV/0!	18750	99.80	1	0.457	0.016	0.061	0.001	0.274	0.0543	0.0014	373	58	381	11	382	7	100.3
COP-1B - 15	1.50E+08	2.617	0.835	3.13	4	8	188	1447	98.84	1	0.603	0.035	0.069	0.002	0.399	0.0638	0.0034	660	110	478	23	432	11	90.3
COP-1B - 16	1.61E+08	8.913	3.778	2.36	-5	12	-240	19260	99.75	1	0.447	0.017	0.060	0.001	0.251	0.0547	0.0018	383	73	374	12	376	6	100.5
COP-1B - 17	1.49E+08	7.43	4.55	1.63	-3	10	-313	15090	99.80	1	0.439	0.016	0.059	0.001	0.250	0.0543	0.0017	360	66	368	11	367	6	99.6
COP-1B - 18	1.48E+08	7.841	3.171	2.47	-5	11	-220	15920	99.73	1	0.431	0.018	0.057	0.001	0.128	0.0544	0.0021	365	82	363	13	360	7	99.0
COP-1B - 19	1.46E+08	48.8	18.44	2.65	21	10	46	4445	99.54	1	0.447	0.011	0.057	0.001	0.445	0.0570	0.0008	485	31	376	8	358	5	95.2
COP-1B - 20	1.24E+08	9.93	7.24	1.37	-11	11	-100	18250	99.52	1	0.460	0.022	0.059	0.002	0.601	0.0559	0.0017	452	75	383	16	367	9	95.8
COP-1B - 21	1.44E+08	10.85	3.35	3.24	8	9	114	2797	99.49	1	0.453	0.018	0.058	0.001	0.404	0.0562	0.0018	440	71	379	12	362	7	95.6
COP-1B - 22	1.54E+08	7.81	2.714	2.88	2	9	512	10071	99.84	1	0.466	0.016	0.062	0.001	0.423	0.0546	0.0015	387	64	387	11	385	6	99.5
COP-1B - 23	1.55E+08	6.22	2.798	2.22	1	11	1100	13120	99.82	1	0.449	0.020	0.060	0.001	0.098	0.0548	0.0022	378	86	375	14	375	7	100.0
COP-1B - 24	1.51E+08	5.93	2.669	2.22	4	10	232	2871	99.74	1	0.422	0.018	0.057	0.001	0.154	0.0543	0.0020	362	80	358	12	356	6	99.5
COP-1B - 25	1.52E+08	3.23	1.618	2.00	8	10	132	893	99.64	1	0.453	0.022	0.059	0.001	0.054	0.0561	0.0026	411	96	378	15	369	7	97.6
COP-1B - 26	1.56E+08	5.12	1.995	2.57	-5	9	-181	10300	99.96	1	0.422	0.022	0.057	0.001	0.150	0.0538	0.0025	350	100	355	16	357	7	100.6
COP-1B - 27	1.55E+08	13.19	10.794	1.22	6	11	183	4473	99.78	1	0.420	0.015	0.057	0.001	0.391	0.0539	0.0016	360	66	357	11	360	6	100.8
COP-1B - 28	1.48E+08	19.6	6.45	3.04	2	9	460	19700	99.78	1	0.444	0.013	0.059	0.001	0.250	0.0543	0.0012	367	51	373	9	371	6	99.4
COP-1B - 29	1.46E+08	8.82	4.13	2.14	1	10	817	14483	99.69	1	0.444	0.015	0.059	0.001	0.171	0.0550	0.0016	389	62	372	11	367	6	98.6
COP-1B - 30	1.48E+08	10.21	3.36	3.04	3	10	333	6860	99.86	1	0.435	0.015	0.058	0.001	0.240	0.0539	0.0014	348	57	366	10	366	6	100.0
COP-1B - 31	1.47E+08	10.51	5.51	1.91	0	11		21000	99.73	1	0.438	0.016	0.059	0.001	0.200	0.0543	0.0015	366	60	368	11	368	6	99.9
COP-1B - 32	1.39E+08	5.57	1.97	2.83	5	11	220	2190	99.75	1	0.450	0.022	0.060	0.001	0.149	0.0545	0.0025	360	100	376	16	373	8	99.1
COP-1B - 33	1.39E+08	89.17	55.3	1.61	74	11	15	1976	98.93	1	0.430	0.010	0.051	0.001	0.455	0.0612	0.0007	646	23	363	6	321	5	88.3
COP-1B - 34	1.51E+08	7.83	3.4	2.30	-3	10	-297	16010	99.78	1	0.442	0.018	0.059	0.001	0.076	0.0546	0.0020	368	78	370	12	369	7	99.7
COP-1B - 35	1.52E+08	7.729	2.779	2.78	7	9	123	2172	99.74	1	0.426	0.014	0.057	0.001	0.018	0.0547	0.0016	382	65	359	10	354	6	98.6
COP-1B - 36	1.48E+08	6.41	2.755	2.33	3	10	333	4450	99.77	1	0.454	0.021	0.060	0.001	0.263	0.0547	0.0022	376	86	379	14	376	7	99.1
COP-1B - 37	1.45E+08	8.19	3.49	2.35	16	11	69	1018	99.78	1	0.447	0.016	0.060	0.001	0.240	0.0542	0.0017	358	67	374	11	374	6	100.0
COP-1B - 38	1.45E+08	13.37	8.95	1.49	1	11	1100	26720	99.74	1	0.444	0.013	0.060	0.001	0.183	0.0541	0.0012	361	48	373	9	373	6	99.9
COP-1B - 39	1.73E+08	54.5	19.52	2.79	38	17	45	3061	99.78	1	0.437	0.011	0.058	0.001	0.192	0.0564	0.0011	465	45	368	8	361	6	98.2
COP-1B - 40	1.28E+08	9.9	5.89	1.68	10	12	120	1825	99.24	1	0.489	0.018	0.060	0.001	0.171	0.0586	0.0019	530	74	404	13	374	6	92.6
COP-1B - 41	1.55E+08	11.16	8.05	1.39	7	11	157	3237	99.96	1	0.422	0.014	0.058	0.001	0.111	0.0535	0.0015	334	62	358	10	364	6	101.6
COP-1B - 42	1.50E+08	6.94	2.479	2.80	-9	9	-100	14530	99.65	1	0.454	0.018	0.060	0.001	0.265	0.0554	0.0019	398	75	378	13	373	7	98.6
COP-1B - 43	1.73E+08	15.84	8.68	1.82	1	13	1300	34230	99.78	1	0.425	0.015	0.058	0.001	0.052	0.0548	0.0018	390	74	359	11	360	7	100.4
COP-1B - 44	1.66E+08	3.906	1.536	2.54	-19	13	-68	14920	99.21	1	0.957	0.047	0.105	0.003	0.553	0.0671	0.0026	819	85	679	25	645	17	95.0
COP-1B - 45	1.61E+08	7.53	3.59	2.10	0	10		15840	99.89	1	0.425	0.022	0.059	0.001	0.427	0.0532	0.0023	313	90	358	15	367	7	102.5

Table B1. Continued.

Sample	Zr90 cps	U (ppm)	Th (ppm)	Th/U	^{204}Pb cps[1]	2σ error on 204 cps	% error on 204 cps	cps ^{206}Pb/^{204}Pb	%Pb*	C*	Isotopic ratios ^{207}Pb/^{235}U	2σ ±	^{206}Pb/^{238}U	2σ ±	err. corr.	^{207}Pb/^{206}Pb	2σ ±	Calculated ages ^{207}Pb/^{206}Pb	2σ ±	^{207}Pb/^{235}U	2σ ±	^{206}Pb/^{238}U	2σ ±	% conc
COP-1B - 46	1.33E+08	7.41	2.244	3.30	8	11	138	3028	98.93	1	0.966	0.037	0.102	0.002	0.464	0.0677	0.0020	840	63	684	19	627	13	91.7
COP-1B - 47	1.22E+08	39.8	22.5	1.77	0	14		75100	99.75	1	0.497	0.012	0.064	0.001	0.079	0.0554	0.0010	421	41	409	8	401	6	97.9
COP-1B - 48	1.52E+08	9.445	5.521	1.71	6	9	157	3155	99.51	1	0.450	0.015	0.057	0.001	0.131	0.0570	0.0016	470	62	377	10	360	6	95.6
COP-1B - 49	1.54E+08	6.991	3.18	2.20	-4	10	-225	13840	99.44	1	0.438	0.018	0.056	0.001	0.266	0.0570	0.0020	459	76	368	13	350	6	95.2
COP-1B - 50	1.51E+08	9.75	5.9	1.65	1	9	1314	28000	99.77	1	0.433	0.018	0.058	0.001	0.215	0.0544	0.0020	364	78	364	12	362	7	99.5
COP-1B - 51	1.36E+08	8.57	3.53	2.43	12	14	117	1309	99.18	1	0.450	0.023	0.055	0.001	0.177	0.0583	0.0028	510	110	376	16	346	7	91.9
COP-1B - 52	1.44E+08	8.02	2.86	2.80	1	11	1100	17300	99.71	1	0.499	0.020	0.065	0.001	0.392	0.0555	0.0019	408	77	410	14	403	9	98.3
COP-1B - 53	1.58E+08	6.92	3.98	1.74	0	11		14460	99.79	1	0.432	0.020	0.058	0.001	0.312	0.0541	0.0021	356	85	363	14	364	7	100.4
COP-1B - 54	1.42E+08	12.58	6.69	1.88	11	10	88	2336	99.81	1	0.480	0.015	0.064	0.001	0.327	0.0548	0.0014	399	58	398	10	397	8	99.9
COP-1B - 55	1.51E+08	7.48	3.07	2.44	-2	10	-426	15750	99.85	1	0.454	0.017	0.061	0.001	0.286	0.0540	0.0017	349	67	379	12	381	6	100.6
COP-1B - 56	1.50E+08	5.448	2.669	2.04	-3	9	-281	11080	99.45	1	0.464	0.020	0.059	0.001	0.162	0.0571	0.0023	453	85	385	14	369	6	95.7
COP-1B - 57	1.62E+08	6.445	2.768	2.33	0	11		14040	99.75	1	0.450	0.017	0.060	0.001	0.218	0.0551	0.0018	393	71	377	12	373	6	98.9
COP-1B - 58	1.61E+08	17.7	11.3	1.57	11	11	100	3318	99.29	1	0.465	0.014	0.057	0.001	0.103	0.0591	0.0013	556	49	387	10	359	5	92.7
COP-1B - 59	1.48E+08	6.56	3.424	1.92	5	9	166	2500	99.76	1	0.448	0.017	0.059	0.001	0.077	0.0547	0.0018	374	69	374	12	371	6	99.2
COP-1B - 60	1.78E+08	14.82	5.455	2.72	-1	17	-1700	32410	99.89	1	0.417	0.020	0.058	0.001	0.090	0.0538	0.0025	350	100	354	14	361	7	102.0
Flagstaffe Lake Igneous Complex FLIC-2																								
FLC-2 - 1	1.18E+08	496	18.33	27.06	12	14	117	2250	99.69	1	0.530	0.019	0.0687	0.0012	0.289	0.0559	0.0017	429	66	431	12	428	7	99.4
FLC-2 - 2	1.20E+08	362	21.7	16.68	13	16	123	1415	99.58	1	0.507	0.022	0.0645	0.0012	0.027	0.0570	0.0024	463	90	415	15	403	8	97.1
FLC-2 - 3	1.16E+08	302	63.7	4.74	2	13	650	8200	99.82	1	0.504	0.021	0.0670	0.0012	0.235	0.0548	0.0021	374	80	415	14	418	7	100.7
FLC-2 - 4	1.34E+08	1840	86.6	21.25	24	15	63	4167	99.84	1	0.484	0.013	0.0646	0.0013	0.260	0.0543	0.0012	376	49	401	9	403	8	100.6
FLC-2 - 5	1.38E+08	409	45.4	9.01	2	15	750	11500	99.76	1	0.504	0.022	0.0651	0.0012	0.284	0.0558	0.0022	423	83	414	15	407	7	98.3
FLC-2 - 6	1.09E+08	376	49.5	7.60	-6	11	-183	-3102	99.72	1	0.503	0.018	0.0652	0.0015	0.374	0.0560	0.0017	424	68	413	12	407	9	98.6
FLC-2 - 7	1.25E+08	315	47.2	6.67	2	15	750	8700	99.66	1	0.541	0.024	0.0699	0.0017	0.268	0.0567	0.0023	450	85	441	17	435	10	98.7
FLC-2 - 8	1.08E+08	446	197	2.26	0	11			99.78	1	0.508	0.016	0.0670	0.0012	0.321	0.0549	0.0014	390	58	416	11	418	7	100.5
FLC-2 - 9	1.03E+08	245.1	148.2	1.65	-7	15	-214	-1689	99.89	1	0.486	0.023	0.0647	0.0016	0.380	0.0538	0.0021	355	90	400	16	404	10	101.0
FLC-2 - 10	1.32E+08	681	40.3	16.90	-17	25	-147	-2147	99.66	1	0.528	0.019	0.0675	0.0016	0.165	0.0564	0.0020	457	77	430	13	421	9	98.0
FLC-2 - 11	1.10E+08	269	53.8	5.00	4	12	300	3525	100.08	1	0.502	0.021	0.0687	0.0014	0.265	0.0530	0.0021	329	88	411	14	429	9	104.3
FLC-2 - 12	1.15E+08	327	34.2	9.56	1	12	1200	17500	99.69	1	0.521	0.023	0.0668	0.0014	0.285	0.0560	0.0021	423	80	424	15	417	9	98.3
FLC-2 - 13	1.33E+08	802	30.9	25.95	-5	19	-380	-8760	99.75	1	0.510	0.014	0.0662	0.0014	0.411	0.0561	0.0014	448	56	418	10	413	9	98.9
FLC-2 - 14	1.12E+08	407	113.5	3.59	-5	12	-240	-4198	99.77	1	0.505	0.018	0.0664	0.0011	0.052	0.0550	0.0019	384	73	413	12	415	7	100.4
FLC-2 - 15	1.30E+08	408	28.2	14.47	-21	16	-76	-1033	99.88	1	0.494	0.025	0.0662	0.0014	0.165	0.0540	0.0026	350	100	407	17	413	9	101.4
FLC-2 - 16	1.36E+08	756	149	5.07	-9	27	-300	-4478	99.70	1	0.511	0.020	0.0669	0.0016	0.057	0.0551	0.0023	405	93	419	14	418	10	99.7
FLC-2 - 17	1.12E+08	638	72.4	8.81	1	12	1200	32500	99.80	1	0.493	0.014	0.0654	0.0011	0.129	0.0547	0.0013	384	54	407	9	408	7	100.4
FLC-2 - 18	1.09E+08	523	61.7	8.48	0	12			99.76	1	0.544	0.017	0.0710	0.0015	0.295	0.0557	0.0014	420	58	440	11	442	9	100.4
FLC-2 - 19	1.25E+08	1271	47.9	26.53	-7	19	-271	-9486	99.77	1	0.500	0.014	0.0652	0.0012	0.013	0.0552	0.0013	424	58	412	10	407	7	99.0
FLC-2 - 20	1.19E+08	471	50.7	9.29	9	11	122	2672	99.75	1	0.472	0.014	0.0623	0.0011	0.186	0.0548	0.0014	387	54	392	9	389	7	99.4
FLC-2 - 21	1.11E+08	1403	38.6	36.35	9	10	111	7744	99.64	1	0.504	0.012	0.0646	0.0011	0.332	0.0567	0.0010	472	38	414	8	403	7	97.5
FLC-2 - 22	1.12E+08	432	20.5	21.07	-2	16	-800	-12100	99.76	1	0.535	0.017	0.0697	0.0013	0.239	0.0558	0.0015	433	58	435	11	434	8	99.8
FLC-2 - 23	1.13E+08	1034	5.79	178.58	2	12	600	25650	99.75	1	0.481	0.012	0.0636	0.0011	0.200	0.0549	0.0011	397	44	399	8	397	6	99.7
FLC-2 - 24	1.18E+08	422	42.7	9.88	17	11	65	1259	99.43	1	0.489	0.016	0.0614	0.0011	0.122	0.0578	0.0016	511	62	405	11	384	7	94.8

Table B1. Continued.

Sample	Zr90 cps	U (ppm)	Th (ppm)	Th/U	^{204}Pb cps[1]	2σ error on 204 cps	% error on 204 cps	cps ^{206}Pb/^{204}Pb	%Pb*	C*	Isotopic ratios ^{207}Pb/^{235}U	2σ ±	^{206}Pb/^{238}U	2σ ±	err. corr.	^{207}Pb/^{206}Pb	2σ ±	Calculated ages ^{207}Pb/^{206}Pb	2σ ±	^{207}Pb/^{235}U	2σ ±	^{206}Pb/^{238}U	2σ ±	% conc
FLC-2 - 25	1.11E+08	505	41.9	12.05	8	11	138	3513	99.18	1	0.585	0.020	0.0692	0.0012	0.167	0.0612	0.0018	622	65	466	13	432	7	92.6
FLC-2 - 26	1.10E+08	1102	1110	0.99	7	13	186	7500	99.75	1	0.490	0.013	0.0636	0.0010	0.259	0.0558	0.0012	431	48	404	9	397	6	98.3
FLC-2 - 27	1.24E+08	499	69.9	7.14	21	18	86	1314	99.96	1	0.508	0.018	0.0689	0.0015	0.201	0.0534	0.0017	333	72	416	12	430	9	103.3
FLC-2 - 28	1.29E+08	1099	114	9.64	-4	16	-400	-14000	99.64	1	0.460	0.015	0.0596	0.0011	0.492	0.0562	0.0015	446	59	384	10	373	7	97.2
FLC-2 - 29	1.07E+08	949	81.4	11.66	-10	12	-120	-4540	99.71	1	0.495	0.013	0.0652	0.0010	0.292	0.0552	0.0011	408	45	408	9	407	6	99.8
FLC-2 - 30	1.30E+08	926	26.5	34.94	5	20	400	9320	99.53	1	0.504	0.018	0.0640	0.0014	0.141	0.0569	0.0019	476	72	414	12	400	9	96.5
FLC-2 - 31	1.35E+08	453	34.6	13.09	4	27	675	6000	99.56	1	0.535	0.031	0.0668	0.0013	0.445	0.0576	0.0030	500	120	435	21	417	8	95.8
FLC-2 - 32	1.35E+08	660	20.6	32.04	1	23	2300	34100	99.73	1	0.489	0.022	0.0647	0.0015	0.328	0.0545	0.0021	379	87	403	15	404	9	100.2
FLC-2 - 33	1.09E+08	804	31.8	25.28	6	12	200	6433	99.84	1	0.487	0.014	0.0646	0.0012	0.193	0.0544	0.0013	382	54	402	10	404	7	100.4
FLC-2 - 34	1.13E+08	890	37.4	23.80	11	12	109	4109	99.52	1	0.515	0.014	0.0650	0.0011	0.243	0.0575	0.0013	495	49	421	10	406	7	96.4
FLC-2 - 35	1.21E+08	737	32	23.03	-5	13	-260	-7780	99.88	1	0.482	0.015	0.0648	0.0011	0.299	0.0538	0.0014	349	56	399	10	405	7	101.4
FLC-2 - 36	1.35E+08	939	32.8	28.63	6	18	300	8617	99.76	1	0.490	0.016	0.0645	0.0011	0.218	0.0550	0.0016	401	67	404	11	403	7	99.6
FLC-2 - 37	1.13E+08	786	46.4	16.94	5	12	240	8660	99.75	1	0.555	0.020	0.0712	0.0017	0.435	0.0563	0.0016	444	59	447	12	443	10	99.2
FLC-2 - 38	1.15E+08	366	21.9	16.71	2	11	550	9700	99.67	1	0.510	0.015	0.0659	0.0011	0.026	0.0561	0.0016	443	62	418	10	411	7	98.4
FLC-2 - 39	1.08E+08	447	67.1	6.66	13	12	92	1606	99.57	1	0.487	0.015	0.0620	0.0011	0.308	0.0570	0.0014	474	56	402	10	388	6	96.4
FLC-2 - 40	1.27E+08	797	24.8	32.14	-6	27	-450	-6617	99.63	1	0.498	0.021	0.0641	0.0013	0.279	0.0562	0.0020	446	81	410	14	400	8	97.6
FLC-2 - 41	1.25E+08	1498	182	8.23	94	38	40	765	97.13	2	0.452	0.100	0.0569	0.0016	0.783	0.0571	0.0095	790	200	372	76	357	10	95.9
FLC-2 - 42	1.35E+08	817	55.6	14.69	9	21	233	5089	99.74	1	0.506	0.018	0.0663	0.0014	0.202	0.0552	0.0018	411	72	415	12	414	8	99.8
FLC-2 - 43	1.21E+08	529	27.3	19.38	-11	19	-173	-2500	99.75	1	0.504	0.016	0.0659	0.0012	0.211	0.0555	0.0016	420	63	414	11	411	7	99.3
FLC-2 - 43b - 1	1.22E+08	760	29.3	25.94	4	15	375	9525	99.64	1	0.480	0.013	0.0624	0.0010	0.175	0.0558	0.0013	441	50	398	9	390	6	98.1
FLC-2 - 44	1.30E+08	1840	65.9	27.92	3	25	833	33033	99.74	1	0.521	0.015	0.0677	0.0013	0.196	0.0556	0.0015	430	63	426	10	422	8	99.2
FLC-2 - 45	1.13E+08	328	41.3	7.94	-7	11	-157	-2470	99.79	1	0.508	0.019	0.0668	0.0012	0.135	0.0552	0.0019	391	76	415	13	417	7	100.4
FLC-2 - 46	1.11E+08	217	53.3	4.07	8	12	150	1459	99.93	1	0.523	0.021	0.0693	0.0015	0.186	0.0549	0.0021	378	82	425	14	432	9	101.6
FLC-2 - 47	1.10E+08	356	14.5	24.55	-8	11	-138	-2238	99.67	1	0.505	0.015	0.0651	0.0012	0.192	0.0559	0.0013	449	57	415	10	407	7	98.0
FLC-2 - 48	1.04E+08	349	17.88	19.52	-8	13	-163	-2225	99.85	1	0.522	0.017	0.0693	0.0013	0.092	0.0546	0.0017	384	64	427	11	432	8	101.2
FLC-2 - 49	1.28E+08	828	47.8	17.32	11	15	136	4073	99.77	1	0.486	0.014	0.0648	0.0012	0.023	0.0545	0.0015	379	62	402	10	405	7	100.7
FLC-2 - 50	1.10E+08	231	45.1	5.12	-10	12	-120	-1197	99.90	1	0.509	0.022	0.0674	0.0013	0.111	0.0545	0.0021	377	87	416	15	420	8	101.0
FLC-2 - 51	1.32E+08	665	17.25	38.55	-14	22	-157	-2586	100.00	1	0.482	0.016	0.0664	0.0014	0.153	0.0524	0.0016	292	67	399	11	414	8	103.8
FLC-2 - 52	1.12E+08	920	40.9	22.49	8	12	150	5690	99.79	1	0.486	0.012	0.0643	0.0010	0.315	0.0549	0.0010	399	39	402	8	402	6	99.9
FLC-2 - 53	1.08E+08	161.1	51.5	3.13	1	11	1100	7720	99.54	1	0.514	0.025	0.0655	0.0015	0.339	0.0573	0.0026	454	94	421	17	409	9	97.1
FLC-2 - 54	1.16E+08	196.7	42.8	4.60	1	14	1400	10740	99.84	1	0.529	0.026	0.0695	0.0014	0.117	0.0553	0.0025	391	94	429	17	433	8	100.9
FLC-2 - 54b - 1	1.09E+08	527	13.35	39.48	-5	11	-220	-5222	99.84	1	0.489	0.015	0.0649	0.0011	0.147	0.0548	0.0015	385	59	404	10	405	6	100.4
FLC-2 - 55	1.22E+08	790	38.8	20.36	13	14	108	3231	99.78	1	0.502	0.016	0.0661	0.0012	0.289	0.0552	0.0014	407	58	413	10	412	7	99.9
Flagstaffe Lake Igneous Complex FLIC-5																								
FLC-5 - 3	7.21E+06	86.5	48.4	1.79	0	22			76.00	1	3.930	0.720	0.1150	0.0140	0.720	0.2660	0.0430	3070	320	1560	170	698	83	44.7
FLC-5 - 1	1.04E+08	171	84.2	2.03	-2	12	-600	-3880	98.73	1	0.570	0.033	0.0643	0.0016	0.241	0.0641	0.0034	680	110	454	21	402	10	88.5
FLC-5 - 2	1.26E+08	344.4	66.3	5.19	4	12	300	4518	99.82	1	0.470	0.016	0.0620	0.0011	0.372	0.0551	0.0017	395	67	390	11	388	7	99.3
FLC-5 - 4	5.09E+07	160.3	112.2	1.43	18	14	78	204	97.95	1	0.668	0.054	0.0674	0.0022	0.486	0.0711	0.0050	840	150	508	33	420	13	82.7
FLC-5 - 5	1.20E+08	227.5	147.2	1.55	-3	11	-367	-3900	99.57	1	0.496	0.019	0.0637	0.0012	0.049	0.0568	0.0021	450	79	408	13	398	7	97.6
FLC-5 - 6	1.18E+08	162.5	58.9	2.76	-2	15	-750	-4030	98.72	1	0.525	0.025	0.0596	0.0014	0.281	0.0639	0.0028	736	92	430	16	373	8	86.8

Table B1. Continued.

Sample	Zr90 cps	U (ppm)	Th (ppm)	Th/U	^{204}Pb cps[1]	2σ error on 204 cps	% error on 204 cps	cps $^{206}Pb/^{204}Pb$	%Pb*	C*	Isotopic ratios $^{207}Pb/^{235}U$	2σ ±	$^{206}Pb/^{238}U$	2σ ±	err. corr.	$^{207}Pb/^{206}Pb$	2σ ±	Calculated ages $^{207}Pb/^{206}Pb$	2σ ±	$^{207}Pb/^{235}U$	2σ ±	$^{206}Pb/^{238}U$	2σ ±	% conc
FLC-5 - 7	1.23E+08	151.2	89.7	1.69	-3	13	-433	-2593	99.81	1	0.465	0.023	0.0617	0.0014	0.151	0.0550	0.0026	373	100	385	16	386	9	100.2
FLC-5 - 8	1.26E+08	125.1	70.5	1.77	4	11	275	1688	99.11	1	0.528	0.026	0.0632	0.0012	0.096	0.0608	0.0028	575	100	428	17	395	8	92.3
FLC-5 - 9	3.41E+07	143	42	3.40	10	13	130	183	96.18	1	0.751	0.070	0.0640	0.0024	0.401	0.0849	0.0071	1150	180	554	40	400	15	72.2
FLC-5 - 10	1.03E+08	84.9	61.57	1.38	9	11	122	408	98.29	1	0.574	0.032	0.0624	0.0014	0.141	0.0675	0.0037	770	120	459	21	390	8	85.0
FLC-5 - 11	1.26E+08	170.9	51.9	3.29	14	11	79	629	99.89	1	0.452	0.018	0.0606	0.0012	0.088	0.0538	0.0020	345	83	377	12	379	7	100.6
FLC-5 - 12	1.18E+08	182.8	117.6	1.55	-10	13	-130	-911	99.78	1	0.463	0.022	0.0610	0.0011	0.278	0.0550	0.0023	382	89	384	15	382	7	99.4
FLC-5 - 13	1.24E+08	183	56.3	3.25	-19	12	-63	-483	99.07	1	0.501	0.024	0.0599	0.0012	0.252	0.0609	0.0027	585	95	410	16	375	7	91.4
FLC-5 - 14	1.08E+08	381	52.3	7.28	-5	11	-220	-3748	99.80	1	0.509	0.019	0.0672	0.0013	0.337	0.0550	0.0018	387	71	416	13	419	8	100.8
FLC-5 - 15	1.25E+08	97.6	64.7	1.51	13	11	85	386	99.74	1	0.466	0.026	0.0615	0.0014	0.242	0.0555	0.0029	380	110	388	18	385	9	99.2
FLC-5 - 16	1.21E+08	155.1	71.1	2.18	10	14	140	809	99.75	1	0.480	0.020	0.0631	0.0013	0.013	0.0555	0.0023	398	90	396	14	394	8	99.6
FLC-5 - 17	1.12E+08	476	130.6	3.64	10	13	130	2050	99.73	1	0.460	0.015	0.0605	0.0012	0.166	0.0553	0.0017	404	66	383	11	379	7	98.8
FLC-5 - 18	1.04E+08	276.6	234.5	1.18	17	13	76	705	99.42	1	0.479	0.021	0.0599	0.0012	0.160	0.0577	0.0022	501	86	396	14	375	8	94.6
FLC-5 - 19	1.18E+08	47	39.3	1.20	14	12	86	169	99.19	1	0.521	0.036	0.0629	0.0018	0.070	0.0602	0.0040	560	150	427	26	393	11	92.1
FLC-5 - 20	1.02E+08	253.1	143.9	1.76	5	12	240	2004	99.53	1	0.468	0.018	0.0601	0.0013	0.321	0.0569	0.0020	455	77	388	12	376	8	97.0
FLC-5 - 21	1.32E+08	188	63.4	2.97	1	23	2300	9690	99.70	1	0.493	0.034	0.0643	0.0017	0.598	0.0554	0.0032	400	130	405	23	402	11	99.1
FLC-5 - 22	9.86E+07	121.1	50.7	2.39	-6	13	-217	-830	98.76	1	0.539	0.027	0.0617	0.0014	0.171	0.0637	0.0030	670	100	434	18	386	9	88.9
FLC-5 - 23	9.96E+07	73.3	63.2	1.16	-4	14	-350	-1740	98.69	1	1.474	0.073	0.1428	0.0036	0.328	0.0761	0.0035	1038	95	916	31	860	20	82.8
FLC-5 - 24	1.04E+08	145.3	38.72	3.75	-7	13	-186	-862	99.09	1	0.506	0.028	0.0602	0.0013	0.415	0.0609	0.0030	580	110	412	19	377	8	91.5
FLC-5 - 25	8.86E+07	145.7	55.1	2.64	0	13			98.96	1	0.521	0.032	0.0623	0.0017	0.271	0.0610	0.0036	590	110	426	20	390	10	91.4
FLC-5 - 26	1.24E+08	153.2	91.4	1.68	0	11			99.78	1	0.468	0.022	0.0617	0.0012	0.078	0.0550	0.0025	367	94	387	15	386	7	99.8
FLC-5 - 27	1.24E+08	132.5	40.3	3.29	0	13			99.67	1	0.472	0.023	0.0617	0.0012	0.078	0.0558	0.0027	390	100	390	16	386	7	98.9
FLC-5 - 28	1.18E+08	226.2	157	1.44	3	12	400	3750	99.75	1	0.478	0.019	0.0632	0.0011	0.162	0.0549	0.0020	380	78	395	13	395	7	100.0
FLC-5 - 29	1.21E+08	161.1	35.9	4.49	-10	12	-120	-813	99.49	1	0.479	0.022	0.0612	0.0012	0.221	0.0573	0.0025	461	94	398	16	383	7	96.2
FLC-5 - 30	1.19E+08	92.3	72.2	1.28	0	13			98.65	1	0.553	0.028	0.0625	0.0013	0.066	0.0645	0.0032	690	100	444	18	391	8	88.0
FLC-5 - 31	1.10E+08	161.8	84.4	1.92	8	12	150	1001	99.97	1	0.497	0.023	0.0675	0.0013	0.164	0.0534	0.0023	314	91	407	16	421	8	103.5
FLC-5 - 32	1.22E+08	90.5	136.8	0.66	-4	14	-350	-1203	99.42	1	0.520	0.025	0.0654	0.0015	0.205	0.0579	0.0027	481	99	423	17	408	9	96.5
FLC-5 - 33	1.26E+08	108	68	1.59	-12	12	-100	-500	99.84	1	0.532	0.038	0.0676	0.0017	0.198	0.0555	0.0034	410	130	428	24	422	10	98.6
FLC-5 - 34	1.18E+08	70.1	86.5	0.81	7	13	186	527	99.58	1	0.513	0.037	0.0658	0.0015	0.017	0.0570	0.0041	410	140	418	25	411	9	98.3
FLC-5 - 35	1.20E+08	64.2	50.7	1.27	-5	12	-240	-664	99.89	1	0.490	0.031	0.0647	0.0016	0.148	0.0551	0.0035	360	130	400	22	404	10	101.1
FLC-5 - 36	1.19E+08	88.9	47.9	1.86	-7	12	-171	-674	99.76	1	0.520	0.031	0.0671	0.0016	0.241	0.0562	0.0032	410	120	421	21	419	10	99.4
FLC-5 - 37	1.09E+08	70.3	79.8	0.88	17	14	82	205	99.59	1	0.503	0.034	0.0653	0.0016	0.115	0.0570	0.0040	420	140	409	23	408	10	99.6
FLC-5 - 38	1.16E+08	122.6	52.9	2.32	4	11	275	1550	99.70	1	0.494	0.028	0.0644	0.0014	0.028	0.0560	0.0031	400	120	407	18	402	9	98.8
FLC-5 - 39	1.17E+08	373.4	139.3	2.68	21	12	57	861	99.02	1	0.525	0.022	0.0617	0.0013	0.489	0.0616	0.0020	643	74	426	14	386	8	90.6
FLC-5 - 40	9.58E+07	122.5	129.4	0.95	8	16	200	644	99.76	1	0.464	0.032	0.0614	0.0015	0.047	0.0556	0.0040	380	150	384	23	384	9	100.0
FLC-5 - 41	1.16E+08	161.7	50.3	3.21	16	13	81	499	99.73	1	0.486	0.024	0.0637	0.0013	0.178	0.0555	0.0025	391	94	400	16	398	8	99.5
FLC-5 - 42	1.22E+08	146.9	115.2	1.28	-6	13	-217	-1227	99.69	1	0.464	0.021	0.0607	0.0011	0.062	0.0557	0.0025	411	96	387	15	380	7	98.1
FLC-5 - 43	1.22E+08	121.2	29.2	4.15	-20	12	-60	-306	99.40	1	0.495	0.027	0.0612	0.0013	0.105	0.0584	0.0030	500	110	405	18	383	8	94.5
FLC-5 - 44	1.14E+08	229	113.1	2.02	-6	11	-183	-1830	99.51	1	0.490	0.021	0.0622	0.0011	0.097	0.0575	0.0024	470	89	403	14	389	7	96.5
FLC-5 - 45	1.15E+08	145.9	79.28	1.84	2	12	600	3575	99.69	1	0.489	0.022	0.0638	0.0013	0.079	0.0558	0.0025	404	93	402	15	398	8	99.1
FLC-5 - 45b - 1	1.16E+08	108.8	55.01	1.98	1	11	1100	5444	99.71	1	0.495	0.024	0.0640	0.0013	0.057	0.0562	0.0027	430	100	408	17	400	8	98.0

Table B1. Continued.

Sample	Zr90 cps	U (ppm)	Th (ppm)	Th/U	^{204}Pb cps[1]	2σ error on 204 cps	% error on 204 cps	cps ^{206}Pb/^{204}Pb	%Pb*	C*	Isotopic ratios ^{207}Pb/^{235}U	2σ ±	^{206}Pb/^{238}U	2σ ±	err. corr.	^{207}Pb/^{206}Pb	2σ ±	Calculated ages ^{207}Pb/^{206}Pb	2σ ±	^{207}Pb/^{235}U	2σ ±	^{206}Pb/^{238}U	2σ ±	% conc
FLC-5 - 46	1.20E+08	140.8	63	2.23	-5	11	-220	-1390	99.55	1	0.469	0.024	0.0606	0.0012	0.270	0.0569	0.0027	441	100	391	16	379	8	97.0
FLC-5 - 47	1.22E+08	132.3	63.8	2.07	18	11	61	353	99.75	1	0.450	0.025	0.0594	0.0012	0.325	0.0550	0.0027	380	100	375	17	372	7	99.2
FLC-5 - 48	1.22E+08	178.9	115	1.56	-6	13	-217	-1527	99.75	1	0.480	0.021	0.0630	0.0013	0.130	0.0551	0.0022	401	89	397	14	394	8	99.1
FLC-5 - 49	9.72E+07	130.2	39.4	3.30	2	14	700	8195	98.93	1	1.996	0.082	0.1766	0.0036	0.221	0.0820	0.0031	1229	74	1111	27	1048	20	84.8
FLC-5 - 50	1.14E+08	164	61.1	2.68	-8	14	-175	-993	99.57	1	0.484	0.024	0.0612	0.0013	0.064	0.0572	0.0028	470	100	399	16	383	8	95.9
FLC-5 - 51	1.07E+08	128.5	124	1.04	0	11			98.87	1	0.521	0.026	0.0608	0.0014	0.073	0.0626	0.0031	630	100	423	17	380	9	89.9
FLC-5 - 52	1.12E+08	67.9	74.7	0.91	-6	11	-183	-548	99.53	1	0.512	0.034	0.0648	0.0016	0.134	0.0576	0.0037	440	130	414	23	405	10	97.8
Flagstaffe Lake Igneous Complex FLIC-6																								
FLC-6 - 45	1.80E+08	187.4	39.3	4.77	120	15	12.5	320	86.70	3	4.510	0.360	0.212	0.010	0.610	0.1541	0.0060	2368	70	1723	68	1241	51	48.5
FLC-6 - 1	2.03E+08	1640	255	6.43	16	11	68.8	6750	99.84	1	0.487	0.016	0.064	0.003	0.591	0.0550	0.0009	403	36	403	11	403	15	100.0
FLC-6 - 2	1.93E+08	498.5	52.8	9.44	23	10	43.5	1356	98.47	1	0.569	0.021	0.062	0.002	0.095	0.0664	0.0017	804	53	457	13	388	14	85.0
FLC-6 - 3	1.86E+08	1570	125.2	12.54	45	12	26.7	2191	99.28	1	0.513	0.016	0.062	0.002	0.716	0.0599	0.0007	596	27	420	10	388	14	92.3
FLC-6 - 4	1.90E+08	296.4	121.2	2.45	7	11	157.1	2574	99.77	1	0.465	0.021	0.062	0.002	0.099	0.0546	0.0020	387	83	389	15	385	14	99.1
FLC-6 - 6	1.95E+08	230.9	48.89	4.72	1	9	1000.0	15567	99.71	1	0.476	0.022	0.062	0.002	0.296	0.0558	0.0021	424	83	395	16	386	15	97.8
FLC-6 - 7	1.43E+08	450	123.4	3.65	81	23	28.4	278	94.55	1	0.785	0.040	0.059	0.003	0.234	0.0964	0.0043	1534	89	586	23	369	16	62.9
FLC-6 - 8	1.80E+08	249.6	127.5	1.96	-1	10	-1385.7	-21186	99.62	1	0.476	0.021	0.062	0.002	0.153	0.0557	0.0020	411	76	396	13	388	15	98.0
FLC-6 - 9	1.90E+08	1227	57.3	21.41	2	9	505.6	43889	99.81	1	0.497	0.017	0.066	0.002	0.456	0.0550	0.0014	404	57	409	12	409	14	99.9
FLC-6 - 9b - 1	1.79E+08	349	27.2	12.83	3	11	366.7	7400	99.67	1	0.508	0.023	0.066	0.003	0.244	0.0557	0.0021	417	81	416	16	413	16	99.4
FLC-6 - 10	1.76E+08	76.2	41.4	1.84	5	8	159.6	854	100.13	1	0.444	0.043	0.062	0.003	0.122	0.0527	0.0052	250	180	371	30	387	17	104.4
FLC-6 - 11	1.84E+08	902	62.9	14.34	9	9	98.9	6303	99.77	1	0.494	0.015	0.064	0.002	0.155	0.0557	0.0009	430	36	407	10	403	14	98.8
FLC-6 - 12	1.70E+08	823	67.1	12.27	18	9	47.5	2524	99.68	1	0.471	0.015	0.061	0.002	0.200	0.0557	0.0015	427	60	391	11	385	14	98.2
FLC-6 - 15	1.87E+08	736.2	156.3	4.71	29	12	41.4	1603	98.95	1	0.556	0.022	0.064	0.003	0.267	0.0632	0.0017	701	55	448	14	401	15	89.4
FLC-6 - 16	1.64E+08	201	42.6	4.72	2	10	500.0	5335	99.64	1	0.486	0.033	0.064	0.003	0.238	0.0562	0.0035	410	120	399	22	399	15	100.1
FLC-6 - 17	1.73E+08	582	165	3.53	3	8	336.0	13216	99.74	1	0.472	0.025	0.062	0.002	0.324	0.0554	0.0027	412	110	393	17	390	14	99.2
FLC-6 - 18	1.50E+08	1221	108.7	11.23	233	29	12.4	294	94.50	3	0.494	0.074	0.067	0.003	0.501	0.0517	0.0053	686	140	401	50	418	20	104.1
FLC-6 - 19	1.87E+08	450	111.4	4.04	18	9	51.1	1455	99.31	1	0.488	0.020	0.060	0.002	0.399	0.0594	0.0020	561	73	403	13	376	15	93.4
FLC-6 - 20	1.98E+08	288	109.9	2.62	13	13	100.0	2034	99.66	1	0.821	0.034	0.097	0.004	0.769	0.0608	0.0022	635	80	606	20	598	24	98.7
FLC-6 - 21	2.06E+08	930	60.3	15.42	15	18	120.0	4247	99.81	1	0.559	0.036	0.074	0.003	0.763	0.0554	0.0030	416	120	450	23	457	18	101.6
FLC-6 - 22	1.63E+08	7962	1262	6.31	31	12	38.7	13142	99.85	1	0.454	0.013	0.060	0.002	0.545	0.0553	0.0006	422	24	380	9	375	13	98.7
FLC-6 - 24	1.81E+08	326.1	69	4.73	4	10	250.0	4860	99.67	1	0.480	0.026	0.062	0.002	0.104	0.0562	0.0029	431	110	397	18	390	14	98.2
FLC-6 - 25	2.06E+08	1573	85.1	18.48	23	21	91.3	4261	99.60	1	0.509	0.017	0.064	0.002	0.227	0.0576	0.0012	510	47	418	12	401	14	96.0
FLC-6 - 26	1.73E+08	772	248.2	3.11	111	19	17.1	422	96.50	3	0.434	0.089	0.063	0.003	0.688	0.0488	0.0061	630	150	356	64	396	20	111.2
FLC-6 - 27	1.97E+08	189	26.8	7.05	8	16	200.0	2094	99.17	1	0.861	0.058	0.097	0.004	0.272	0.0646	0.0039	740	130	629	32	594	23	94.4
FLC-6 - 28	2.08E+08	1680	94.8	17.72	13	14	107.7	8369	99.80	1	0.505	0.016	0.066	0.003	0.127	0.0553	0.0011	420	46	415	11	413	15	99.5
FLC-6 - 29	2.08E+08	1170	86.5	13.53	5	17	340.0	14740	99.84	1	0.491	0.018	0.064	0.003	0.362	0.0551	0.0013	411	53	406	12	403	15	99.3
FLC-6 - 34b - 1	2.00E+08	445	65.5	6.79	7	14	200.0	4343	99.74	1	0.560	0.021	0.072	0.003	0.404	0.0559	0.0014	436	59	451	14	449	17	99.5
FLC-6 - 30	1.97E+08	1481	128	11.57	25	17	68.0	3764	99.51	1	0.531	0.018	0.066	0.003	0.101	0.0581	0.0016	524	64	432	12	412	15	95.3
FLC-6 - 31	1.58E+08	229.4	83.4	2.75	12	10	85.3	2523	99.66	1	1.354	0.059	0.144	0.006	0.361	0.0677	0.0022	841	67	867	25	868	32	95.0
FLC-6 - 32	1.97E+08	607	42.7	14.22	-1	18	-1800.0	-37500	99.80	1	0.470	0.023	0.062	0.002	0.155	0.0546	0.0022	380	92	391	16	389	14	99.4
FLC-6 - 33	1.79E+08	1816	2608	0.70	42	10	23.8	2614	99.09	1	0.531	0.017	0.063	0.002	0.429	0.0611	0.0010	635	35	432	11	392	15	90.7

Table B1. Continued.

Sample	Zr90 cps	U (ppm)	Th (ppm)	Th/U	^{204}Pb cps^{1}	2σ error on 204 cps	% error on 204 cps	cps ^{206}Pb/^{204}Pb	%Pb*	C*	Isotopic ratios ^{207}Pb/^{235}U	2σ ±	^{206}Pb/^{238}U	2σ ±	err. corr.	^{207}Pb/^{206}Pb	2σ ±	Calculated ages ^{207}Pb/^{206}Pb	2σ ±	^{207}Pb/^{235}U	2σ ±	^{206}Pb/^{238}U	2σ ±	% conc
FLC-6 - 34_1	1.81E+08	1765	398.8	4.43	127	16	12.6	815	97.64	3	0.452	0.046	0.060	0.003	0.508	0.0541	0.0027	500	71	379	30	374	15	98.6
FLC-6 - 35	1.81E+08	1900	231.6	8.20	61	12	19.7	1848	98.99	1	0.536	0.017	0.062	0.002	0.699	0.0620	0.0009	667	34	436	11	390	14	89.4
FLC-6 - 36	1.66E+08	193.1	52.07	3.71	13	10	76.9	845	99.57	1	0.505	0.025	0.064	0.003	0.030	0.0569	0.0025	459	98	415	18	400	15	96.5
FLC-6 - 37	1.48E+08	3480	37.8	92.06	22	16	72.7	7136	99.56	1	0.420	0.013	0.054	0.002	0.048	0.0561	0.0010	451	40	356	9	340	12	95.4
FLC-6 - 38	1.91E+08	3420	211	16.21	57	30	52.6	3544	99.51	1	0.542	0.060	0.067	0.007	0.386	0.0587	0.0013	553	34	440	21	416	36	94.5
FLC-6 - 39	1.88E+08	605	121.3	4.99	14	11	78.6	2621	99.55	1	0.504	0.026	0.064	0.003	0.635	0.0568	0.0023	472	90	414	18	401	16	96.8
FLC-6 - 40	1.46E+08	1782	151.7	11.75	54	17	31.5	1450	98.89	1	0.526	0.019	0.061	0.003	0.589	0.0628	0.0014	693	47	428	13	380	15	88.6
FLC-6 - 41	1.49E+08	539	119.6	4.51	17	11	64.7	1824	99.36	1	0.631	0.028	0.076	0.003	0.463	0.0606	0.0021	604	77	495	17	469	18	94.8
FLC-6 - 42	1.76E+08	333.6	37.06	9.00	0	10			99.82	1	0.484	0.023	0.064	0.003	0.127	0.0550	0.0021	390	85	400	16	399	15	99.9
FLC-6 - 43	1.96E+08	417.7	80.8	5.17	18	15	83.3	1371	99.65	1	0.451	0.025	0.059	0.003	0.518	0.0559	0.0023	430	88	377	17	367	16	97.4
FLC-6 - 44	2.01E+08	802	25.69	31.22	-6	16	-266.7	-8983	99.49	1	0.572	0.022	0.071	0.003	0.116	0.0588	0.0020	548	74	459	14	442	17	96.2
FLC-6 - 46	1.73E+08	168.1	302	0.56	23	12	52.2	614	97.96	1	0.944	0.036	0.091	0.004	0.107	0.0754	0.0022	1063	58	673	19	563	21	83.6
FLC-6 - 47	1.77E+08	1109	1245	0.89	92	13	14.1	815	97.93	1	0.733	0.027	0.073	0.003	0.357	0.0728	0.0021	1000	58	557	17	456	16	81.8
FLC-6 - 48	1.76E+08	367	100.7	3.64	37	11	29.7	595	98.37	1	0.621	0.032	0.067	0.003	0.732	0.0681	0.0025	852	78	488	19	416	17	85.1
FLC-6 - 49	1.69E+08	328.8	132.7	2.48	50	11	22.0	369	96.03	1	0.753	0.034	0.063	0.003	0.095	0.0862	0.0033	1316	66	567	20	396	15	69.9
FLC-6 - 50	1.62E+08	230	62.4	3.69	9	11	122.2	1430	99.76	1	0.489	0.025	0.064	0.003	0.322	0.0553	0.0024	393	93	402	18	401	15	99.7
FLC-6 - 51	1.99E+08	1690	33.4	50.60	4	18	450.0	27725	99.84	1	0.553	0.025	0.071	0.003	0.673	0.0563	0.0016	457	64	446	16	445	18	99.7
FLC-6 - 52	1.58E+08	449	69	6.51	24	14	58.3	1021	98.91	1	0.551	0.025	0.064	0.003	0.006	0.0630	0.0025	685	82	445	16	399	15	89.7
FLC-6 - 53	1.71E+08	355	45.3	7.84	6	8	135.0	3550	99.81	1	0.515	0.021	0.067	0.003	0.247	0.0557	0.0017	420	65	421	14	420	16	99.7
FLC-6 - 54	1.78E+08	166.7	43	3.88	3	9	348.1	3789	99.53	1	0.519	0.024	0.066	0.003	0.156	0.0570	0.0022	460	83	423	16	414	15	97.8
Rumford pluton RUM-1																								
RUM-1 - 4-junk	~~*6.24E+07*~~	712	63.7	0.09	154	18	12	89	100	-	0.53	0.077	0.0643	0.0023	0.8676	0.039	0.027	1990	200	402	14	490	51	82.0
RUM-1 - 1	*1.33E+08*	230.7	181.8	0.79	-7	14	-200	-1074	100	1	0.47	0.021	0.062	0.0008	0.196	0.056	0.0024	470	86	388	5	394	14	98.5
RUM-1 - 2	*1.22E+08*	323	229	0.71	-9	11	-122	-1096	100	1	0.453	0.015	0.06015	0.001	0.0472	0.0551	0.0019	413	76	376.5	5.9	380	10	99.1
RUM-1 - 3	*1.29E+08*	320	104.3	0.33	1	13	1300	11300	100	1	0.482	0.022	0.0629	0.0011	0.0455	0.056	0.0026	450	99	393.1	6.8	397	15	99.0
RUM-1 - 5	*1.23E+08*	492.6	509	1.03	3.5	8.7	249	4240	100	1	0.436	0.012	0.05928	0.0008	0.0347	0.0537	0.0015	341	62	371.2	4.8	366.5	8.2	101.3
RUM-1 - 6	*1.25E+08*	849	158.8	0.19	22	11	50	1236	100	1	0.559	0.016	0.06221	0.001	0.5382	0.0657	0.0014	785	43	389	5.9	449	11	86.6
RUM-1 - 7	*1.24E+08*	763	931	1.22	13	11	85	1818	100	1	0.481	0.01	0.06034	0.0007	0.2499	0.0586	0.0012	550	48	377.7	4.3	398.1	7.1	94.9
RUM-1 - 8	*1.32E+08*	225	218.4	0.97	12	13	108	633	100	1	0.492	0.018	0.0637	0.0011	0.0317	0.0559	0.0022	430	84	398.2	6.8	404	12	98.6
RUM-1 - 9	*1.36E+08*	286.3	399.9	1.40	4	15	375	2318	100	1	0.463	0.018	0.0595	0.0009	0.2054	0.057	0.0023	450	87	372.4	5.3	385	13	96.7
RUM-1 - 10	*1.33E+08*	140	100	0.71	-10	16	-160	-479	100	1	0.504	0.028	0.0642	0.0013	0.0954	0.0566	0.0036	470	120	402.5	7.8	412	19	97.7
RUM-1 - 11	*1.19E+08*	253.9	244	0.96	18	17	94	427	100	1	0.455	0.022	0.05935	0.0009	0.2247	0.0563	0.0027	440	95	371.7	5.4	379	15	98.1
RUM-1 - 12	*1.23E+08*	459	423	0.92	2	10	500	6965	100	1	0.448	0.011	0.05964	0.0008	0.0498	0.0556	0.0016	422	63	373.4	4.6	376.2	8.2	99.3
Songo pluton SG-7b																								
SG-7B - 1	1.14E+08	278.2	67.4	4.13	-3	11	-367	-4113	99.68	1	0.429	0.014	0.057	0.001	0.207	0.0549	0.0020	382	77	363	11	360	6	99.1
SG-7B - 2	1.12E+08	286.4	168.2	1.70	1	13	1300	12700	99.79	1	0.438	0.015	0.058	0.001	0.317	0.0544	0.0018	375	72	367	11	363	5	98.8
SG-7B - 3	1.00E+08	372.2	185.4	2.01	8	12	150	1970	99.87	1	0.438	0.017	0.059	0.001	0.152	0.0539	0.0021	345	83	368	12	368	5	100.0
SG-7B - 4	1.09E+08	240.4	135.6	1.77	3	10	333	3503	99.77	1	0.437	0.019	0.058	0.001	0.124	0.0543	0.0023	344	89	366	13	366	6	100.0
SG-7B - 5	1.23E+08	331	55	6.02	2	17	850	7480	99.75	1	0.438	0.023	0.059	0.001	0.135	0.0546	0.0028	370	110	368	16	366	7	99.5
SG-7B - 6	1.05E+08	206.5	145	1.42	18	16	89	502	99.71	1	0.440	0.018	0.059	0.001	0.167	0.0549	0.0025	375	95	372	12	367	6	98.7

Table B1. Continued.

Sample	Zr90 cps	U (ppm)	Th (ppm)	Th/U	^{204}Pb cps[1]	2σ error on 204 cps	% error on 204 cps	cps $^{206}Pb/^{204}Pb$	%Pb*	C*	Isotopic ratios $^{207}Pb/^{235}U$	2σ ±	$^{206}Pb/^{238}U$	2σ ±	err. corr.	$^{207}Pb/^{206}Pb$	2σ ±	Calculated ages $^{207}Pb/^{206}Pb$	2σ ±	$^{207}Pb/^{235}U$	2σ ±	$^{206}Pb/^{238}U$	2σ ±	% conc
SG-7B - 7	1.07E+08	445.7	244	1.83	14	12	86	1445	99.86	1	0.454	0.012	0.061	0.001	0.052	0.0537	0.0015	339	61	379	9	383	5	101.0
SG-7B - 8	1.11E+08	268.3	192.5	1.39	4	12	300	3063	99.79	1	0.450	0.017	0.060	0.001	0.204	0.0545	0.0020	360	80	376	12	375	5	99.7
SG-7B - 9	1.29E+08	247.3	142.2	1.74	-2	20	-1000	-5920	99.74	1	0.449	0.034	0.059	0.001	0.196	0.0552	0.0041	370	150	374	23	371	8	99.1
SG-7B - 10	1.09E+08	302.9	209.9	1.44	0	14			99.75	1	0.439	0.018	0.059	0.001	0.215	0.0542	0.0022	355	88	368	13	367	6	99.8
SG-7B - 11	1.15E+08	390.1	73.3	5.32	-7	12	-171	-2406	99.62	1	0.412	0.013	0.054	0.001	0.118	0.0553	0.0018	398	71	350	10	339	4	97.0
SG-7B - 12	1.01E+08	272	180	1.51	-7	12	-171	-1561	99.73	1	0.417	0.019	0.056	0.001	0.213	0.0541	0.0024	356	98	353	14	350	5	99.2
SG-7B - 13	1.14E+08	118.8	87.5	1.36	0	13			99.70	1	0.455	0.025	0.060	0.001	0.157	0.0554	0.0031	380	110	378	17	374	7	98.8
SG-7B - 14	1.21E+08	349.8	226.7	1.54	32	18	56	503	97.67	1	0.601	0.026	0.060	0.001	0.118	0.0727	0.0032	979	91	476	17	376	6	79.1
SG-7B - 15	1.07E+08	153.9	84.1	1.83	18	12	67	369	99.80	1	0.434	0.022	0.058	0.001	0.102	0.0538	0.0027	340	110	364	15	363	6	99.7
SG-7B - 16	9.97E+07	333.7	174.5	1.91	8	15	188	1874	99.88	1	0.459	0.020	0.061	0.001	0.104	0.0540	0.0024	344	95	382	14	384	6	100.4
SG-7B - 16b - 1	1.13E+08	223.3	137.7	1.62	-11	11	-100	-953	99.85	1	0.457	0.017	0.062	0.001	0.062	0.0539	0.0021	337	81	380	12	385	6	101.2
SG-7B - 17	1.11E+08	241	125.4	1.92	-4	12	-300	-2700	99.88	1	0.433	0.017	0.058	0.001	0.134	0.0538	0.0022	333	85	363	12	364	5	100.2
SG-7B - 18	1.15E+08	335	264	1.27	-4	13	-325	-3775	99.92	1	0.433	0.015	0.059	0.001	0.017	0.0533	0.0019	335	79	364	11	367	5	100.9
SG-7B - 19	1.35E+08	380.3	187	2.03	3	26	867	6250	99.61	1	0.448	0.023	0.059	0.001	0.191	0.0559	0.0033	420	130	375	16	367	8	98.0
SG-7B - 20	1.02E+08	308.8	227.4	1.36	4	11	275	3313	99.57	1	0.471	0.017	0.060	0.001	0.069	0.0563	0.0020	444	79	391	12	377	5	96.4
SG-7B - 21	1.20E+08	271.6	150	1.81	-1	14	-1400	-12250	99.76	1	0.418	0.017	0.056	0.001	0.406	0.0545	0.0020	368	79	355	11	351	6	99.0
SG-7B - 22	1.08E+08	571	471	1.21	79	16	20	289	93.26	1	0.794	0.031	0.055	0.001	0.389	0.1063	0.0047	1693	90	590	18	343	6	58.1
SG-7B - 23	9.06E+07	891	1275	0.70	-8	20	-250	-3963	99.50	1	0.407	0.012	0.053	0.001	0.030	0.0560	0.0018	440	70	346	9	330	4	95.3
SG-7B - 24	9.90E+07	296	112.2	2.64	-8	14	-175	-1529	99.64	1	0.438	0.019	0.057	0.001	0.069	0.0555	0.0025	405	94	368	13	358	6	97.4
SG-7B - 25	1.13E+08	200	165	1.21	10	15	150	906	99.67	1	0.458	0.022	0.060	0.001	0.152	0.0558	0.0028	430	110	382	16	374	8	97.9
SG-7B - 26	1.10E+08	180.8	115.4	1.57	4	12	300	2055	99.78	1	0.449	0.019	0.060	0.001	0.141	0.0544	0.0023	351	88	375	13	376	6	100.1
SG-7B - 27	1.12E+08	340.3	181	1.88	4	12	300	3583	99.73	1	0.411	0.015	0.055	0.001	0.085	0.0541	0.0020	357	79	349	10	345	5	98.8
SG-7B - 28	1.14E+08	318.3	132.4	2.40	7	10	143	2014	99.95	1	0.414	0.015	0.057	0.001	0.083	0.0530	0.0020	303	78	350	11	355	5	101.5
SG-7B - 29	1.16E+08	340	101.9	3.34	10	13	130	1568	99.93	1	0.424	0.014	0.058	0.001	0.227	0.0530	0.0016	325	67	358	10	362	6	101.0
SG-7B - 30	1.27E+08	281	210	1.34	17	20	118	765	98.95	1	0.508	0.038	0.059	0.001	0.563	0.0626	0.0042	640	140	414	26	367	8	88.7
SG-7B - 31	9.52E+07	255.8	200	1.28	-7	12	-171	-1447	98.48	1	0.554	0.024	0.061	0.001	0.040	0.0657	0.0031	750	100	448	17	384	6	85.6
SG-7B - 32	1.31E+08	168.8	73.8	2.29	-11	15	-136	-741	99.84	1	0.438	0.030	0.060	0.002	0.155	0.0537	0.0037	330	140	367	21	373	11	101.6
SG-7B - 33	1.03E+08	295	137.6	2.14	-8	15	-188	-1628	99.75	1	0.450	0.020	0.060	0.001	0.087	0.0549	0.0026	370	100	379	15	375	6	99.0
SG-7B - 34	1.05E+08	468	341	1.37	16	12	75	1209	98.99	1	0.501	0.017	0.059	0.001	0.433	0.0616	0.0020	630	69	411	12	371	5	90.2
SG-7B - 35	9.39E+07	885	182	4.86	15	18	120	2261	99.27	1	0.439	0.012	0.054	0.001	0.011	0.0586	0.0017	538	65	369	9	341	5	92.3
SG-7B - 36	1.10E+08	151.7	113.9	1.33	-2	11	-550	-3405	100.00	1	0.433	0.019	0.060	0.001	0.163	0.0529	0.0024	294	93	363	14	373	6	102.6
SG-7B - 37	1.12E+08	278.6	66.3	4.20	1	11	1100	12390	99.77	1	0.434	0.018	0.058	0.001	0.105	0.0547	0.0022	368	86	364	12	361	5	99.2
SG-7B - 38	1.28E+08	304	157.8	1.93	13	23	177	1122	99.87	1	0.439	0.022	0.060	0.001	0.264	0.0536	0.0026	330	100	368	15	373	7	101.3
SG-7B - 39	1.12E+08	248	167	1.49	2	13	650	5370	99.82	1	0.427	0.019	0.058	0.001	0.132	0.0540	0.0024	333	90	359	13	361	6	100.5
SG-7B - 40	1.11E+08	268.1	119.2	2.25	17	13	76	720	99.73	1	0.452	0.015	0.060	0.001	0.132	0.0550	0.0019	385	74	377	11	374	5	99.3
SG-7B - 41	1.20E+08	248.7	149	1.67	-2	13	-650	-5960	99.85	1	0.455	0.019	0.061	0.001	0.274	0.0543	0.0022	361	86	380	13	381	5	100.4
SG-7B - 42	9.38E+07	553	575	0.96	3	19	633	6800	99.67	1	0.396	0.017	0.052	0.001	0.193	0.0547	0.0022	384	92	338	12	329	4	97.4
SG-7B - 43	1.12E+08	173.6	102.3	1.70	7	13	186	1113	99.77	1	0.440	0.021	0.058	0.001	0.211	0.0548	0.0025	365	97	368	15	365	6	99.3
SG-7B - 44	1.10E+08	209.8	142.8	1.47	5	13	260	1848	99.16	1	0.469	0.021	0.057	0.001	0.307	0.0598	0.0025	557	90	389	14	357	5	91.6
SG-7B - 44b - 1	1.08E+08	152	91.8	1.66	12	12	100	535	99.91	1	0.433	0.025	0.059	0.001	0.025	0.0538	0.0031	310	110	362	17	367	7	101.3

Table B1. Continued.

Sample	Zr90 cps	U (ppm)	Th (ppm)	Th/U	^{204}Pb cps[1]	2σ error on 204 cps	% error on 204 cps	cps ^{206}Pb/^{204}Pb	%Pb*	C*	Isotopic ratios ^{207}Pb/^{235}U	2σ ±	^{206}Pb/^{238}U	2σ ±	err. corr.	^{207}Pb/^{206}Pb	2σ ±	Calculated ages ^{207}Pb/^{206}Pb	2σ ±	^{207}Pb/^{235}U	2σ ±	^{206}Pb/^{238}U	2σ ±	% conc
SG-7B - 45	1.11E+08	367	120.8	3.04	-5	10	-200	-3240	99.95	1	0.421	0.012	0.057	0.001	0.148	0.0532	0.0015	320	62	356	8	360	5	101.2
SG-7B - 46	1.10E+08	183.4	111.7	1.64	1	12	1200	7940	99.74	1	0.430	0.018	0.058	0.001	0.027	0.0544	0.0024	344	92	362	13	361	6	99.8
SG-7B - 47	1.11E+08	202	112.6	1.79	-1	12	-1200	-8610	99.89	1	0.426	0.017	0.058	0.001	0.062	0.0538	0.0022	334	87	359	12	361	6	100.6
SG-7B - 48	1.10E+08	224.6	111.9	2.01	4	11	275	2590	100.00	1	0.450	0.018	0.061	0.001	0.266	0.0533	0.0020	314	80	375	13	383	6	102.1
SG-7B - 49	1.14E+08	357	306	1.17	0	12			99.54	1	0.430	0.014	0.056	0.001	0.073	0.0557	0.0019	425	70	362	10	352	5	97.3
SG-7B - 50	1.16E+08	265.3	142.8	1.86	9	11	122	1341	99.83	1	0.430	0.015	0.058	0.001	0.201	0.0538	0.0019	338	75	362	11	364	5	100.5
North Jay pluton NJq-1																								
~~NJq-1 - 8~~	~~*176*~~	~~5E+09~~	~~6E+10~~	~~11.61~~	~~-6~~	~~12~~	~~-200~~	~~-40167~~	~~100~~	~~1~~	~~0.418~~	~~0.0085~~	~~0.05612~~	~~0.0008~~	~~0.3742~~	~~0.0542~~	~~0.0012~~	~~382~~	~~51~~	~~352~~	~~4.7~~	~~354.4~~	~~6.1~~	~~99.3~~
NJq-1 - 1	*1.33E+08*	842	913	1.08	263	25	10	125	100	2	0.488	0.046	0.061	0.0018	0.7316	0.059	0.017	1230	290	381.7	11	371	85	102.9
NJq-1 - 3	*1.38E+08*	746	49.2	0.07	33	14	42	873	100	2	0.457	0.02	0.06852	0.0014	0.6048	0.0491	0.012	1050	250	427.2	8.3	398	29	107.3
NJq-1 - 4	*1.20E+08*	5438	269.8	0.05	34	14	41	4909	100	2	0.437	0.0097	0.06139	0.0008	0.0308	0.0513	0.0029	375	100	384.1	4.9	367	92	104.7
NJq-1 - 5	*1.40E+08*	431.4	47.7	0.11	33	15	45	1339	100	2	2.04	0.098	0.1809	0.0067	0.4939	0.0822	0.0065	1260	130	1072	36	1133	120	94.6
NJq-1 - 7	*1.56E+08*	5340	222.5	0.04	287	32	11	602	100	2	0.393	0.027	0.0546	0.0016	0.5241	0.053	0.0033	450	81	342.5	9.8	335	85	102.2
NJq-1 - 9	*1.20E+08*	701.3	565	0.81	162	19	12	248	100	2	0.76	0.065	0.1103	0.0022	0.6157	0.0489	0.0084	1030	180	674.4	13	553	33	122.0
NJq-1 - 10	*1.34E+08*	1035	69.6	0.07	3	11	367	26033	100	1	1.334	0.029	0.14176	0.002	0.3031	0.0688	0.0016	896	47	854.5	11	860.9	13	99.3
NJq-1 - 11	*1.33E+08*	1313	139.7	0.11	143	18	13	324	100	2	0.436	0.034	0.06298	0.0011	0.4102	0.0494	0.0064	700	130	393.7	6.7	367	0	107.3
NJq-1 - 12	*1.41E+08*	1291	166.2	0.13	-1	15	-1500	-42940	100	1	0.445	0.012	0.0608	0.0009	0.1444	0.0534	0.0015	337	65	380.5	5.7	373.4	8.2	101.9
NJq-1 - 14	*1.16E+08*	466	387	0.83	12	24	200	2040	100	1	0.936	0.03	0.1095	0.0023	0.255	0.061	0.0017	649	68	670	14	670	17	100.0
NJq-1 - 15	*1.11E+08*	2241	105.2	0.05	623	59	9	151	100	2	0.591	0.2	0.0798	0.0016	0.4086	0.0521	0.0043	560	110	495	9.6	479	79	103.3
NJq-1 - 16	*1.20E+08*	3592	322	0.09	1185	59	5	108	100	2	0.519	0.11	0.0608	0.0006	0.4636	0.0598	0.003	790	88	380.6	3.7	417	66	91.3
NJq-1 - 18	*1.20E+08*	966	214.3	0.22	90	20	22	267	100	2	0.38	0.023	0.0465	0.0012	0.5969	0.059	0.014	1260	220	293.2	7.3	323	57	90.8
NJq-1 - 19	*1.04E+08*	1209	245	0.20	26	15	58	1161	100	1	0.508	0.014	0.05841	0.0009	0.1014	0.0636	0.0019	720	65	366	5.2	418	9.3	87.6
NJq-1 - 20	*1.44E+08*	962	146.5	0.15	18	13	72	1779	100	1	0.437	0.012	0.05948	0.0009	0.1485	0.0536	0.0016	358	68	372.4	5.6	367.5	8.5	101.3
NJq-1 - 22	*1.30E+08*	257.8	74.9	0.29	-20	12	-60	-403	100	1	0.427	0.018	0.0589	0.0011	0.297	0.0534	0.0023	335	90	368.9	6.9	365	14	101.1
NJq-1 - 23	*1.45E+08*	870	139.7	0.16	45	15	33	1338	100	2	1.558	0.085	0.1201	0.005	0.5218	0.097	0.0071	1558	130	731	28	955	59	76.5
NJq-1 - 24	*1.05E+08*	864	900	1.04	350	30	9	81	100	2	0.35	0.094	0.0594	0.0015	0.6567	0.044	0.014	1300	280	372	8.8	320	89	116.3
NJq-1 - 25	*1.33E+08*	2000	85.5	0.04	-14.4	9.6	-67	-4806	100	1	0.463	0.012	0.06222	0.001	0.5472	0.0547	0.0015	388	60	389.1	5.8	385.7	8	100.9
NJq-1 - 26	*1.26E+08*	490.1	396.1	0.81	116	19	16	146	100	2	0.55	0.1	0.058	0.0014	0.7733	0.063	0.017	1640	240	363.4	8.3	380	95	95.6
NJq-1 - 27	*1.48E+08*	346	237.5	0.69	2	15	750	5815	100	1	0.44	0.017	0.05815	0.001	0.0345	0.0556	0.0022	420	87	364.4	5.9	369	12	98.8
NJq-1 - 29	*1.19E+08*	314	213	0.68	22	18	82	1161	100	1	2.096	0.11	0.1617	0.0081	0.7203	0.0942	0.0027	1527	54	965	46	1149	43	84.0
NJq-1 - 31	*1.25E+08*	2270	813	0.36	121	21	17	727	100	2	0.577	0.032	0.07232	0.0014	0.4925	0.0579	0.0031	630	99	450.1	8.3	459	120	98.1
NJq-1 - 32	*1.39E+08*	2140	130.5	0.06	14	13	93	5114	100	1	0.444	0.016	0.06018	0.0013	0.3565	0.0542	0.0016	374	62	376.7	8.1	372.5	11	101.1
NJq-1 - 33	*1.19E+08*	547.3	362	0.66	56	16	29	440	100	2	0.75	0.067	0.0869	0.0019	0.459	0.062	0.011	1220	150	537	12	480	120	111.9
Cape Cod Hill pluton CCH-1																								
CCH-1 - 1	*1.16E+08*	829	6	0.29	2.5	9.8	392	9356	100	1	0.43	0.011	0.05874	0.0007	0.2906	0.0531	0.0012	333	50	365.5	8.1	368.3	4.2	100.8
CCH-1 - 2	*1.17E+08*	631	3	0.05	-5	11	-220	-4040	100	1	0.483	0.015	0.06344	0.001	0.4403	0.0551	0.0014	405	56	399.2	10	396.5	5.9	99.3
CCH-1 - 3	*1.16E+08*	457	0	0.04	-5	12	-240	-2652	100	1	0.438	0.014	0.05973	0.0008	0.1825	0.0533	0.0016	326	66	369.2	9.8	373.9	4.6	101.3
CCH-1 - 4	*8.53E+07*	589	1	0.04	-10	19	-190	-1391	100	1	0.538	0.019	0.0701	0.0009	0.2101	0.0562	0.0019	430	78	436	13	436.5	5.2	100.1
CCH-1 - 5	*1.17E+08*	334	0	0.04	-9	11	-122	-1072	100	1	0.447	0.017	0.05876	0.0008	0.1537	0.0548	0.0019	393	77	374	12	368.1	4.6	98.4
CCH-1 - 6	*1.19E+08*	3400	12	0.06	47	14	30	2166	100	2	0.439	0.015	0.0605	0.0015	0.3682	0.0544	0.0022	515	62	369	87	378.7	8.8	102.6

Table B1. Continued.

Sample	Zr90 cps	U (ppm)	Th (ppm)	Th/U	^{204}Pb cps^{1}	2σ error on 204 cps	% error on 204 cps	cps ^{206}Pb/^{204}Pb	%Pb*	C*	Isotopic ratios ^{207}Pb/^{235}U	2σ ±	^{206}Pb/^{238}U	2σ ±	err. corr.	^{207}Pb/^{206}Pb	2σ ±	Calculated ages ^{207}Pb/^{206}Pb	2σ ±	^{207}Pb/^{235}U	2σ ±	^{206}Pb/^{238}U	2σ ±	% conc
CCH-1 - 7	*1.14E+08*	780	8	0.13	86	13	15	266	100	2	0.46	0.19	0.0605	0.0016	0.8392	0.06	0.02	1180	220	420	25	378.4	9.7	90.1
CCH-1 - 8	*1.16E+08*	1980	3	0.04	-1	12	-1200	-61000	100	1	0.487	0.012	0.0638	0.0014	0.7361	0.0553	0.00085	418	33	402.3	8	398.3	8.8	99.0
CCH-1 - 9	*1.17E+08*	611	5	0.50	-1	11	-1100	-17790	100	1	0.436	0.012	0.05933	0.0007	0.0808	0.0535	0.0014	352	59	367.8	8.5	371.5	3.9	101.0
CCH-1 - 10	*1.20E+08*	357	5	0.48	-2	10	-500	-5390	100	1	0.476	0.016	0.05971	0.0007	0.0892	0.0569	0.0019	473	73	397	11	373.9	4.4	94.2
CCH-1 - 11	*1.19E+08*	337	7	0.65	1	13	1300	10100	100	1	0.482	0.017	0.05991	0.0008	0.0618	0.0584	0.002	520	74	400	11	375	4.9	93.8
CCH-1 - 12	*1.29E+08*	*240*	*2*	*0.38*	*-13*	*18*	*-138*	*-1565*	*100*	*1*	*1.654*	*0.052*	*0.1661*	*0.002*	*0.371*	*0.0714*	*0.0021*	*976*	*61*	*992*	*20*	*990*	*12*	*99.8*
CCH-1 - 13	*1.32E+08*	843	6	0.24	14	21	150	1981	100	1	0.482	0.014	0.06336	0.0007	0.148	0.0557	0.0013	457	50	401	9.6	396	4.3	98.8
CCH-1 - 14	*1.31E+08*	261	14	0.49	4	17	425	2055	100	1	0.458	0.016	0.0605	0.0009	0.0364	0.0548	0.0021	400	79	381	11	378.5	5.4	99.3
CCH-1 - 15	*1.27E+08*	1520	15	0.04	10	14	140	4910	100	1	0.49	0.012	0.0637	0.001	0.7306	0.0558	0.00099	443	39	404.1	8.3	398.2	6.2	98.5
CCH-1 - 16	*1.20E+08*	13190	12	0.01	79	20	25	4823	100	2	0.438	0.0083	0.05901	0.0006	0.2992	0.0537	0.0012	361	40	370.1	150	369.6	3.7	99.9
CCH-1 - 17	*1.19E+08*	510	30	0.76	4.4	9.7	220	3584	100	1	0.458	0.014	0.06173	0.0009	0.2489	0.0543	0.0016	373	65	382.3	9.4	386.1	5.5	101.0
CCH-1 - 18	*1.24E+08*	3120	100	0.29	34	17	50	2524	100	2	0.393	0.0084	0.05387	0.0007	0.4616	0.0532	0.0025	501	76	337	50	338.2	4.3	100.4
CCH-1 - 19	*1.24E+08*	217	19	0.74	3	10	333	2150	100	1	0.449	0.018	0.0592	0.0011	0.0619	0.0555	0.0022	420	89	377	13	370.6	6.5	98.3
CCH-1 - 20	*1.26E+08*	160	4	0.57	8	12	150	601	100	1	0.433	0.025	0.0573	0.0012	0.0188	0.0545	0.0031	330	110	362	18	359.2	7.3	99.2
CCH-1 - 21	*1.19E+08*	641	6	0.49	-2	11	-550	-9590	100	1	0.442	0.013	0.05868	0.0007	0.0699	0.0544	0.0015	378	62	371.1	9.1	367.6	4.5	99.1
CCH-1 - 22	*1.19E+08*	1349	7	0.10	-5	11	-220	-8272	100	1	0.45	0.0093	0.06026	0.0006	0.1481	0.0544	0.00098	384	41	376.8	6.5	377.2	3.7	100.1
CCH-1 - 23	*1.19E+08*	281	2	0.49	2	11	550	4140	100	1	0.44	0.017	0.05872	0.0008	0.1115	0.0535	0.0021	358	84	370	12	367.8	5.1	99.4
CCH-1 - 24	*1.10E+08*	619	29	0.69	1	13	1300	16630	100	1	0.42	0.012	0.05616	0.0008	0.2483	0.0538	0.0014	346	58	355	8.8	352.2	4.8	99.2
CCH-1 - 25	*1.22E+08*	1890	5	0.05	1	11	1100	57800	100	1	0.458	0.011	0.0601	0.0011	0.7498	0.0551	0.00087	419	36	382	7.7	376.2	6.7	98.5
CCH-1 - 26	*1.20E+08*	823	2	0.03	-4	10	-250	-6875	100	1	0.498	0.012	0.0657	0.001	0.3062	0.0547	0.0012	385	47	410	8.3	410.2	5.7	100.0
CCH-1 - 27	*1.16E+08*	4570	12	0.02	1	11	1100	143000	100	1	0.471	0.0098	0.06347	0.001	0.7811	0.054	0.00062	371	25	392.4	6.6	396.6	6	101.1
CCH-1 - 28	*1.14E+08*	5080	5	0.02	-5.3	9.6	-181	-28868	100	1	0.466	0.0077	0.0617	0.0006	0.49	0.0544	0.00057	390	23	388	5.3	386.2	3.5	99.5
CCH-1 - 29	*1.24E+08*	283	3	0.68	4	13	325	2180	100	1	0.493	0.022	0.0602	0.0009	0.0242	0.0594	0.0027	550	90	405	15	376.7	5.5	93.0
CCH-1 - 30	*1.17E+08*	190	12	0.75	-5.4	8.7	-161	-1081	100	1	0.451	0.023	0.06149	0.001	0.3547	0.0532	0.0025	305	96	380	16	384.6	6.2	101.2
CCH-1 - 31	*1.24E+08*	487	0	0.04	2	10	500	7560	100	1	0.464	0.013	0.0611	0.0008	0.0356	0.0553	0.0016	402	63	387.6	9	382.3	4.8	98.6
CCH-1 - 32	*1.19E+08*	311	4	0.62	7	12	171	1333	100	1	0.458	0.02	0.05972	0.001	0.1466	0.0548	0.0023	407	91	381	14	373.9	5.9	98.1
CCH-1 - 33	*1.04E+08*	1440	5	0.21	9	23	256	4473	100	1	0.458	0.011	0.06071	0.0007	0.3674	0.0546	0.0016	398	55	382.9	7.5	379.9	4.4	99.2
CCH-1 - 34	*1.17E+08*	132	4	0.69	-5	11	-220	-810	100	1	0.462	0.028	0.0611	0.0012	0.1448	0.056	0.0032	420	120	383	20	382.4	7.3	99.8
CCH-1 - 35	*1.20E+08*	313	5	0.61	4.8	9.4	196	2006	100	1	0.445	0.019	0.06096	0.0008	0.2131	0.0525	0.0024	286	91	374	14	381.4	4.9	102.0
CCH-1 - 36	*1.15E+08*	858	2	0.10	4	15	375	6075	100	1	0.487	0.016	0.05994	0.0007	0.4065	0.0591	0.0017	566	60	402	11	375.3	4.4	93.4
CCH-1 - 37	*1.22E+08*	3150	15	0.15	33	12	36	2961	100	2	0.451	0.013	0.05979	0.0008	0.3681	0.0547	0.0021	523	61	377	82	374.3	5.1	99.3
CCH-1 - 38	*1.19E+08*	1025	7	0.12	19	11	58	1621	100	1	0.454	0.011	0.06052	0.0006	0.0642	0.0542	0.0012	365	49	380.6	7.4	378.8	3.7	99.5
CCH-1 - 39	*1.18E+08*	361	18	1.03	7	12	171	1450	100	1	0.432	0.019	0.05684	0.0008	0.1988	0.0547	0.0024	370	92	363	13	356.3	5.1	98.2
CCH-1 - 40	*1.19E+08*	194	7	0.70	-3	10	-333	-1887	100	1	0.434	0.021	0.05852	0.001	0.0223	0.0532	0.0027	310	100	367	15	366.5	6.1	99.9
CCH-1 - 41	*1.18E+08*	385	2	0.33	-1.2	9.9	-825	-9417	100	1	0.442	0.018	0.0591	0.0007	0.2146	0.0534	0.0021	352	78	370	12	370.1	4.5	100.0
CCH-1 - 42	*1.18E+08*	1370	3	0.06	-3	11	-367	-14633	100	1	0.471	0.013	0.06242	0.001	0.5941	0.0552	0.0011	412	44	391	9.2	390.3	6.1	99.8
CCH-1 - 43	*1.25E+08*	2722	16	0.14	24	14	58	3368	100	1	0.468	0.0084	0.05786	0.0005	0.3202	0.0586	0.00078	556	29	391.2	5.8	362.6	3.1	92.7
CCH-1 - 44	*1.27E+08*	914	3	0.22	41	19	46	1024	100	2	0.843	0.084	0.0884	0.0058	0.646	0.0715	0.0052	1020	110	629	39	546	33	86.8
CCH-1 - 45	*1.17E+08*	681	1	0.04	-3	11	-367	-6937	100	1	0.465	0.013	0.062	0.0007	0.1291	0.054	0.0013	365	56	387	8.7	387.7	4	100.2
CCH-1 - 46	*1.21E+08*	320	1	0.19	-1	14	-1400	-10070	100	1	0.452	0.016	0.06132	0.0009	0.2707	0.0531	0.0019	310	76	377	12	383.6	5.5	101.8

Table B1. Continued.

Sample	Zr90 cps	U (ppm)	Th (ppm)	Th/U	^{204}Pb cps[1]	2σ error on 204 cps	% error on 204 cps	cps $^{206}Pb/^{204}Pb$	%Pb*	C*	Isotopic ratios $^{207}Pb/^{235}U$	2σ ±	$^{206}Pb/^{238}U$	2σ ±	err. corr.	$^{207}Pb/^{206}Pb$	2σ ±	Calculated ages $^{207}Pb/^{206}Pb$	2σ ±	$^{207}Pb/^{235}U$	2σ ±	$^{206}Pb/^{238}U$	2σ ±	% conc
CCH-1 - 47	*1.09E+08*	458	3	0.24	-16	12	-75	-1952	100	1	1.462	0.034	0.1437	0.0017	0.1559	0.0741	0.0015	1041	40	918	13	866	9.4	94.3
CCH-1 - 48	*1.23E+08*	1234	18	0.17	10	12	120	3923	100	1	0.493	0.011	0.06192	0.0006	0.0142	0.0575	0.0012	511	45	406.6	7.7	387.3	3.8	95.3
CCH-1 - 49	*1.28E+08*	3640	1	0.01	6	16	267	18517	100	1	0.458	0.0082	0.05884	0.0008	0.473	0.0564	0.00057	467	23	383.5	5.6	368.6	4.8	96.1
CCH-1 - 50	*1.32E+08*	6620	3	0.01	-9	20	-222	-24222	100	1	0.46	0.0095	0.06269	0.0009	0.4455	0.0536	0.00058	351	25	385.2	6.4	391.9	5.7	101.7
Norridgewock DHq-1																								
DHq-1 - 1	1.29E+08	296	2.4	0.41	18	13	72	522	100	1	0.697	0.027	0.06059	0.0009	0.0688	0.0841	0.0034	1295	83	534	16	379.8	5.5	71.1
DHq-1 - 2	1.36E+08	279	1.9	0.47	-1	11	-1100	-9350	100	1	0.454	0.016	0.06193	0.001	0.0191	0.0538	0.0021	333	82	380	11	387.3	5.8	101.9
DHq-1 - 3	1.26E+08	550	12	0.36	-6	12	-200	-2850	100	1	0.45	0.02	0.06	0.0009	0.1769	0.0549	0.0023	405	93	378	14	375.4	5.7	99.3
DHq-1 - 4	1.47E+08	195	9.4	0.66	-3	15	-500	-2100	100	1	0.43	0.024	0.0581	0.001	0.2923	0.056	0.003	400	110	368	16	364	6.3	98.9
DHq-1 - 5	1.50E+08	187	6.3	0.53	1	15	1500	6670	100	1	0.573	0.031	0.0616	0.0011	0.1533	0.0682	0.0037	900	100	456	19	385.3	6.9	84.5
DHq-1 - 6	9.44E+07	256	32	0.80	13	18	138	608	100	1	0.821	0.03	0.0803	0.0017	0.2768	0.0755	0.0025	1050	69	610	18	498	10	81.6
DHq-1 - 7	1.35E+08	297	4.6	0.53	5.4	9.3	172	1798	100	1	0.45	0.017	0.06063	0.0008	0.0212	0.0537	0.0021	345	83	377	11	379.4	4.9	100.6
DHq-1 - 8	1.46E+08	260.2	4.8	0.46	6	19	317	1492	100	1	0.612	0.049	0.0607	0.001	0.4178	0.0739	0.0054	1020	110	490	28	379.8	5.9	77.5
DHq-1 - 9	1.35E+08	455.6	6.9	0.65	1	13	1300	15040	100	1	0.462	0.012	0.05981	0.0007	0.0234	0.0555	0.0016	427	62	384.8	8.2	374.9	4.3	97.4
DHq-1 - 10	1.39E+08	386.8	3.2	0.38	-4	23	-575	-3288	100	1	0.463	0.021	0.0617	0.0009	0.135	0.0562	0.0024	440	86	390	14	385.9	5.5	98.9
DHq-1 - 11	1.34E+08	220.6	2	0.41	-6.9	9.3	-135	-1045	100	1	0.459	0.017	0.06034	0.0008	0.1245	0.0546	0.0022	383	85	382	11	377.7	4.8	98.9
DHq-1 - 12	1.31E+08	173	3.1	0.38	6	12	200	952	100	1	0.436	0.02	0.0617	0.0011	0.0784	0.0517	0.0025	240	95	367	14	385.9	6.7	105.1
DHq-1 - 13	1.27E+08	283.7	8.8	0.60	-22	11	-50	-415	100	1	0.442	0.019	0.0607	0.0011	0.0999	0.0514	0.0022	280	89	374	13	379.6	6.6	101.5
DHq-1 - 14	1.38E+08	2740	14	0.18	21	14	67	4552	100	1	0.492	0.01	0.06273	0.0008	0.5156	0.057	0.00082	484	31	406.2	6.9	392.2	4.7	96.6
DHq-1 - 15	1.27E+08	237.1	3.7	0.65	-7	11	-157	-1056	100	1	0.444	0.019	0.05885	0.001	0.0313	0.0545	0.0025	360	97	374	13	368.6	5.8	98.6
DHq-1 - 16	1.43E+08	759	44	0.99	17	17	100	1446	100	1	0.44	0.013	0.05737	0.0007	0.2377	0.0546	0.0017	412	64	370	9.1	359.6	4	97.2
DHq-1 - 17	1.32E+08	246.8	2.3	0.56	13	12	92	605	100	1	0.436	0.019	0.0581	0.0009	0.0999	0.0536	0.0027	360	99	366	13	364.1	5.6	99.5
DHq-1 - 13b - 1	1.18E+08	360.4	2.4	0.39	1	18	1800	10620	100	1	0.445	0.022	0.05874	0.0009	0.1271	0.0541	0.0027	400	96	372	15	367.9	5.2	98.9
DHq-1 - 18	1.40E+08	281	1.6	0.59	-11	11	-100	-854	100	1	0.446	0.016	0.0592	0.0009	0.05	0.054	0.0021	357	83	375	11	371	5.5	98.9
DHq-1 - 19	1.48E+08	401	14	0.56	5	13	260	2738	100	1	0.45	0.015	0.06	0.0008	0.1136	0.0554	0.0019	390	71	379	10	375.6	4.9	99.1
DHq-1 - 20	1.30E+08	861.1	6.6	0.70	7.5	9.4	125	3688	100	1	0.49	0.0099	0.06045	0.0007	0.0997	0.0583	0.0012	543	46	404.6	6.7	378.4	4.2	93.5
DHq-1 - 21	1.37E+08	418	8.6	0.70	23	14	61	578	100	1	0.44	0.02	0.05846	0.0008	0.0798	0.0541	0.0025	345	92	369	14	366.2	4.6	99.2
DHq-1 - 22	1.31E+08	302.9	1.5	0.31	-1	11	-1100	-10050	100	1	0.542	0.021	0.06165	0.0009	0.2781	0.0633	0.0023	705	80	439	14	385.6	5.6	87.8
DHq-1 - 23	1.32E+08	354.8	3.6	0.56	15	11	73	753	100	1	0.445	0.015	0.05986	0.0008	0.1928	0.0545	0.0018	373	71	374	11	374.7	5	100.2
DHq-1 - 24	1.39E+08	330	8.1	0.62	4	14	350	2703	100	1	0.447	0.017	0.05845	0.0011	0.1796	0.0553	0.0019	412	74	375	12	366.2	6.3	97.7
DHq-1 - 25	1.40E+08	323.1	1.8	0.49	-1	11	-1100	-10640	100	1	0.45	0.014	0.059	0.0008	0.2507	0.0555	0.002	400	78	376	10	369.2	5.1	98.2
DHq-1 - 26	1.35E+08	156.1	3.5	0.68	22	11	50	227	100	1	0.473	0.033	0.0603	0.0011	0.065	0.0581	0.0038	500	120	391	22	377.2	6.7	96.5
DHq-1 - 27	1.33E+08	383.5	10	0.62	-3	11	-367	-3917	100	1	0.46	0.015	0.0577	0.0008	0.1717	0.058	0.0019	506	73	383	11	361.6	5.1	94.4
DHq-1 - 28	1.30E+08	239	9.4	0.54	0.3	9.1	3033	24567	100	1	0.436	0.017	0.0582	0.0009	0.2433	0.0539	0.002	346	81	369	12	364.6	5.3	98.8
DHq-1 - 29	1.30E+08	347.8	9.1	0.53	1	11	1100	11150	100	1	0.449	0.016	0.06006	0.0008	0.1285	0.0538	0.0019	353	76	375	11	375.9	5.1	100.2
DHq-1 - 30	1.34E+08	253.3	2	0.52	-8.1	9.2	-114	-1010	100	1	0.452	0.019	0.05983	0.0009	0.081	0.0559	0.0024	423	93	379	14	374.6	5.5	98.8
DHq-1 - 31	1.28E+08	433.5	2.7	0.61	14	12	86	963	100	1	0.52	0.015	0.05927	0.0008	0.1047	0.0634	0.0021	711	68	424	10	371.1	4.9	87.5
DHq-1 - 32	1.27E+08	735	26	0.44	84	18	21	268	100	2	0.35	0.031	0.0552	0.0013	0.7214	0.046	0.012	1100	180	310	110	346.2	7.7	111.7
DHq-1 - 33	1.29E+08	192.8	1.8	0.44	5	13	260	1252	100	1	0.468	0.019	0.0617	0.0011	0.2787	0.0555	0.0025	390	95	391	14	386.1	6.6	98.7
DHq-1 - 34	1.29E+08	221.5	5.2	0.60	7	10	143	1016	100	1	0.461	0.021	0.06041	0.0009	0.0144	0.0547	0.0025	400	100	384	15	378.1	5.3	98.5

Table B1. Continued.

Sample	Zr90 cps	U (ppm)	Th (ppm)	Th/U	^{204}Pb cps[1]	2σ error on 204 cps	% error on 204 cps	cps ^{206}Pb/^{204}Pb	%Pb*	C*	Isotopic ratios ^{207}Pb/^{235}U	2σ ±	^{206}Pb/^{238}U	2σ ±	err. corr.	^{207}Pb/^{206}Pb	2σ ±	Calculated ages ^{207}Pb/^{206}Pb	2σ ±	^{207}Pb/^{235}U	2σ ±	^{206}Pb/^{238}U	2σ ±	% conc
DHq-1 - 35	1.38E+08	241.6	6.7	0.64	13	11	85	622	100	1	0.458	0.019	0.0608	0.0011	0.0927	0.0537	0.0026	410	93	385	13	380.3	6.5	98.8
DHq-1 - 36	1.28E+08	381.8	12	1.13	17	11	65	707	100	1	0.451	0.016	0.05971	0.0007	0.0186	0.0551	0.002	401	79	380	11	373.8	4.4	98.4
DHq-1 - 37	1.29E+08	227.9	3.2	0.63	18	16	89	392	100	1	0.424	0.022	0.0564	0.001	0.1028	0.0561	0.0029	420	100	357	16	353.9	6	99.1
DHq-1 - 38	1.30E+08	325.8	3.4	0.51	4	10	250	2763	100	1	0.488	0.017	0.06364	0.001	0.1351	0.0557	0.0019	445	78	403	12	397.7	6	98.7
DHq-1 - 39	1.36E+08	180	4.4	0.56	24	14	58	252	100	1	0.458	0.035	0.0602	0.0012	0.258	0.0539	0.0043	400	140	381	24	376.6	7.4	98.8
DHq-1 - 40	1.43E+08	319.9	2.9	0.45	-8	14	-175	-1389	100	1	0.469	0.015	0.0618	0.0008	0.3465	0.0548	0.0017	382	69	389	11	386.7	5.1	99.4
DHq-1 - 41	1.33E+08	274	4.3	0.66	-12.8	9.6	-75	-701	100	1	0.444	0.016	0.05904	0.0009	0.102	0.0546	0.0023	360	87	373	11	369.8	5.3	99.1
DHq-1 - 41b - 1	1.29E+08	191	4.7	0.83	-8	11	-138	-734	100	1	0.425	0.022	0.05829	0.001	0.0265	0.054	0.003	330	110	361	16	365.1	6.2	101.1
DHq-1 - 42	1.44E+08	197.7	2.6	0.67	-9	16	-178	-718	100	1	0.441	0.02	0.0588	0.001	0.3191	0.0541	0.0027	340	100	368	14	368	5.8	100.0
DHq-1 - 43	1.11E+08	216.9	3.3	0.75	9	16	178	661	100	1	0.421	0.018	0.0577	0.001	0.0055	0.0532	0.0024	360	90	360	13	361.8	6.3	100.5
DHq-1 - 44	1.27E+08	345.8	3.4	0.56	3	20	667	3563	100	1	0.434	0.017	0.0578	0.0008	0.2906	0.0544	0.0022	360	82	368	12	362.5	4.7	98.5
DHq-1 - 45	1.33E+08	347.7	6.2	0.82	-2	16	-800	-5770	100	1	0.47	0.017	0.0618	0.0009	0.0156	0.0545	0.0019	394	75	390	11	386.2	5.7	99.0
DHq-1 - 46	1.34E+08	345.4	8.6	0.77	4	12	300	2765	100	1	0.458	0.016	0.06009	0.0009	0.0869	0.0563	0.002	439	80	382	11	376.1	5.4	98.5
DHq-1 - 47	1.37E+08	437	16	0.66	-12	18	-150	-1157	100	1	0.44	0.014	0.05792	0.0007	0.0492	0.0551	0.0018	390	71	369	9.9	362.9	4.1	98.3
DHq-1 - 48	1.17E+08	635	18	0.68	1	13	1300	18080	100	1	0.432	0.013	0.05784	0.0007	0.0208	0.0529	0.0016	340	61	368	8.7	362.4	4.2	98.5
DHq-1 - 49	1.29E+08	257.3	8.2	0.56	11.6	9.7	84	711	100	1	0.461	0.02	0.06126	0.0009	0.0052	0.0541	0.0023	363	90	383	14	383.2	5.2	100.1
DHq-1 - 50	1.37E+08	196.5	5.3	0.61	-7	17	-243	-977	100	1	0.476	0.021	0.0629	0.0009	0.0212	0.0547	0.0024	380	93	396	15	393.1	5.7	99.3
DHq-1 - 51	1.35E+08	252	18	0.60	12	13	108	652	100	1	0.431	0.02	0.0579	0.001	0.25	0.0543	0.0024	345	93	364	14	363.4	5.8	99.8
DHq-1 - 52	1.28E+08	316.1	3.4	0.47	1	20	2000	10240	100	1	0.706	0.027	0.0657	0.0009	0.3756	0.0799	0.003	1160	69	545	16	410.3	5.2	75.3
DHq-1 - 53	1.28E+08	404.3	2.7	0.52	-13	11	-85	-964	100	1	0.437	0.015	0.05859	0.0008	0.0748	0.0541	0.002	361	77	371	11	367	4.7	98.9
DHq-1 - 54	1.31E+08	252.4	5.2	0.67	-14	10	-71	-561	100	1	0.477	0.02	0.0593	0.001	0.2321	0.0569	0.0023	480	90	394	14	371.2	5.8	94.2
DHq-1 - 55	1.40E+08	393.5	11	0.75	19	16	84	706	100	1	0.529	0.014	0.0625	0.0009	0.0898	0.0608	0.0019	620	68	430	9.9	392.3	5.5	91.2
DHq-1 - 56	1.31E+08	178.8	4.4	0.46	14	12	86	425	100	1	0.477	0.022	0.0624	0.0012	0.1015	0.0535	0.0027	370	100	395	15	390.2	7.5	98.8
DHq-1 - 57	1.31E+08	186.3	2.7	0.57	14	14	100	431	100	1	0.493	0.019	0.0605	0.001	0.2185	0.0577	0.0021	500	83	405	13	378.7	6	93.5
DHq-1 - 58	1.26E+08	237.8	5.8	0.63	1	10	1000	7366	100	1	0.451	0.018	0.06002	0.0009	0.083	0.0534	0.0022	335	88	376	13	375.7	5.4	99.9
DHq-1 - 59	1.30E+08	222.4	3.2	0.88	1	12	1200	7020	100	1	0.45	0.019	0.05918	0.0009	0.1126	0.0553	0.0023	410	90	377	13	370.6	5.4	98.3
DHq-1 - 60	1.25E+08	505	20	0.87	-7	17	-243	-2310	100	1	0.466	0.012	0.05994	0.0009	0.4134	0.0556	0.0014	430	56	387	8.6	375.2	5.2	97.0

APPENDIX B: Continued

Table B2. LA-ICP-MS U-Pb isotopic analyses of zircon standards (University of New Brunswick).

Corrections = C* — cps = counts per second — 1 = (after Hg correction)

1 threshold 204cps for no correction: 80 cps

2 threshold % for 204-based correction: 21 % error

3 threshold % for 208-based correction: 98.5 %Pb*

Sample	Zr90 cps	U (ppm)	Th (ppm)	Th/U	^{204}Pb cps[1]	2σ error on 204 cps	% error on 204 cps	cps ^{206}Pb/^{204}Pb	%Pb*	C*	Isotopic ratios ^{207}Pb/^{235}U	2σ ±	^{206}Pb/^{238}U	2σ ±	err. corr.	^{207}Pb/^{206}Pb	2σ ±	Calculated ages ^{207}Pb/^{206}Pb	2σ ±	^{207}Pb/^{235}U	2σ ±	^{206}Pb/^{238}U	2σ ±	% conc
11/05/2016																								
Plesovice - 1	*1.44E+08*	502.9	43.69	0.09	3	12	400	5026.6667	100	1	0.396	0.014	0.05332	0.0009	0.0552	0.0545	0.0021	364	83	334.8	5.7	338	10	99.1
Plesovice - 2	*1.37E+08*	567.1	46.77	0.08	1	11	1100	16480	100	1	0.395	0.013	0.0545	0.0009	0.1141	0.0535	0.0018	332	75	342.1	5.5	338.5	9.4	101.1
Plesovice - 3	*1.29E+08*	399.1	30.8	0.08	-3	11	-366.67	-3763.333	100	1	0.388	0.015	0.05477	0.0009	0.2096	0.052	0.0021	296	91	343.7	5.6	336	11	102.3
Plesovice - 4	*1.34E+08*	674.9	60.96	0.09	-1	12	-1200	-19490	100	1	0.401	0.013	0.05415	0.0009	0.2491	0.0538	0.0018	351	74	339.9	5.3	342	9.1	99.4
Plesovice - 5	*1.49E+08*	767.4	63.1	0.08	16	22	137.5	1456.875	100	1	0.397	0.012	0.05368	0.0008	0.089	0.0539	0.0018	392	74	337.1	5.1	339	8.6	99.4
Plesovice - 6	*1.34E+08*	531	46.87	0.09	8	13	162.5	1916.25	100	1	0.391	0.013	0.05406	0.0009	0.0048	0.0527	0.0018	314	79	339.4	5.5	334	9.8	101.6
12/05/2016																								
Plesovice - 1	*1.23E+08*	956	2	0.11	-13	11	-85	-1959	100	1	0.39	0.0098	0.05359	0.0006	0.3151	0.0537	0.0012	342	49	334.1	7.2	336.5	3.7	100.7
Plesovice - 2	*1.13E+08*	445	1	0.08	5	11	220	2246	100	1	0.392	0.013	0.05344	0.0007	0.1395	0.053	0.0016	334	68	334.9	9.2	335.6	4.2	100.2
Plesovice - 3	*1.15E+08*	1048	1	0.14	-12.6	9.3	-74	-2137	100	1	0.395	0.0092	0.05363	0.0006	0.2418	0.0533	0.001	340	45	337.4	6.7	336.7	3.4	99.8
Plesovice - 4	*1.17E+08*	745	1	0.10	1	11	1100	19440	100	1	0.394	0.011	0.05341	0.0006	0.1163	0.0537	0.0013	349	56	336.4	8	335.4	3.6	99.7
Plesovice - 5	*1.21E+08*	765	1	0.10	11	11	100	1838	100	1	0.398	0.012	0.05334	0.0006	0.4666	0.0537	0.0013	341	54	339.6	8.3	335	3.4	98.6
Plesovice - 6	*1.28E+08*	674	1	0.11	5	16	320	3714	100	1	0.393	0.012	0.05302	0.0006	0.2316	0.0536	0.0015	330	60	338	8.2	333	3.6	98.5
Plesovice - 7	*1.01E+08*	787	2	0.10	5	16	320	3832	100	1	0.401	0.01	0.05355	0.0006	0.1984	0.0545	0.0012	389	51	342	7.7	336.3	3.5	98.3
15/12/2016																								
Plesovice - 1	1.01E+08	481.8	39.93	12.07	17	12	70.6	1051	99.68	1	0.406	0.011	0.054	0.001	0.219	0.0548	0.0015	383	58	345	8	337	4	97.6
Plesovice - 2	1.15E+08	713.5	68.8	10.37	9	16	177.8	3159	99.75	1	0.398	0.012	0.054	0.001	0.143	0.0539	0.0017	348	68	340	9	338	5	99.3
Plesovice - 3	1.11E+08	629.8	58.48	10.77	2	13	650.0	12290	99.66	1	0.405	0.013	0.054	0.001	0.040	0.0547	0.0018	377	71	345	9	338	4	98.0
Plesovice - 4	1.14E+08	798.8	82.4	9.69	9	13	144.4	3573	99.78	1	0.397	0.011	0.054	0.001	0.136	0.0535	0.0014	335	59	339	8	339	5	100.0
Plesovice - 5	1.10E+08	564	50.6	11.15	-5	13	-260.0	-4330	100.11	1	0.379	0.012	0.054	0.001	0.120	0.0511	0.0016	248	71	326	9	337	5	103.4
Plesovice - 6	1.01E+08	590	49.8	11.85	2	12	600.0	10880	99.80	1	0.398	0.009	0.054	0.001	0.280	0.0537	0.0012	345	51	340	7	338	4	99.6
Plesovice - 7	1.15E+08	700.3	66.03	10.61	11	17	154.5	2501	99.95	1	0.383	0.012	0.054	0.001	0.203	0.0520	0.0015	273	66	329	9	337	5	102.5
16/12/2016																								
Plesovice - 1	1.15E+08	527.3	43.97	11.99	0	11			99.93	1	0.392	0.013	0.0539	0.0009	0.220	0.0527	0.0016	299	65	335	10	339	6	101.1
Plesovice - 2	1.15E+08	717.4	75.1	9.55	-10	12	-120.0	-2954.00	99.82	1	0.395	0.011	0.0540	0.0009	0.167	0.0533	0.0013	326	54	339	8	339	5	100.2
Plesovice - 3	1.12E+08	408.5	33.11	12.34	-1	13	-1300.0	-16410.00	99.84	1	0.395	0.015	0.0539	0.0009	0.152	0.0532	0.0018	316	72	337	11	338	6	100.4
Plesovice - 4	1.14E+08	519.2	43.92	11.82	1	12	1200.0	20960.00	99.85	1	0.396	0.012	0.0541	0.0009	0.203	0.0531	0.0014	320	58	338	9	340	6	100.5
Plesovice - 5	1.07E+08	405	32.68	12.39	8	13	162.5	1953.75	99.97	1	0.388	0.011	0.0540	0.0009	0.095	0.0522	0.0014	279	57	332	8	339	6	102.0
Plesovice - 6	1.08E+08	489	41.6	11.75	-1	11	-1100.0	-19100.00	99.86	1	0.395	0.013	0.0541	0.0010	0.170	0.0529	0.0016	309	63	337	9	340	6	100.7
Plesovice - 7	1.05E+08	903.8	130.4	6.93	7	13	185.7	4945.71	99.91	1	0.390	0.011	0.0535	0.0009	0.145	0.0525	0.0012	304	53	334	8	336	5	100.7
Plesovice - 8	1.13E+08	643.9	59.75	10.78	-4	11	-275.0	-6510.00	99.84	1	0.394	0.015	0.0540	0.0010	0.206	0.0529	0.0018	307	73	337	11	339	6	100.7
Plesovice - 9	1.05E+08	631.8	59.45	10.63	0	14			99.92	1	0.384	0.013	0.0534	0.0009	0.023	0.0521	0.0017	271	68	330	10	336	5	101.9

Table B2. Continued.

Sample	Zr90 cps	U (ppm)	Th (ppm)	Th/U	^{204}Pb cps[1]	2σ error on 204 cps	% error on 204 cps	cps ^{206}Pb/^{204}Pb	%Pb*	C*	Isotopic ratios ^{207}Pb/^{235}U	2σ ±	^{206}Pb/^{238}U	2σ ±	err. corr.	^{207}Pb/^{206}Pb	2σ ±	Calculated ages ^{207}Pb/^{206}Pb	2σ ±	^{207}Pb/^{235}U	2σ ±	^{206}Pb/^{238}U	2σ ±	% conc
Plesovice - 10	1.02E+08	811.2	85.4	9.50	-6	10	-166.7	-5171.67	99.85	1	0.396	0.012	0.0540	0.0009	0.112	0.0532	0.0014	324	57	338	9	339	5	100.2
02/02/217																								
Plesovice - 1	1.73E+08	730.8	68.2	10.72	18	10	53.6	1815	99.84	1	0.387	0.013	0.053	0.002	0.011	0.0528	0.0013	304	53	332	10	333	12	100.5
Plesovice - 1	1.78E+08	730.3	68.1	10.72	19	11	57.9	1789	99.85	1	0.385	0.014	0.053	0.002	0.022	0.0526	0.0014	295	58	331	10	333	12	100.8
Plesovice - 2	1.71E+08	604.5	54.1	11.17	7	9	126.8	3921	99.71	1	0.403	0.015	0.054	0.002	0.024	0.0545	0.0015	373	59	343	11	338	12	98.5
Plesovice - 2	1.80E+08	604.5	54.1	11.17	7	11	157.1	4150	99.81	1	0.398	0.016	0.054	0.002	0.089	0.0537	0.0016	340	65	340	11	339	12	99.8
Plesovice - 3	1.57E+08	617.9	54.16	11.41	15	12	80.0	1875	99.92	1	0.383	0.014	0.053	0.002	0.356	0.0525	0.0012	297	53	328	10	332	12	101.2
Plesovice - 3	1.71E+08	619	54.41	11.38	13	11	84.6	2262	99.90	1	0.382	0.013	0.053	0.002	0.182	0.0526	0.0011	300	47	328	10	332	12	101.0
Plesovice - 4	1.68E+08	665.7	59.31	11.22	3	9	284.4	9575	99.78	1	0.376	0.013	0.051	0.002	0.082	0.0531	0.0013	317	52	323	10	322	12	99.7
Plesovice - 4	1.68E+08	665.7	59.3	11.23	3	9	272.7	9288	99.76	1	0.375	0.013	0.051	0.002	0.100	0.0530	0.0013	314	52	323	10	322	12	99.8
Plesovice - 5	1.64E+08	585	51	11.47	5	10	217.8	6044	99.81	1	0.392	0.014	0.053	0.002	0.236	0.0536	0.0014	342	56	335	11	334	12	99.7
Plesovice - 5	1.64E+08	587	51.3	11.44	11	9	89.5	2571	99.76	1	0.393	0.014	0.053	0.002	0.165	0.0541	0.0013	360	51	336	10	332	12	98.9
Plesovice - 6	1.61E+08	559	48.7	11.48	8	10	125.0	3161	99.85	1	0.390	0.014	0.054	0.002	0.338	0.0530	0.0013	314	54	334	10	336	12	100.8
Plesovice - 6	1.61E+08	559	48.7	11.48	8	10	125.0	3161	99.85	1	0.390	0.014	0.054	0.002	0.338	0.0530	0.0013	314	54	334	10	336	12	100.8
Plesovice - 7	1.63E+08	613.4	52.96	11.58	7	9	134.3	4154	99.65	1	0.397	0.014	0.052	0.002	0.046	0.0544	0.0014	367	57	339	10	330	12	97.3
Plesovice - 7	1.78E+08	613.6	52.93	11.59	11	11	100.0	2635	99.66	1	0.394	0.015	0.053	0.002	0.080	0.0540	0.0016	350	65	337	11	330	12	98.1
Plesovice - 8	1.62E+08	658.4	59.57	11.05	0	10	9500.0	293600	99.81	1	0.391	0.014	0.053	0.002	0.017	0.0534	0.0014	327	56	334	10	335	12	100.0
Plesovice - 8	1.62E+08	658.4	59.57	11.05	0	10	9500.0	293600	99.81	1	0.391	0.014	0.053	0.002	0.017	0.0534	0.0014	327	56	334	10	335	12	100.0
Plesovice - 9	1.63E+08	791.8	77.53	10.21	1	9	657.1	25464	99.91	1	0.386	0.013	0.053	0.002	0.125	0.0525	0.0011	295	46	331	9	335	12	101.4
Plesovice - 9	1.63E+08	791.8	77.53	10.21	1	9	657.1	25464	99.91	1	0.386	0.013	0.053	0.002	0.125	0.0525	0.0011	295	46	331	9	335	12	101.4
Plesovice - 10	1.61E+08	1185	159.2	7.44	11	9	81.6	4632	99.81	1	0.391	0.012	0.053	0.002	0.138	0.0533	0.0009	333	38	335	9	335	12	100.0
Plesovice - 10	1.61E+08	1185	159.2	7.44	11	9	81.6	4632	99.81	1	0.391	0.012	0.053	0.002	0.138	0.0533	0.0009	333	38	335	9	335	12	100.0
Plesovice - 11	1.59E+08	618.1	53.99	11.45	3	9	268.8	8459	99.81	1	0.391	0.014	0.053	0.002	0.149	0.0535	0.0013	333	54	335	10	334	12	99.7
Plesovice - 11	1.59E+08	618.1	53.99	11.45	3	9	268.8	8459	99.81	1	0.391	0.014	0.053	0.002	0.149	0.0535	0.0013	333	54	335	10	334	12	99.7
Plesovice - 12	1.60E+08	747.9	71.37	10.48	1	10	1650.0	55317	99.73	1	0.390	0.013	0.052	0.002	0.194	0.0535	0.0011	337	47	334	10	329	12	98.5
Plesovice - 12	1.73E+08	748.6	71.46	10.48	-3	12	-400.0	-11450	99.73	1	0.389	0.015	0.052	0.002	0.179	0.0535	0.0014	334	59	334	11	330	12	98.8
Plesovice - 13	1.54E+08	473.6	38.91	12.17	16	10	63.5	1328	99.93	1	0.392	0.015	0.054	0.002	0.108	0.0528	0.0015	301	62	335	11	339	12	101.2
Plesovice - 13	1.56E+08	473.6	38.93	12.17	16	10	60.1	1313	99.93	1	0.392	0.015	0.054	0.002	0.126	0.0528	0.0015	303	61	335	11	339	12	101.1
Plesovice - 14	1.67E+08	412.2	37.35	11.04	7	13	185.7	2681	99.71	1	0.395	0.018	0.053	0.002	0.154	0.0543	0.0022	364	87	337	13	331	12	98.3
Plesovice - 14	1.58E+08	412.2	37.29	11.05	9	9	104.6	2086	99.57	1	0.403	0.015	0.053	0.002	0.093	0.0554	0.0017	404	66	343	11	331	12	96.5
Plesovice - 15	1.56E+08	610.3	54.76	11.14	17	8	49.1	1560	99.82	1	0.388	0.013	0.053	0.002	0.247	0.0532	0.0012	321	49	332	10	333	12	100.2
Plesovice - 15	1.56E+08	610.3	54.76	11.14	17	8	49.1	1560	99.82	1	0.388	0.013	0.053	0.002	0.247	0.0532	0.0012	321	49	332	10	333	12	100.2
Plesovice - 16	1.56E+08	612.7	55.4	11.06	6	9	143.8	4202	99.71	1	0.395	0.015	0.053	0.002	0.261	0.0540	0.0014	352	55	338	11	332	12	98.5
Plesovice - 16	1.56E+08	612.7	55.4	11.06	6	9	143.8	4202	99.71	1	0.395	0.015	0.053	0.002	0.261	0.0540	0.0014	352	55	338	11	332	12	98.5
Plesovice - 17	1.57E+08	972.6	105.7	9.20	7	9	123.6	6025	99.75	1	0.393	0.013	0.053	0.002	0.174	0.0533	0.0010	329	44	336	9	334	12	99.3
Plesovice - 17	1.57E+08	972.6	105.7	9.20	7	9	123.6	6025	99.75	1	0.393	0.013	0.053	0.002	0.174	0.0533	0.0010	329	44	336	9	334	12	99.3
Plesovice - 18	1.53E+08	518.7	43.51	11.92	8	8	103.8	2849	99.85	1	0.395	0.015	0.055	0.002	0.221	0.0531	0.0014	317	59	337	11	344	13	102.0
Plesovice - 18	1.63E+08	518.7	43.51	11.92	9	10	111.1	2609	99.81	1	0.397	0.016	0.055	0.002	0.270	0.0537	0.0017	342	69	339	12	343	13	101.2
Plesovice - 19	1.58E+08	412.1	33.25	12.39	8	10	125.0	2281	100.09	1	0.379	0.015	0.054	0.002	0.114	0.0513	0.0016	242	66	326	11	338	12	103.6
Plesovice - 19	1.53E+08	412.1	33.25	12.39	9	9	101.1	1989	100.05	1	0.381	0.015	0.054	0.002	0.094	0.0515	0.0015	250	62	327	11	337	12	103.2

Table B2. Continued.

Sample	Zr90 cps	U (ppm)	Th (ppm)	Th/U	^{204}Pb cps[1]	2σ error on 204 cps	% error on 204 cps	cps ^{206}Pb/^{204}Pb	%Pb*	C*	Isotopic ratios ^{207}Pb/^{235}U	2σ ±	^{206}Pb/^{238}U	2σ ±	err. corr.	^{207}Pb/^{206}Pb	2σ ±	Calculated ages ^{207}Pb/^{206}Pb	2σ ±	^{207}Pb/^{235}U	2σ ±	^{206}Pb/^{238}U	2σ ±	% conc
Plesovice - 20	1.53E+08	676	62.46	10.82	0	8	7700.0	288900	99.90	1	0.380	0.013	0.052	0.002	0.004	0.0525	0.0012	292	52	327	10	329	12	100.7
Plesovice - 20	1.56E+08	676.3	62.48	10.82	1	8	922.2	32467	99.89	1	0.378	0.014	0.052	0.002	0.081	0.0524	0.0014	291	57	325	10	328	12	100.8
18/04/2017																								
Plesovice - 1	1.68E+08	23.35	1.955	11.94	7	13	185.7	6687	99.81	1	0.399	0.011	0.054	0.001	0.523	0.0536	0.0010	342	41	340	8	340	5	99.9
Plesovice - 2	1.58E+08	31.53	3.043	10.36	19	11	57.9	3175	99.28	1	0.434	0.011	0.054	0.001	0.187	0.0583	0.0013	527	48	366	8	338	5	92.5
Plesovice - 3	1.59E+08	17.74	1.775	9.99	2	11	550.0	17270	99.96	1	0.389	0.013	0.054	0.001	0.157	0.0521	0.0015	272	63	333	10	339	5	101.9
Plesovice - 4	1.57E+08	21.17	1.776	11.92	5	10	190.4	7856	99.95	1	0.387	0.011	0.054	0.001	0.113	0.0520	0.0012	273	49	333	8	338	5	101.7
Plesovice - 5	1.56E+08	18.53	1.499	12.36	1	11	1100.0	35120	99.88	1	0.396	0.012	0.054	0.001	0.205	0.0530	0.0013	314	54	338	9	339	5	100.1
Plesovice - 6	1.53E+08	40.55	4.885	8.30	15	12	80.0	4975	99.27	1	0.437	0.012	0.054	0.001	0.692	0.0586	0.0008	547	29	367	8	338	5	91.9
Plesovice - 7	1.52E+08	16.72	1.574	10.62	-4	10	-264.9	30780	99.79	1	0.397	0.013	0.054	0.001	0.378	0.0535	0.0013	337	51	339	9	337	5	99.6
Plesovice - 8	1.50E+08	17.78	1.736	10.24	4	12	300.0	8128	99.71	1	0.404	0.013	0.054	0.001	0.360	0.0545	0.0013	376	53	344	9	337	5	98.1
Plesovice - 9	1.49E+08	27.41	2.476	11.07	-4	9	-230.0	50200	99.84	1	0.393	0.011	0.054	0.001	0.381	0.0528	0.0010	319	44	337	8	338	5	100.3
Plesovice - 10	1.43E+08	19.28	2.133	9.04	6	9	143.8	5352	99.79	1	0.397	0.011	0.054	0.001	0.329	0.0536	0.0011	340	45	339	8	338	6	99.9
Plesovice - 11	1.39E+08	21.34	1.858	11.49	-5	11	-220.0	36520	99.75	1	0.396	0.012	0.053	0.001	0.303	0.0539	0.0012	355	49	338	9	335	5	98.9
Plesovice - 12	1.41E+08	15.95	1.321	12.07	-2	10	-500.0	27530	99.75	1	0.393	0.012	0.053	0.001	0.290	0.0537	0.0013	339	55	336	9	333	5	99.2
Plesovice - 13	1.51E+08	12.49	1.012	12.34	-1	12	-1200.0	23180	99.92	1	0.389	0.014	0.054	0.001	0.473	0.0525	0.0015	296	61	335	11	341	6	101.8
Plesovice - 14	1.41E+08	16.91	1.636	10.34	10	10	100.0	2953	99.86	1	0.398	0.013	0.054	0.001	0.388	0.0533	0.0013	328	52	339	9	339	5	99.8
Plesovice - 15	1.39E+08	9.581	0.776	12.35	4	9	244.4	4544	99.67	1	0.400	0.015	0.053	0.001	0.269	0.0543	0.0017	356	68	341	11	335	6	98.2
11/05/2016																								
FC-1 - 1	*1.40E+08*	215.6	132.7	0.62	-5	11	-220	-4434	100	1	1.935	0.052	0.1861	0.0029	0.1438	0.0762	0.0022	1088	59	1099.8	16	1091	18	100.8
FC-1 - 2	*1.41E+08*	418.4	279.3	0.67	1	11	1100	43250	100	1	1.947	0.047	0.1858	0.0026	0.0242	0.0762	0.002	1109	55	1099.3	14	1096	16	100.3
FC-1 - 3	*1.41E+08*	236.6	136.8	0.58	-1	11	-1100	-24500	100	1	1.943	0.051	0.186	0.0027	0.0967	0.0759	0.0023	1079	60	1099.3	15	1094	18	100.5
FC-1 - 4	*1.42E+08*	232.5	114	0.49	7	12	171	3410	100	1	2.008	0.051	0.1859	0.0029	0.3519	0.0764	0.0022	1100	56	1098.9	16	1118	18	98.3
FC-1 - 5	*1.41E+08*	248.8	79.9	0.32	-6	12	-200	-4243	100	1	1.949	0.051	0.1858	0.0029	0.2568	0.076	0.0022	1089	59	1098	16	1099	18	99.9
FC-1 - 6	*1.40E+08*	200.1	95.42	0.48	3	12	400	6880	100	1	1.929	0.058	0.186	0.0034	0.0576	0.0762	0.0024	1108	64	1100	18	1094	20	100.5
FC-1 - 7	*1.39E+08*	188	93.4	0.50	-10	11	-110	-1921	100	1	1.9	0.058	0.186	0.0028	0.0414	0.0759	0.0025	1088	69	1099.5	15	1082	21	101.6
FC-1 - 8	*1.35E+08*	209.7	133.6	0.64	1	15	1500	21040	100	1	1.95	0.062	0.1857	0.0031	0.2822	0.0764	0.0025	1099	65	1099	17	1096	21	100.3
FC-1 - 9	*1.38E+08*	297.1	163.1	0.55	0.6	8.8	1467	50933	100	1	1.962	0.051	0.1859	0.0028	0.0664	0.0761	0.0022	1106	57	1099	15	1103	18	99.6
FC-1 - 10	*1.37E+08*	182.4	99.1	0.54	-10	10	-100	-1880	100	1	1.984	0.055	0.1861	0.003	0.185	0.0762	0.0023	1111	61	1100	16	1115	17	98.7
FC-1 - 11	*1.37E+08*	181.9	73.39	0.40	-6	11	-183	-3070	100	1	1.926	0.058	0.1856	0.003	0.2116	0.0759	0.0024	1089	65	1097	17	1091	21	100.5
FC-1 - 12	*1.36E+08*	271.4	166.4	0.61	-2	12	-600	-13720	100	1	1.97	0.051	0.186	0.0029	0.2142	0.0764	0.0022	1100	58	1099.4	16	1105	17	99.5
FC-1 - 13	*1.36E+08*	441.9	257	0.58	-4	12	-300	-11133	100	1	1.942	0.045	0.1858	0.0027	0.198	0.076	0.002	1103	51	1098.6	14	1095	15	100.4
FC-1 - 14	*1.35E+08*	250.9	149	0.59	-7.7	9.8	-127	-3291	100	1	1.946	0.053	0.1861	0.0029	0.437	0.0764	0.0021	1101	56	1099.9	16	1097	18	100.3
FC-1 - 15	*1.32E+08*	313.5	158.2	0.50	11	11	100	2823	100	1	1.957	0.049	0.1867	0.0029	0.2487	0.0755	0.0021	1084	57	1103.2	16	1101	17	100.2
FC-1 - 16	*1.32E+08*	166	69.45	0.42	9	9.4	104	1819	100	1	1.964	0.064	0.1849	0.003	0.3118	0.077	0.0025	1128	64	1093	16	1100	22	99.4
FC-1 - 17	*1.33E+08*	127.6	40.92	0.32	-14.9	8.2	-55	-840	100	1	1.943	0.067	0.1858	0.0032	0.1536	0.0761	0.0028	1094	75	1099	18	1094	23	100.5
FC-1 - 18	*1.32E+08*	250.2	146.6	0.59	6	10	167	4167	100	1	1.96	0.053	0.186	0.0029	0.2118	0.0761	0.0023	1099	60	1100	16	1102	19	99.8
FC-1 - 19	*1.30E+08*	122.8	74.49	0.61	-4	11	-275	-3033	100	1	1.933	0.069	0.1858	0.0034	0.0318	0.0762	0.0031	1080	83	1098	19	1094	24	100.4
12/05/2016																								
FC-1 - 1	*1.19E+08*	128	1	0.60	1	13	1300	11460	100	1	1.927	0.084	0.1851	0.0034	0.0341	0.0769	0.0033	1105	90	1092	30	1094	18	100.2

Table B2. Continued.

Sample	Zr90 cps	U (ppm)	Th (ppm)	Th/U	^{204}Pb cps[1]	2σ error on 204 cps	% error on 204 cps	cps ^{206}Pb/^{204}Pb	%Pb*	C*	Isotopic ratios ^{207}Pb/^{235}U	2σ ±	^{206}Pb/^{238}U	2σ ±	err. corr.	^{207}Pb/^{206}Pb	2σ ±	Calculated ages ^{207}Pb/^{206}Pb	2σ ±	^{207}Pb/^{235}U	2σ ±	^{206}Pb/^{238}U	2σ ±	% conc
FC-1 - 2	*1.15E+08*	617	4	0.71	-0.6	8.7	-1450	-92050	100	1	1.958	0.032	0.1867	0.0017	0.3041	0.0764	0.00095	1106	26	1100.6	11	1103	9.3	100.2
FC-1 - 3	*1.14E+08*	230	1	0.51	-6	10	-167	-3377	100	1	1.914	0.047	0.1844	0.0023	0.2816	0.0759	0.0016	1094	44	1089	16	1091	12	100.2
FC-1 - 4	*1.14E+08*	212	1	0.47	-5.3	9.3	-175	-3549	100	1	1.951	0.046	0.1855	0.0022	0.2265	0.0758	0.0016	1088	43	1097	16	1097	12	100.0
FC-1 - 5	*1.15E+08*	245	1	0.53	-6.6	9.7	-147	-3285	100	1	1.937	0.043	0.186	0.0023	0.1646	0.076	0.0014	1090	37	1092	15	1100	12	100.7
FC-1 - 6	*1.20E+08*	209	1	0.51	-3	14	-467	-6370	100	1	1.943	0.053	0.1845	0.0024	0.173	0.0769	0.0019	1107	50	1094	18	1091	13	99.7
FC-1 - 7	*1.27E+08*	159	1	0.37	3	22	733	4873	100	1	1.941	0.1	0.1844	0.0045	0.4137	0.0764	0.0035	1107	89	1092	34	1091	24	99.9
FC-1 - 9	*1.15E+08*	447	3	0.61	-3	12	-400	-13763	100	1	1.96	0.041	0.187	0.0022	0.2679	0.0752	0.0013	1075	33	1100	14	1105	12	100.5
FC-1 - 10	*1.16E+08*	259	2	0.63	-12	11	-92	-1963	100	1	1.976	0.05	0.1866	0.0021	0.1271	0.0764	0.0019	1101	47	1109	16	1103	12	99.4
FC-1 - 11	*1.14E+08*	193	1	0.62	-3	11	-367	-5880	100	1	1.949	0.056	0.1844	0.0025	0.1341	0.0766	0.0021	1104	57	1097	20	1091	14	99.5
FC-1 - 12	*1.18E+08*	493	3	0.54	-14.9	9.6	-64	-3076	100	1	1.979	0.039	0.1868	0.0019	0.1641	0.0761	0.0012	1098	33	1107	13	1104	10	99.7
FC-1 - 13	*1.16E+08*	250	2	0.63	4.4	9.7	220	5186	100	1	1.958	0.048	0.1869	0.0022	0.1884	0.0763	0.0016	1094	42	1101	17	1104	12	100.3
FC-1 - 14	*1.22E+08*	268	2	0.57	13	15	115	1935	100	1	1.921	0.048	0.1854	0.0025	0.1303	0.0754	0.0021	1086	55	1089	17	1096	14	100.6
FC-1 - 15	*1.17E+08*	520	2	0.55	6	9.8	163	7952	100	1	1.983	0.038	0.1861	0.0017	0.2477	0.0767	0.0012	1116	31	1109	13	1100	9.4	99.2
FC-1 - 16	*1.16E+08*	209	1	0.63	9.5	9.8	103	1993	100	1	1.932	0.043	0.1854	0.0024	0.2991	0.0755	0.0016	1074	43	1091	15	1096	13	100.5
FC-1 - 18	*1.15E+08*	151	1	0.38	7	10	143	1940	100	1	1.97	0.053	0.1853	0.0024	0.2514	0.0769	0.0018	1112	47	1106	18	1095	13	99.0
FC-1 - 19	*1.14E+08*	174	1	0.42	-2	10	-500	-7795	100	1	1.951	0.054	0.1851	0.0023	0.1625	0.0763	0.0019	1110	49	1095	19	1094	13	99.9
FC-1 - 20	*1.14E+08*	225	1	0.51	6	11	183	3377	100	1	1.944	0.044	0.185	0.0022	0.1065	0.0769	0.0016	1115	42	1099	15	1095	12	99.6
FC-1 - 21	*1.15E+08*	298	2	0.58	-4	11	-275	-6753	100	1	1.92	0.043	0.187	0.0022	0.2301	0.0754	0.0014	1074	40	1091	16	1105	12	101.3
15/12/2016																								
FC-1 - 1	1.08E+08	213.5	105.95	2.02	-7	12	-171.4	-4177	99.64	1	1.964	0.036	0.185	0.002	0.169	0.0767	0.0014	1103	37	1101	12	1096	12	99.9
FC-1 - 2	1.08E+08	208.7	104.9	1.99	10	12	120.0	2906	99.69	1	1.963	0.037	0.186	0.002	0.214	0.0765	0.0015	1098	39	1103	13	1102	13	99.3
FC-1 - 3	1.04E+08	116.5	63	1.85	2	13	650.0	8055	99.64	1	1.910	0.051	0.186	0.003	0.021	0.0747	0.0023	1040	63	1085	19	1100	15	93.0
FC-1 - 4	1.07E+08	171.2	64.8	2.64	9	12	133.3	2569	99.64	1	1.939	0.044	0.185	0.002	0.349	0.0761	0.0016	1085	43	1092	15	1092	13	98.6
FC-1 - 5	1.09E+08	345.2	228.8	1.51	8	12	150.0	6050	99.76	1	1.947	0.030	0.187	0.002	0.222	0.0755	0.0012	1076	32	1096	10	1104	12	96.7
FC-1 - 6	1.10E+08	268.4	151.2	1.78	-5	10	-200.0	-7510	99.64	1	1.955	0.040	0.186	0.002	0.269	0.0763	0.0015	1090	40	1098	14	1099	12	98.5
FC-1 - 7	1.10E+08	258.3	152.3	1.70	-14	13	-92.9	-2583	99.64	1	1.947	0.040	0.186	0.002	0.216	0.0761	0.0015	1086	39	1095	14	1097	12	98.3
FC-1 - 8	1.08E+08	493.1	273.8	1.80	-1	11	-1100.0	-68500	99.78	1	1.970	0.026	0.187	0.002	0.303	0.0762	0.0010	1096	26	1104	9	1107	11	98.6
FC-1 - 9	1.03E+08	246.8	141.9	1.74	-1	12	-1200.0	-31900	99.61	1	1.937	0.035	0.184	0.002	0.147	0.0765	0.0014	1097	38	1092	12	1088	13	99.5
FC-1 - 10	1.09E+08	444.4	258.7	1.72	-7	11	-157.1	-8827	99.83	1	1.952	0.024	0.186	0.002	0.179	0.0760	0.0010	1095	25	1098	8	1102	11	99.4
FC-1 - 11	1.08E+08	205.5	70.47	2.92	3	12	400.0	9350	99.51	1	1.981	0.038	0.184	0.002	0.097	0.0777	0.0015	1135	41	1107	13	1090	13	96.2
FC-1 - 12	1.08E+08	309.9	193.3	1.60	2	13	650.0	21165	99.78	1	1.937	0.034	0.186	0.002	0.353	0.0759	0.0012	1085	32	1093	12	1098	12	98.6
FC-1 - 13	1.10E+08	270	170.9	1.58	8	12	150.0	4711	99.71	1	1.949	0.034	0.187	0.002	0.179	0.0759	0.0013	1090	37	1097	12	1102	12	98.8
FC-1 - 14	1.08E+08	239	133.9	1.78	6	11	183.3	5463	99.75	1	1.927	0.038	0.185	0.002	0.335	0.0753	0.0013	1068	36	1089	13	1095	13	96.6
FC-1 - 16	1.08E+08	243.2	127.5	1.91	-4	10	-236.6	-8180	99.69	1	1.960	0.034	0.186	0.002	0.245	0.0766	0.0013	1102	35	1100	12	1099	12	100.0
FC-1 - 17	1.08E+08	331.5	197.9	1.68	0	13			99.81	1	1.950	0.030	0.187	0.002	0.294	0.0756	0.0011	1083	31	1097	10	1105	12	97.7
FC-1 - 18	1.09E+08	206.3	103.2	2.00	-2	13	-650.0	-14165	99.58	1	1.965	0.042	0.185	0.003	0.351	0.0772	0.0015	1115	41	1101	14	1094	13	98.3
FC-1 - 1	1.24E+08	563.3	366.6	1.54	14	11	78.6	6214	99.83	1	1.964	0.042	0.1873	0.0029	0.342	0.0761	0.0011	1094	29	1103	14	1107	16	98.6
FC-1 - 2	1.22E+08	358.4	210	1.71	-5	10	-200.0	-10758	99.76	1	1.952	0.043	0.1848	0.0028	0.357	0.0766	0.0011	1106	29	1098	15	1093	15	99.0
FC-1 - 3	1.20E+08	512.6	269.6	1.90	4	11	275.0	19300	99.79	1	1.969	0.044	0.1873	0.0029	0.420	0.0764	0.0012	1101	31	1104	15	1107	16	99.4
FC-1 - 4	1.21E+08	108.8	41.2	2.64	10	13	130.0	1647	99.64	1	1.956	0.062	0.1862	0.0034	0.285	0.0763	0.0020	1084	53	1097	21	1100	18	97.5

Table B2. Continued.

Sample	Zr90 cps	U (ppm)	Th (ppm)	Th/U	^{204}Pb cps[1]	2σ error on 204 cps	% error on 204 cps	cps $^{206}Pb/^{204}Pb$	%Pb*	C*	Isotopic ratios $^{207}Pb/^{235}U$	2σ ±	$^{206}Pb/^{238}U$	2σ ±	err. corr.	$^{207}Pb/^{206}Pb$	2σ ±	Calculated ages $^{207}Pb/^{206}Pb$	2σ ±	$^{207}Pb/^{235}U$	2σ ±	$^{206}Pb/^{238}U$	2σ ±	% conc
FC-1 - 5	1.17E+08	167.9	74.54	2.25	-7	13	-185.7	-3454	99.68	1	1.939	0.049	0.1842	0.0031	0.102	0.0765	0.0016	1104	40	1093	17	1090	17	98.6
FC-1 - 6	1.19E+08	257.3	137.7	1.87	-7	12	-171.4	-5420	99.79	1	1.929	0.048	0.1855	0.0030	0.377	0.0752	0.0013	1072	37	1089	17	1097	16	97.1
FC-1 - 7	1.19E+08	182.1	112.2	1.62	5	12	240.0	5332	99.61	1	1.941	0.054	0.1839	0.0032	0.184	0.0766	0.0018	1096	47	1093	19	1088	17	99.9
FC-1 - 8	1.16E+08	270.8	172.1	1.57	-3	12	-400.0	-13173	99.79	1	1.953	0.048	0.1875	0.0031	0.356	0.0756	0.0014	1077	37	1098	17	1108	17	96.6
FC-1 - 9	1.13E+08	289.7	92.7	3.13	-3	12	-400.0	-13517	99.77	1	1.912	0.046	0.1839	0.0030	0.287	0.0754	0.0014	1078	35	1084	16	1088	16	98.9
FC-1 - 10	1.14E+08	291.4	182.2	1.60	-6	12	-200.0	-6898	99.67	1	1.971	0.046	0.1859	0.0031	0.252	0.0770	0.0013	1113	35	1105	16	1099	17	98.9
FC-1 - 11	1.13E+08	298.1	187.5	1.59	5	12	240.0	8360	99.65	1	1.963	0.049	0.1850	0.0030	0.293	0.0766	0.0014	1108	38	1101	17	1094	16	99.2
FC-1 - 12	1.09E+08	159.1	56.8	2.80	-6	14	-233.3	-3657	99.74	1	1.948	0.057	0.1878	0.0032	0.352	0.0751	0.0018	1056	48	1095	20	1109	18	93.5
FC-1 - 13	1.12E+08	202.3	95.3	2.12	-9	12	-133.3	-3161	99.66	1	1.910	0.051	0.1844	0.0031	0.024	0.0752	0.0018	1059	48	1083	18	1091	17	96.1
FC-1 - 15	1.11E+08	189.2	118.4	1.60	-1	12	-1200.0	-26680	99.66	1	1.945	0.055	0.1857	0.0032	0.227	0.0759	0.0018	1079	48	1094	19	1098	17	97.3
FC-1 - 16	1.12E+08	164.2	91	1.80	13	11	84.6	1812	99.74	1	1.930	0.058	0.1869	0.0031	0.223	0.0747	0.0019	1043	51	1089	20	1105	17	92.4
FC-1 - 17	1.11E+08	348.6	226.7	1.54	-4	12	-300.0	-12400	99.69	1	1.991	0.046	0.1867	0.0030	0.027	0.0772	0.0013	1119	33	1111	15	1104	16	99.0
FC-1 - 18	1.10E+08	243.2	126.7	1.92	-12	11	-91.7	-2876	99.74	1	1.973	0.052	0.1883	0.0031	0.350	0.0759	0.0015	1081	41	1106	17	1112	17	96.1
FC-1 - 19	1.11E+08	375.2	214.8	1.75	1	11	1100.0	53300	99.78	1	1.949	0.046	0.1856	0.0030	0.460	0.0762	0.0013	1093	33	1097	16	1098	16	99.2
FC-1 - 20	1.10E+08	300.2	169.9	1.77	1	11	1100.0	42350	99.83	1	1.938	0.042	0.1856	0.0029	0.307	0.0757	0.0012	1085	30	1095	14	1098	16	98.6
FC-1 - 21	1.08E+08	323.7	190.3	1.70	-2	12	-600.0	-22480	99.70	1	1.967	0.048	0.1865	0.0031	0.316	0.0765	0.0014	1101	36	1103	17	1102	17	99.5
FC-1 - 22	1.09E+08	202.6	101.3	2.00	24	13	54.2	1185	99.66	1	1.949	0.048	0.1836	0.0033	0.282	0.0769	0.0014	1118	39	1097	16	1086	18	97.1
02/02/2017																								
FC-1 - 1	1.72E+08	229.7	136.5	1.68	8	9	119.2	4655	99.69	1	1.957	0.061	0.186	0.007	0.283	0.0761	0.0013	1089	34	1099	21	1100	38	98.2
FC-1 - 2	1.74E+08	217.8	100.7	2.16	7	8	125.8	5382	99.72	1	1.933	0.064	0.186	0.007	0.272	0.0760	0.0015	1082	41	1090	22	1097	38	98.4
FC-1 - 4	1.65E+08	694	328	2.12	1	9	1566.7	189667	99.81	1	1.965	0.055	0.186	0.007	0.474	0.0764	0.0008	1102	21	1103	19	1101	38	99.8
FC-1 - 5	1.66E+08	469.9	282.6	1.66	3	9	306.9	26069	99.86	1	1.935	0.057	0.186	0.007	0.486	0.0759	0.0009	1087	24	1092	20	1098	37	99.1
FC-1 - 6	1.66E+08	270.9	151.8	1.78	3	9	364.0	17420	99.76	1	1.958	0.058	0.186	0.007	0.375	0.0766	0.0011	1104	28	1100	20	1098	38	99.6
FC-1 - 7	1.65E+08	333.6	192.9	1.73	6	10	160.7	8815	99.77	1	1.952	0.059	0.186	0.007	0.189	0.0754	0.0011	1071	31	1098	20	1101	38	95.7
FC-1 - 8	1.62E+08	327.9	144.2	2.27	-1	7	-514.3	-36500	99.74	1	1.951	0.058	0.186	0.007	0.235	0.0764	0.0011	1101	28	1099	21	1097	38	99.7
FC-1 - 9	1.61E+08	201.7	102.15	1.97	1	10	1000.0	31230	99.70	1	1.950	0.064	0.186	0.007	0.281	0.0762	0.0015	1088	40	1096	22	1100	38	98.4
FC-1 - 10	1.59E+08	346	214.6	1.61	4	9	222.0	12949	99.77	1	1.959	0.059	0.186	0.007	0.442	0.0764	0.0011	1100	30	1100	20	1100	38	99.8
FC-1 - 11	1.57E+08	348.6	217	1.61	8	9	106.0	6383	99.78	1	1.944	0.060	0.186	0.007	0.447	0.0761	0.0011	1092	29	1095	21	1097	38	99.3
FC-1 - 12	1.59E+08	147.7	110.2	1.34	5	10	179.2	4370	99.71	1	1.965	0.065	0.187	0.007	0.306	0.0759	0.0015	1082	40	1104	22	1104	38	96.7
FC-1 - 13	1.56E+08	387	240	1.61	10	10	100.0	5750	99.74	1	1.946	0.057	0.185	0.007	0.239	0.0762	0.0011	1095	29	1096	20	1096	38	99.7
FC-1 - 14	1.58E+08	326.4	203.5	1.60	6	8	147.4	8954	99.81	1	1.956	0.057	0.186	0.007	0.101	0.0757	0.0012	1087	29	1100	19	1101	38	98.0
FC-1 - 15	1.56E+08	251	124.5	2.02	12	10	77.2	3127	99.73	1	1.949	0.059	0.186	0.007	0.166	0.0762	0.0013	1094	33	1097	20	1098	38	99.4
FC-1 - 16	1.58E+08	281.3	155.1	1.81	6	9	165.5	8091	99.70	1	1.952	0.060	0.186	0.007	0.202	0.0760	0.0012	1090	31	1098	21	1099	38	98.6
FC-1 - 17	1.56E+08	262.1	148.3	1.77	11	11	100.0	3717	99.78	1	1.966	0.062	0.187	0.007	0.274	0.0758	0.0013	1086	34	1105	20	1103	38	97.3
FC-1 - 18	1.53E+08	386.5	210.7	1.83	7	9	135.8	8552	99.76	1	1.935	0.059	0.185	0.007	0.442	0.0769	0.0011	1113	29	1092	20	1093	38	97.1
FC-1 - 19	1.58E+08	268	162.8	1.65	8	9	108.8	5263	99.75	1	1.959	0.058	0.186	0.007	0.248	0.0763	0.0011	1096	29	1101	20	1102	38	99.2
FC-1 - 20	1.55E+08	175.4	85.6	2.05	6	8	134.5	4641	99.69	1	1.949	0.063	0.186	0.007	0.276	0.0756	0.0014	1074	37	1099	21	1098	38	96.3
18/04/2017																								
FC-1 - 2	1.78E+08	4.5	2.0	2.24	0	10	-4800.0	32790	99.59	1	1.965	0.054	0.186	0.003	0.010	0.0771	0.0017	1118	45	1102	18	1100	16	97.9
FC-1 - 3	1.72E+08	7.4	3.2	2.29	0	10		53200	99.75	1	1.948	0.050	0.186	0.003	0.329	0.0759	0.0012	1084	32	1096	17	1100	15	97.9

Table B2. Continued.

Sample	Zr90 cps	U (ppm)	Th (ppm)	Th/U	^{204}Pb cps[1]	2σ error on 204 cps	% error on 204 cps	cps ^{206}Pb/^{204}Pb	%Pb*	C*	Isotopic ratios ^{207}Pb/^{235}U	2σ ±	^{206}Pb/^{238}U	2σ ±	err. corr.	^{207}Pb/^{206}Pb	2σ ±	Calculated ages ^{207}Pb/^{206}Pb	2σ ±	^{207}Pb/^{235}U	2σ ±	^{206}Pb/^{238}U	2σ ±	% conc
FC-1 - 4	1.68E+08	8.5	4.6	1.83	-5	9	-193.6	60100	99.74	1	1.977	0.047	0.186	0.003	0.325	0.0767	0.0010	1108	27	1107	16	1101	15	99.9
FC-1 - 5	1.76E+08	7.3	4.4	1.66	0	12	#DIV/0!	52590	99.86	1	1.920	0.047	0.185	0.003	0.434	0.0757	0.0011	1082	29	1087	16	1091	16	99.1
FC-1 - 6	1.78E+08	3.4	1.6	2.15	-7	11	-157.1	24700	99.69	1	1.920	0.060	0.187	0.004	0.174	0.0753	0.0020	1061	54	1086	21	1102	19	95.8
FC-1 - 7	1.65E+08	6.1	3.5	1.74	6	11	183.3	7118	99.75	1	1.948	0.048	0.186	0.003	0.251	0.0754	0.0011	1076	32	1096	17	1099	16	96.7
FC-1 - 8	1.80E+08	10.1	6.0	1.67	15	15	100.0	4926	99.83	1	1.971	0.048	0.188	0.003	0.300	0.0766	0.0013	1109	33	1105	17	1109	17	99.5
FC-1 - 10	1.60E+08	4.3	1.8	2.40	-5	10	-200.0	28890	99.60	1	1.948	0.055	0.185	0.003	0.249	0.0762	0.0016	1089	42	1095	19	1093	16	98.7
FC-1 - 12	1.63E+08	3.0	1.3	2.30	5	10	200.0	4014	99.57	1	1.931	0.059	0.183	0.003	0.227	0.0765	0.0017	1093	46	1089	20	1085	17	99.8
FC-1 - 13	1.55E+08	8.3	5.2	1.59	3	10	396.0	21836	99.71	1	1.973	0.050	0.188	0.003	0.119	0.0763	0.0013	1094	34	1105	17	1109	16	98.2
FC-1 - 14	1.49E+08	5.3	3.2	1.63	3	10	293.9	10273	99.63	1	1.954	0.055	0.187	0.003	0.095	0.0761	0.0017	1083	45	1097	19	1103	17	97.5
FC-1 - 15	1.50E+08	3.5	1.8	1.99	4	12	300.0	5648	99.55	1	1.982	0.070	0.185	0.004	0.138	0.0772	0.0023	1116	60	1106	24	1096	19	99.0
FC-1 - 16	1.46E+08	11.3	7.4	1.53	-2	9	-430.0	70100	99.83	1	1.932	0.045	0.185	0.003	0.452	0.0757	0.0010	1083	26	1093	15	1095	16	98.6
FC-1 - 17	1.47E+08	7.0	3.6	1.96	2	10	500.0	22500	99.73	1	1.965	0.048	0.187	0.003	0.382	0.0767	0.0012	1107	31	1104	17	1105	17	99.5
FC-1 - 18	1.33E+08	6.1	2.8	2.13	8	13	162.5	4529	99.64	1	1.946	0.066	0.184	0.003	0.139	0.0756	0.0022	1075	56	1095	22	1090	18	96.6
FC-1 - 19	1.49E+08	2.8	1.0	2.70	2	10	633.3	11847	99.40	1	1.953	0.065	0.184	0.003	0.129	0.0770	0.0022	1099	57	1096	22	1089	18	99.9
FC-1 - 20	1.46E+08	5.4	3.2	1.67	-2	11	-550.0	34300	99.71	1	1.970	0.052	0.188	0.003	0.390	0.0763	0.0014	1093	36	1105	19	1108	16	98.2
FC-1 - 21	1.49E+08	2.8	1.1	2.52	-3	10	-306.3	17890	99.59	1	1.927	0.061	0.185	0.003	0.239	0.0754	0.0020	1067	50	1087	21	1094	18	96.4